Analytica Chimica Acta 1316 (2024) 342880

Contents lists available at ScienceDirect

Analytica Chimica Acta

journal homepage: www.elsevier.com/locate/aca

A review of biocompatible polymer-functionalized two-dimensional materials: Emerging contenders for biosensors and bioelectronics applications

Tahreem Zahra [a], Umme Javeria [a], Hasan Jamal [b], Mirza Mahmood Baig [a,c], Farid Akhtar [d,**], Urooj Kamran [d,e,*]

[a] Department of Chemistry, University of Narowal, Narowal, Punjab, 51600, Pakistan
[b] Division of Energy Technology, Daegu Gyeongbuk Institute of Science & Technology, 333, Techno Jungang-Daero, Hyeonpung-Myeon, Dalseong-Gun, Daegu, 42988, Republic of Korea
[c] Department of Chemistry, University of Ulsan, Ulsan, 44610, Republic of Korea
[d] Division of Materials Science, Luleå University of Technology, 97187, Luleå, Sweden
[e] Institute of Advanced Machinery Design Technology, Korea University, 145 Anam-ro, Seongbuk-gu, Seoul, Republic of Korea

HIGHLIGHTS

- Improved properties of polymer-2D materials for biosensing/bioelectronics.
- Discussion of diverse range of polymer-functionalized 2D materials as biosensors.
- Insight analysis of their synthesis methods and applications.
- Critical overview of challenges and future aspects of polymer-2D materials.

GRAPHICAL ABSTRACT

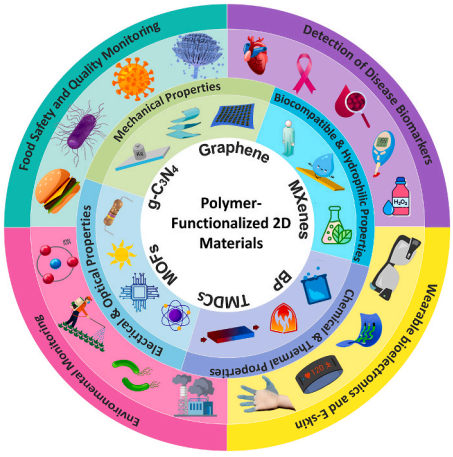

ARTICLE INFO

Keywords:
Bioelectronics
Biosensors
2D materials
Polymer-functionalization
Biocompatible

ABSTRACT

Bioelectronics, a field pivotal in monitoring and stimulating biological processes, demands innovative nano-materials as detection platforms. Two-dimensional (2D) materials, with their thin structures and exceptional physicochemical properties, have emerged as critical substances in this research. However, these materials face challenges in biomedical applications due to issues related to their biological compatibility, adaptability, functionality, and nano-bio surface characteristics. This review examines surface modifications using covalent and

* Corresponding author. Division of Materials Science, Luleå University of Technology, 97187, Luleå, Sweden.
** Corresponding author.
E-mail addresses: farid.akhtar@ltu.se (F. Akhtar), malikurooj9@gmail.com (U. Kamran).

https://doi.org/10.1016/j.aca.2024.342880
Received 10 March 2024; Received in revised form 14 June 2024; Accepted 15 June 2024
Available online 18 June 2024

non-covalent-based polymer-functionalization strategies to overcome these limitations by enhancing the biological compatibility, adaptability, and functionality of 2D nanomaterials. These surface modifications aim to create stable and long-lasting therapeutic effects, significantly paving the way for the practical application of polymer-functionalized 2D materials in biosensors and bioelectronics. The review paper critically summarizes the surface functionalization of 2D nanomaterials with biocompatible polymers, including g-C_3N_4, graphene family, MXene, BP, MOF, and TMDCs, highlighting their current state, physicochemical structures, synthesis methods, material characteristics, and applications in biosensors and bioelectronics. The paper concludes with a discussion of prospects, challenges, and numerous opportunities in the evolving field of bioelectronics.

1. Introduction

In recent years, the intersection of biotechnology, nanotechnology, and materials science has led to remarkable advancements in the development of biosensors and bioelectronics for various electronic and biomedical applications [1]. Since Luigi Galvani uncovered the concept of 'bioelectricity' in the 1780s, bioelectronics has emerged as a dynamic area of study involving the integration of electronics with biology and biotechnology [2]. Bioelectronics integrates biologically derived sensing components like DNA, cells, proteins, and antibodies with electronic components such as electrodes, field-effect transistors (FETs), optical resonators, and electrode arrays to create functional biosensors with exceptional sensitivity and specificity [3–5], as depicted in Fig. 1. These biosensor tools are designed to identify and observe biological interactions and physiological signals. They achieve this identification through electrical or optical measurements, capturing changes in parameters such as potential, current, conductance, or resonant frequency [6,7]. With successful applications across many domains, including pharmaceutical testing, clinical diagnosis, environmental surveillance, and food quality management, these biosensors and bioelectronics devices offer viable alternatives to traditional chemical and physical sensors as well as methods [8,9].

Despite substantial success in various healthcare applications, current bioelectronic devices face limitations in spatial resolution, biocompatibility, and sensitivity due to mechanical properties and size discrepancies compared to the biological elements they aim to detect.

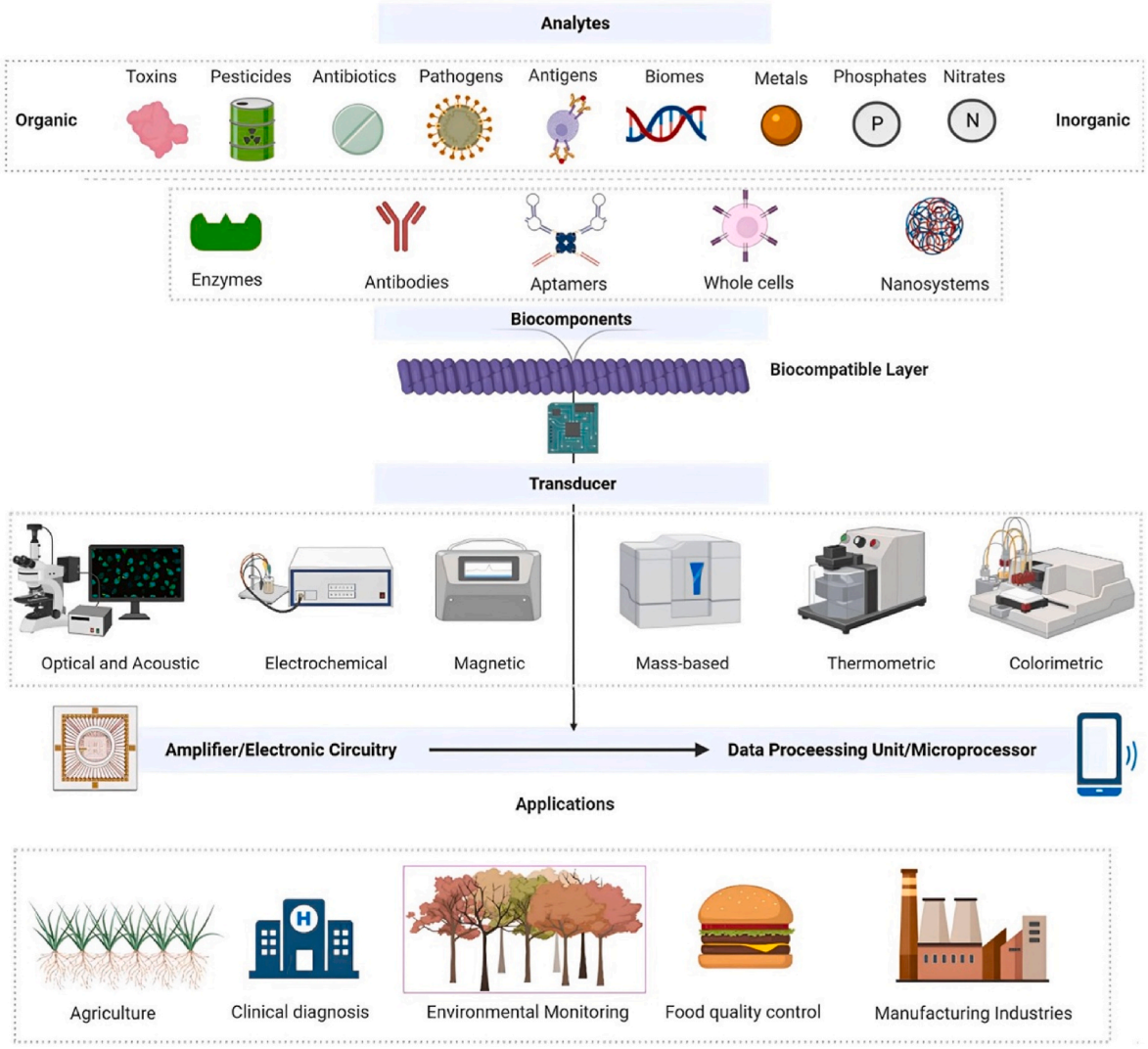

Fig. 1. Diagram depicting the essential elements of a biosensor and the detection module for various applications. Reprinted from Ref. [18]. with permission from Elsevier.

For instance, essential components involved in neuronal communication (e.g., synapses and ion channels) operate on a nanometre scale relevant to intercellular communication. Nano-electronic devices offer a means of building effective interfaces for cellular communication, serving as foundational units for seamlessly integrating electronics with biological systems [10]. However, conventional devices often differ significantly in rigidity from natural tissue, resulting in shear motion at tissue-electronic interfaces that deteriorates stimulation and recording capabilities with time. Matching electronic tools' structural, mechanical, and biochemical properties with natural tissue could enable stable integration and create new scientific and technological possibilities [11,12].

Material compatibility with biological systems is also crucial for device stability, recording reliability, and potential health risks. Investigating the impact of materials on cells and tissues before their use is essential [13]. For instance, silicon-based electronics have demonstrated utility in various biochemical and biological monitoring technologies, such as bio-photoelectric imaging tubes, biosensors, and biochips [14]. Despite their proven utility, these electronics encounter challenges like decreased carrier mobility, limited flexibility, and high short-channel properties in sub-10 nm nodes. Specifically, the quest for ultra-thin, rigid silicon-based components to enhance flexibility poses significant hurdles in integration and processing. Recently, nanomaterials and their composites have emerged, offering exceptional characteristics in combination with low modulus to create top-performing photoelectric and electronic devices capable of tolerating substantial mechanical deformation [13,15].

The primary challenge in developing these nano-biosensors lies in their capacity to reliably identify specific biomolecules or target analytes for disease diagnostics and medical interventions [16]. Consequently, when designing nano-bioelectrodes as sensing platforms, the utmost consideration revolves around achieving high selectivity and sensitivity [17]. The latest biosensors use advanced nanomaterials as sensing platforms and incorporate efficient data processing techniques for various healthcare uses. These biosensors aim to balance efficiency, stability, and multifunctionality by integrating them with state-of-the-art technologies. Overcoming their main challenges involves designing complex functional nanoplatforms and controlling their physiochemical properties [18]. Since 2004, Andre Geim and Konstantin Novoselov have successfully isolated one layer of graphene from monolithic graphite through the micromechanical cleavage method at the University of Manchester. Noteworthy attention has been directed towards nanomaterials in a two-dimensional (2D) form [19,20]. These ultra-thin atomic layers, around 5–10 nm thick or a small number of thin layers linked together by van der Waals forces, offer broader possibilities [21]. The discovery of graphene has spurred the exploration of various 2D layered materials with remarkable mechanical, electronic, optical, and biological attributes [22–24]. Collaborative endeavours of chemists, physicists, and material scientists have explored a variety of 2D nanocrystals, encompassing transition metal dichalcogenides (TMDCs) [25], MXenes [26,27], graphitic carbon nitride (g-C_3N_4) [28,29], transition metal oxide [30], and black phosphorus (BP) [31,32] with diverse applications, including biomedicine. Beyond their 2D structure and ultra-thin nature, these emerging materials showcase distinct electronic, optical, and physicochemical characteristics like efficient carrier transfer, extensive surface areas, transparency, biocompatibility, flexible layered structures, robust interfacial attractions with cells, DNA, biomolecules, proteins, and other biological entities [33,34]. Consequently, these distinctive attributes make them suitable not only for bioelectronic and biosensor devices but also for overcoming the limitations of silicon-based electronics [35].

Despite the impressive strides made in developing bioelectronic devices combined with nanotechnology, they still need to match the effectiveness of biological systems in performing tasks like molecular recognition, catalyzing chemical reactions, and reacting and adapting to changes in their surroundings. As a result, the collaboration between 2D materials and polymers has led to significant progress in bio-interfaces, offering exciting prospects for regulating biomolecular interactions within bioelectrodes and mimicking natural environments to enhance electronic capabilities [36]. Polymers, known for their adaptability, biocompatibility, and ease of synthesis, are frequently employed in surface functionalization. The ultrathin structures and extensive surface areas of 2D materials make incorporating various elements, like polymers. This synergy between polymers and 2D materials has driven the development of innovative nanodevices that can be processed with solvents, stable monitoring platforms, and adhesive nanointerfaces [15]. Challenges like agglomeration in 2D materials can also be addressed by blending them with polymers in a thickened solution, where polymers reduce water molecule flow abilities and slow diffusion of 2D materials, contributing to stability and optimal performance [37].

To safely use 2D nanomaterials in medical applications, the primary concern is to ensure their safety in biosystems, including in vitro and in vivo diagnostic scenarios. It has been observed that the chemical composition influences the biocompatibility of 2D materials, and surface modification with polymeric substances like bovine serum albumin (BSA), poly(vinyl pyrrolidone) (PVP), polyethylene glycol (PEG), etc., can enhance their stability, biocompatibility, and physiological dispersibility [38]. For instance, MoS_2 nanosheets (NSs) exfoliated with BSA demonstrated better compatibility with fibroblast cells compared to those without BSA [39]. Such surface modifications are commonly employed to stabilize 2D materials under physiological conditions, improving biological compatibility despite potential toxicity concerns.

There has been a significant surge in interest within the biosensing and bioelectronics fields in recent years, with numerous published studies. However, previous research has predominantly concentrated on specific subsets of this broad field, often examining individual classes of 2D materials for singular applications [40,41] or a single composite of polymer-functionalized 2D materials within a particular domain of biosensing [42]. For instance, Jiang and his team focused on the development, mechanisms, challenges, and future perspectives of graphene-based biosensors for detecting bacterial and viral pathogens [43]. In another review, Alwarappan and colleagues comprehensively discussed the synthesis routes, surface functionalization, and application of MXenes in biosensors [16]. Other researchers have broadly covered recent trends in the design and fabrication of graphene/polymer nanocomposites (GPNs) for sensing applications in environmental and human health monitoring [44]. However, our study broadens the scope of research by exploring the functionalization of various 2D materials with different polymers and covering a wide range of real-life applications of these materials in biosensors. This broad scope is not comprehensively covered by other relative studies with the latest research from 2014 to 2024. The review begins with an overview of the synthesis methods for 2D materials, emphasizing those functionalized with polymers. We then elaborate on the distinctive characteristics that make these materials highly compatible with bioelectronics and biosensors. The discussion will comprehensively address how specific polymer properties enhance the biosensing capabilities of various emerging 2D materials. Furthermore, we outline these composite materials' sensitivity and detection limits in particular applications, illustrating their practical implementations. The applications covered include food safety, environmental monitoring, detection of disease biomarkers, and the development of wearable bioelectronics and electronic skins (E-skins). Finally, the study explores the challenges and prospects of applying functionalized 2D materials in bioelectronics and biosensors, providing insights into future research and development directions in this rapidly evolving field.

2. Synthesis of polymer-functionalized 2D materials

The synthesis of 2D nanomaterials and their derivatives with polymers can be classified into two main categories: top-down and bottom-up approaches. The bottom-up approach can be further subdivided into various methods, including ligand-mediated growth, small molecules

assisted bottom-up approach, polyhydric alcohol method, and hydrothermal method, among others. On the other hand, the top-down method encompasses techniques such as exfoliation methods (such as chemical, micromechanical, ultrasonic, tiny atom assisted, and liquid phase exfoliation), nanolithography, laser ablation, and more [45]. Some commonly used synthesis methods are outlined in this review paper section.

2.1. Chemical vapor deposition

Chemical vapor deposition (CVD) is a high-temperature technique to vaporize and deposit metal on a suitable substrate. This method allows for synthesizing 2D nanomaterials based on transition metals, which provide superior electrical conductivity and more control over the final nanosheet or nanoplate thickness. CVD can create nanosheets in metal, semiconductors, and insulators. High temperatures evaporate the material in an adequate substrate and an inert environment; a tube furnace usually aids this process. The outer tube introduces the precursor and the inert atmosphere. The ability to carefully regulate the qualities incorporated into the nanomaterials, such as shape and crystallinity, is a crucial benefit of the CVD process. This approach allows the synthesis of high-purity 2D materials. CVD is one of the most popular techniques for creating 2D nanomaterials, including graphene, TMDs, and other layered materials. The basic idea is that a precursor gas breaks down on a substrate to form a thin film or 2D substance [45].

Utilizing the expansive surface area and superior quality of 2D materials, particularly those synthesized via CVD, offers a straightforward approach to precisely tailoring the surface or interface within layers of polymer structures. Typically, polymers like thermoplastic poly (methyl methacrylate) (PMMA), polystyrene (PS), polycarbonate (PC), polyolefins, and other compatible materials are employed as support mediums. The 2D sheets can be easily transferred from their growth substrates, such as copper foil or silica, onto the designated polymer support. This process enables the creation of composite films with a 2D sheet serving as the surface layer, which can then be utilized as precursors or foundational elements for subsequent processes, such as the fabrication of nanocomposites or devices [46].

2.2. Liquid phase exfoliation

Among the array of available exfoliation methods, liquid-phase exfoliation (LPE) is the most widely acclaimed technique for producing diverse types of 2D materials, offering precise control over their dimensions by adjusting process parameters. LPE typically involves either sonication-assisted or high-shear exfoliation. Initially, the bulk materials are dispersed in a suitable solvent with or without the aid of a surfactant and then subjected to either sonication or high shear mixing. Throughout the LPE process, the growth and subsequent collapse of micrometer sized bubbles or voids exert forces on the bulk material, effectively separating it into individual sheets [47]. Additionally, surfactants can improve the stability of the exfoliated sheets by intercalating between the layers, preventing their tendency to re-aggregate. LPE is typically conducted under mild conditions without high temperature or pressure. Offering high yield and adjustable parameters, 2D materials acquired via LPE find versatile applications, particularly in the biomedical realm [48,49].

Exfoliating agents that effectively produce water-soluble and functional nanosheets have been found within polymers known for their favourable biocompatibility. PVP, distinguished by its non-ionic and non-toxic properties, has emerged as a widely utilized exfoliating agent. The hydrophilic properties of PVP and substituents present on the nitrogen atom of the pyrrolidone ring endow its structure with similarities to N-methyl pyrrolidone (NMP), thereby contributing to the improved colloidal stability of aqueous nanosheet suspensions. Additionally, nanosheets exfoliated with PVP exhibit commendable biocompatibility, rendering them suitable for diverse bio-applications [50]. Nevertheless, various LPE methodologies and chemical functionalization techniques may influence the biocompatibility of the resultant materials. Hence, evaluating potential adverse effects, such as toxicity, inflammation, or immune responses, is crucial when utilizing 2D materials to ensure their suitability for clinical applications [48,49].

2.3. Micromechanical exfoliation

Atomically thin sheets of diverse 2D inorganic materials can be acquired through micromechanical exfoliation, a method like the one Grim and his colleagues employed for isolating single-layer graphene from highly oriented pyrolytic graphite (HOPG). This technique involves delicately rubbing or peeling commercially available inorganic layers of material against scotch tape on a photoresist surface. As a result, various flakes, including monolayers, adhere to the photoresist surface due to weakening van der Waals forces between adjacent layers. Subsequently, these monolayers are rinsed with acetone and transferred onto an oxidized silicon wafer. Although this method facilitates the extraction of monolayers from bulk materials like WS_2, MoS_2, h-BH, and $NbSe_2$ in a relatively straightforward, rapid, and cost-effective manner, it does come with certain drawbacks. Since monolayers serve as the foundational component of layered materials, separating them from thicker flakes is crucial for understanding the intrinsic properties of these materials. However, the yield of monolayers from this process is notably low, limiting its applicability primarily to laboratory-scale investigations rather than large-scale production for advanced technological applications. Nevertheless, the absence of chemical involvement in this process ensures structural integrity and high crystallinity maintenance, as it relies solely on applying shear force during the peeling procedure [51]. This technique has the potential to synthesize various 2D materials, as demonstrated by Gomez and his team, who utilized a polydimethylsiloxane (PDMS)-based intermediate viscoelastic substrate to achieve high-yield production of atomically thin BP flakes [52].

2.4. Hydrothermal method

Also known as the solvothermal method, this method operates under high temperature and pressure conditions, using water as an aqueous solvent or an organic solvent alongside NaOH as a reducing agent. The reaction mixture is enclosed within a sealed vessel made of Teflon encased in a thick stainless-steel chamber, functioning as an autoclave. Organic solvents are utilized in the solvothermal approach. In the mid-nineteenth century, geologists sought to replicate hydrothermal conditions to mimic the formation of specific rocks and minerals, hence coining the term “hydrothermal.” Granular production has existed for two centuries, based on hydrothermal techniques for single-crystal formation. This method employs a hydrophilic solution within a distinct sealed reaction vessel to create an environment of elevated temperature and pressure by heating and pressurizing the reaction system. This enables compounds that are typically poorly soluble or insoluble under standard conditions to dissolve and recrystallize at high temperatures and pressures [45].

Hydrothermal (or solvothermal) synthesis has garnered considerable attention in 2D material synthesis. Like liquid-exfoliated 2D materials, the hydrothermal method facilitates the synthesis of –O or –OH group-functionalized 2D materials using water as a solvent during the synthesis process. Additionally, incorporating groups other than OH is feasible with carefully selected additives for the reaction. For instance, the synthesis of amino-functionalized graphene and polymer-functionalized MoS_2 using additives such as PEG and PVP has been recognized. Hydrothermal synthesis is particularly adept at producing small particles rather than large and thin sheets [53].

3. Material properties required for biosensors and bioelectronics

2D materials offer distinctive properties that make them compatible with bioelectronics and biosensors, yet they face challenges like poor adaptability, cytotoxicity, low charge carrier mobility, environmental degradation, poor light absorption, and durability. Surface functionalization has emerged as a well-explored and practical strategy to address these challenges. This method allows for manipulating 2D nanomaterial properties while preserving their original lattice structure. Consequently, this approach is ideal for creating 2D material or polymers with unique traits like improved optical absorption, environmental stability, low cytotoxicity, robust mechanical strength, and the capacity to detect chemicals and biomolecules. This section highlights the advantageous properties of these materials in biomedical and flexible/stretchable bioelectronics, highlighting the latent potential of wearable electronics as combined biosensing systems that conform to the skin.

3.1. Mechanical properties

Good mechanical properties like flexibility and durability enable conformal contact with curvilinear, dynamic human skin and make acute health measurements possible. They also play a pivotal role in the lifespan of skin bioelectronics for long-term, continuous health monitoring. For materials used in these applications, finding the right balance in mechanical properties is essential yet challenging [54]. They need to be strong enough to withstand significant deformations while remaining flexible to match the softness of body tissues. The ability to stretch should be over 10 % on flat skins and 60 % on full-range body motions, depending on the device placement and target applications. In past years, the progressive development of 2D materials has emerged as excellent materials for bioelectronic applications because of their robust in-plane covalent or ionic bonds, strength, and atomic-thin structure, offering flexibility and stretchability [38]. However, to further improve the long-term stability, flexibility, and stretchability to ensure the viability of these materials in practical applications, scientists are actively functionalizing 2D materials with various polymer matrices to create 2D material/polymer hybrids with improved mechanical properties [55].

For instance, a GOx/gold/MoS_2/gold nanofilm over a polymer electrode was fabricated to enhance glucose detection by improving electrochemical signals and flexibility [56]. Utilizing a flexible polymer electrode as a substrate, the biosensor demonstrated superior flexibility to conventional Au-coated silicon sensors, as measured by a micro-fatigue tester (Fig. 2A and B). The Au-coated silicon electrode showed a flexure extension value of just 0.0938 mm under a force of

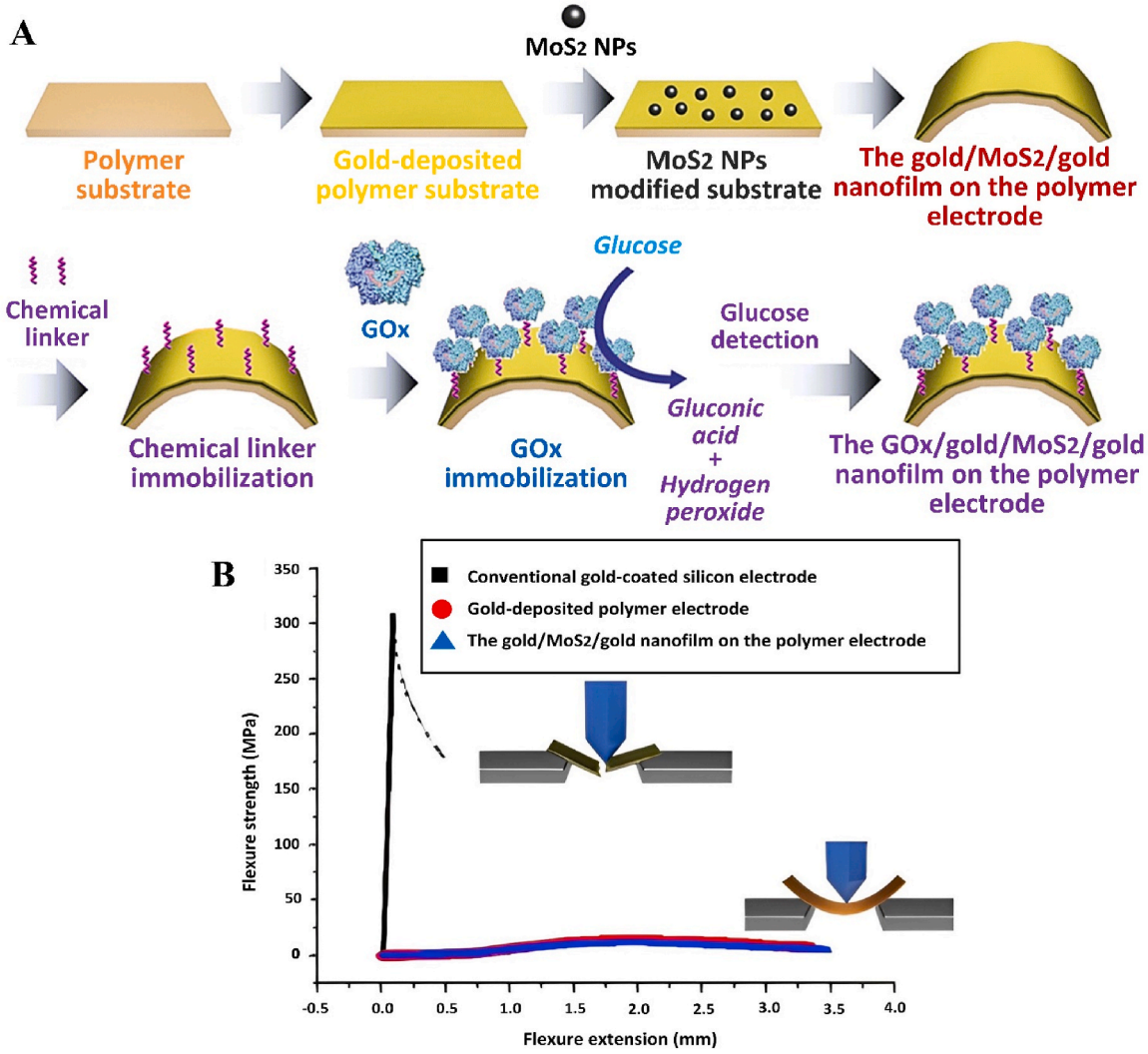

Fig. 2. A) Schematic representation of the construction process of a flexible electrochemical glucose biosensor featuring a GOx/gold/MoS_2/gold nanofilm on a polymer electrode. **B)** Demonstrating the flexibility of nanofilm on polymer electrodes through a flexibility test. Reproduced from Ref. [56]. with permission from *Elsevier*. (For interpretation of the references to colour in this figure legend, the reader is referred to the Web version of this article.)

307.4 MPa. In contrast, the gold/MoS_2/gold nanofilm over an electrode of polymer and Au-deposited polymer showed values of 3.48 mm and 3.36 mm, respectively, under approximately 12 MPa force, highlighting their flexibility. The electrochemical analysis demonstrated an increased signal with the nanofilm compared to conventional electrodes, indicating enhanced sensitivity. Aerometric measurements revealed the biosensor's ability to detect glucose, with a limit of detection (LOD) of 10 nM in a linear range of 500–10 nM and excellent selectivity even in human serum samples. In conclusion, the flexible glucose biosensor developed in this study showed promising potential for wearable biosensing systems due to its enhanced sensitivity, selectivity, and flexibility. Further optimization may be required for practical applications, particularly ensuring uniform layer depth. Wang and coworkers fabricated PP-rGO20 nanocomposites onto microelectrode sites, eliminating the need for post-reduction for neutral interface use [57]. TEM images revealed the polymerization of PEDOT: PSS on the rGO sheet surface. This approach unveiled the internal structure of PP-rGO20 and demonstrated the attachment of PSS to rGO sheets through π-π attractions between PSS and the sp^2 electron-stacking of rGO. The composite enhanced microelectrodes' stability and electrochemical properties and demonstrated robust mechanical stability under cyclic voltammetry (CV) scanning and ultrasonication tests. After 1000 cycles of scanning ($n = 3$), a 29.8 ± 5.1 % decrease in charge storage capacity (CSC) and an 11.6 ± 3.0 % increase in impedance at 1 kHz confirmed the superior mechanical stability of the PP-rGO20-modified electrode during stimulation and recording, even during in-vivo acute implantation. Yet, the study lacks long-term biocompatibility assessment and stability under extended electrical stimulation, highlighting the need for comprehensive evaluation and optimization for practical neural interface applications.

3.2. Electrical and optical properties

Optical and electrical properties depending on band gaps and electronic structures of 2D materials are crucial for biosensing applications [18]. The crystal structure of 2D materials affects photon and electron movement, with atomic thickness offering optical transparency but reducing charge mobility due to electron scattering. For instance, graphene's 0 eV band gap limits its use in optoelectronics for biosystems. Yet, its atomic thickness and high carrier mobility offer high optical transparency and fast response in optoelectronics. Many 2D materials have band gaps and electrical mobility dependent on the thickness of the layers, like MoS_2 transitions from an indirect to a direct band gap with varying numbers of layers. Additionally, BP has a thickness-dependent band gap (0.2–2.1 eV) and high carrier mobility at 10 nm layer thickness. Due to their relative band gaps, these 2D materials, with their more significant absorption coefficients at distinct wavelengths than graphene, are more suitable for optoelectronic devices [38]. However, the unique optical features of graphene-based nanomaterials, including tuneable and broadband absorption, make them valuable for optical sensors in various applications [58]. The bandgap and electrical properties of graphene and other 2D materials can be improved through different means, like hybridization with other nanomaterials, doping, or surface treatments. It is suggested that the optoelectronic properties of 2D nanomaterials can be significantly enhanced through surface functionalization with suitable polymers, opening new possibilities for applications in biosensors and bioelectronics.

Deviations in optical properties could be utilized for biomarker detection, as demonstrated by Zhou and his team, who developed a fibre optic biosensor built on 2D BP for sensing the cancer biomarker called human neuron-specific enolase (NSE) [59]. The nanosheets of BP were bio-functionalized with poly-L-lysine (PLL), serving as a crucial cross-linker to enhance the bio-nano-photonic interface with a significantly improved light-matter interface. Immobilizing the anti-NSE antibody through PLL allowed for the real-time and susceptible detection of NSE, as the linking of NSE by antibody altered the local refractive index. Due to its remarkable performance, they believe this BP-based biosensor opens new possibilities for bio-nano-photonic applications in food safety, healthcare, biomedical, and environmental monitoring. Future work should evaluate the biosensor's performance with clinical samples to validate its practical utility in early cancer diagnosis and disease detection. Photoelectrochemistry (PEC) involves the conversion of light energy into electricity by semiconductors (photoactive material), generating electron-hole pairs that initiate redox reactions at interfaces upon illumination [60]. A PEC sensor for glutathione detection using a nanocomposite of MoS_2 and polyaniline (PANI) was devised as the optoelectronic material [61]. The PANI/nanoMoS_2/GE nanocomposite exhibited a maximum PEC response of 712 nA, surpassing the performance of single material-modified gold electrodes with PANI or MoS_2. This improvement was attributed to the effective prevention of electron-hole pair recombination in PANI/nanoMoS_2, leading to an improved photocurrent response. The optimization of various parameters, such as ultrasonic time (4 h), ratio of PANI to nanoMoS_2 (5:2), and pH (6.0), suggested that the biosensor's performance was sensitive to experimental conditions. Achieving optimal results may require extensive experimentation and fine-tuning, which could increase the time and resources necessary for sensor development.

The enhanced electrical conductivity promotes efficient electron transmission between the solution and the modified electrode. A straightforward co-deposition technique anchors a PEDOT/g-C_3N_4 hybrid film on GCE. The g-C_3N_4 incorporation into PEDOT addressed the low conductivity of g-C_3N_4 and significantly enhanced electron-transfer capabilities [62]. The findings suggested that the modified electrode with the composite film displayed superior electrocatalytic activity for sensing ascorbic acid (AA) and acetaminophen (AP), offering a low LOD and broad linear range. Similarly, real sample analysis using Vitamin C and Paracetamol tablets demonstrated the biosensor's practical feasibility, with satisfactory recovery rates (94.9–104.56 %) indicating reliable detection capability. Yet, addressing further studies focusing on long-term stability, comprehensive selectivity testing, and validation using a diverse range of real samples would strengthen the reliability and applicability of the PEDOT/g-C_3N_4/GCE sensor. In another study, electrochemically deposited PEDOT was utilized as the conductive framework to create a composite with g-C_3N_4, addressing the limited conductivity issue of g-C_3N_4 [63]. The strong interactions and the cooperative influence between E-PEDOT and g-C_3N_4 also greatly enhanced the electron transmission properties and improved the electrochemical catalytic activity of the nanocomposite. Compared to pristine, g-C_3N_4, and E-PEDOT-modified electrodes, the g–C_3N_4–E-PEDOT-modified GCE exhibited superior electrocatalytic activity during AP oxidation. This study achieved a lower LOD for detecting AP of 34.28 nM compared to the above research with an LOD for AP of 0.49 μM. Overall, while both studies showcased innovative approaches and successful applications of composite materials in electrochemical sensing, they differed in the specific composite materials used, target analytes detected, and optimization strategies employed.

3.3. Chemical and thermal properties

The stability of 2D nanomaterials in biosensors and bioelectronic applications is determined by their chemical and thermal properties. Various factors, such as bonding, structure, doping, functional groups, defects, and environmental conditions, can influence the chemical and thermal stability of 2D nanomaterials. In particular, the in-plane thermal conductivity and cross-plane heat resistance of 2D nanomaterials are noteworthy considerations due to their ionic or covalent in-plane bonds and weak van der Waals interactions between layers [38]. In sensing applications, sensors must exhibit stability in both thermal and chemical aspects because the sensing material experiences various heat and chemical treatments throughout the machine processes involved in sensor manufacturing. Even continuous health monitoring relies heavily on the enduring stability of skin electronics. Hence, considerable efforts

have been made to improve the chemical and thermal stability of 2D materials because materials like BP and MXenes are easily susceptible to degradation in ambient conditions, primarily triggered by oxygen and water exposure. For example, the stability of BP NSs is notably impacted by light, which can trigger the formation of various reactive oxygen species (ROS) in the presence of oxygen and water [55]. On the other hand, under oxidative conditions such as elevated temperatures, $Ti_3C_2T_x$ (a type of MXene) transforms TiO_2 due to its exposed 'M' (Mo, Ti, etc.) atoms on both sides, which are unstable due to weak van der Waals attractions. Such conversions may result in the loss of distinctive properties of MXene, including their electrical and thermal conductance, hydrophilic traits, and increased functionality [18]. Therefore, polymer functionalization is a crucial technique to overcome the limitations associated with pristine 2D materials and make them more stable in physiological or manufacturing conditions [18].

For instance, a flexible biosensor utilizing hybrid sensitive films of PANI and $Ti_3C_2T_x$ was crafted to monitor NH_3 volatilization in agriculture [64]. The core-shell structure of $Ti_3C_2T_x$/PANI hybrids ensured the stability of 88 % for 35 days at ambient conditions, with outstanding humidity tolerance of up to 60 % relative humidity (RH) within 10–40 °C making them well-suited for practical applications. The superior performance of the hybrid sensor compared to pure PANI was attributed to factors like increased surface area, enhanced protonation degree of PANI, and the formation of a $Ti_3C_2T_x$/PANI Schottky junction. While the sensor exhibited excellent sensitivity to NH_3 even in high-humidity environments, it showed increased sensitivity to water vapor, especially at high RH levels (>90 %). This high sensitivity to humidity can potentially interfere with accurate NH_3 detection, particularly in environments with fluctuating humidity levels. The RGO-phenol formaldehyde composites are formed by in-situ intercalate polymerization via an interactive oxidation-reduction reaction. It involved the reduction of GO by phenol to RGO and the simultaneous oxidation of phenol to benzoquinone [65]. Here, the phenol non-covalently adsorbed on RGO was a reductant that guided the PF formation on the RGO surface. The interaction between GO and phenol homologs via covalent bonding and π–π stacking ensured strong interfacial interactions and good dispersion, thus resulting in enhanced thermal conductivity and thermal resistance. It was noted that adding RGO to polymer composites enhanced thermal conductivity and stability, particularly with 0.5 wt% RGO loading. However, higher concentrations led to decreased conductivity due to RGO agglomeration. Moreover, other thermal analyses confirmed enhanced thermal resistance and higher decomposition temperatures in RGO-PF composites, indicating their potential for high-performance thermal management applications. Yet, the study primarily focused on the structural and functional properties of RGO and its composites, with limited exploration of their practical applications or scalability.

Here, a novel cholesterol biosensor using a composite material, CSPPy-g-$C_3N_4H^+$, as the matrix was introduced [66]. The composite material, formed by exfoliating g-$C_3N_4H^+$ into thin nanosheets, provided an effective and large surface area. Consequently, the fabricated biosensor exhibited good long-standing storage stability over 45 days despite various potential interfering elements, retaining 94 % of its initial response. It also exhibited repeatability, with an average RSD of ≤3.46 % in ten repeated measurements, confirming excellent performance. The study does not provide a comparative analysis with existing cholesterol biosensors. A comparative evaluation could highlight the advantages and limitations of the proposed biosensor relative to existing technologies, providing valuable context for its performance. A high surface passivation and effective exfoliation of BP nanosheets using a diluted polymer ionic liquid solution were achieved for flexible photoelectrodes. The stability of the resultant PIL-modified BP was significantly enhanced in both aqueous and solid-state environments compared to bare BP [67]. Even after 120 h of exposure to ambient conditions, the modified BP's photocurrent density remained constant at approximately 50 nA cm^{-2}. This impressive stability of the flexible photodetector was credited to the exceptional photostability and ambient of the BP/PIL materials. When this material was exposed to ambient conditions for 100 days, its crystalline nature remained unchanged, showcasing the excellent environmental stability conferred by PIL modification.

3.4. Hydrophilicity and biocompatibility

Skin bioelectronics and biosensor devices are known for their direct interaction with human skin, necessitating careful consideration of biocompatibility, especially for prolonged usage. Extensive work has focused on creating biocompatible active materials and encapsulating layers. This effort has resulted in various biocompatible skin bioelectronics, from sensors and energy devices to integrated circuits [9]. The toxicity of 2D materials stems from variations in synthesis and post-processing steps, altering material composition and degradation characteristics, which can significantly impact the nano-bio interface. Factors like exfoliation and lateral dimensions also influence their toxicity. Notably, for certain materials like TMDs, particularly MoS_2 and BP, higher exfoliation states correlate with increased toxicity due to active edge sites and expanded surface area. Thinner and smaller 2D nanomaterials exhibit excellent toxicity responses due to their enhanced effective surface area. Additionally, material characteristics such as crystal structure, surface functionality, chemical changes, and structural form play roles in toxicity. However, the lack of comprehensive material characterization and toxicological studies hinders a precise assessment of the hazard potential of 2D nanomaterials. To address this concern, biocompatible polymers have emerged as a popular approach to enhance the biocompatibility and stability of inherently toxic 2D materials such as MoS_2 and graphene [68]. Hydrophilicity, linked to biocompatibility, tends to be higher with better biocompatibility. For example, the hydrophobic nature of graphene surfaces can lead to strong interactions with biomolecules, potentially causing pore clogging. While surface modifications like oxidation and coating are possible, they may impact membrane integrity or alter pore size, affecting biosensors' signal-to-noise ratio (S/N) [69]. Hence, researchers are exploring 2D materials with more hydrophilic surfaces for nano-biosensor development.

The biocompatibility and hydrophilicity of graphene (GR) are enhanced by covalently attaching hydrophilic chitosan (CS) biopolymer while maintaining its electronic performance [70]. CS showcases remarkable traits such as superior film-forming capacity, biocompatibility, strong adhesion, non-toxicity, and potential for chemical alterations due to its abundant amino and hydroxyl groups. Leveraging these distinctive characteristics, it is logical to anticipate enhancements in the hydrophilicity and biocompatibility of GR through CS-functionalization via covalent grafting methods. It was observed that the successful grafting of CS onto GR without structural damage allowed for dense Pd NP decoration onto CS-GR sheets through in situ reduction. The resulting electrode modified by Pd NPs/CS-GR exhibited outstanding electrocatalytic activity for glucose oxidase (GOD) and H_2O_2 oxidation, holding promise for various oxidase-based bioelectronics and biosensors. However, the study primarily focused on biosensor performance under controlled laboratory conditions. Further validation in real-world scenarios, including complex sample matrices and interference studies, would be essential to assess its practical utility and reliability in clinical or industrial settings. An eco-friendly method to create PSGO-PEDOT nanosheets has been developed for their applications in bioelectronics and biomaterials [71]. PSGO-PEDOT nanosheets were made using a functional GO template for this purpose. GO underwent two sequential functionalization steps. First, sulfonate groups were added to the GO surfaces to produce sulfonated GO (SGO), providing doping sites for PEDOT. In the next step, catechol groups were introduced onto SGO, resulting in PSGO through PDA functionalization. This process enhanced interactions between PEDOT and PSGO. Furthermore, PDA also reduced PSGO, thereby increasing its conductivity. Consequently, PEDOT

assembled on the PSGO template to form conductive sandwich-like nanosheets with abundant hydrophilic and reductive catechol groups, leading to good water dispersibility and redox activity. These nanosheets then created physical crosslinks dispersed uniformly within a chemically crosslinked polyacrylamide (PAM) hydrogel network. This combined physical and chemical crosslinking imparted toughness and stretchability to the hydrogel, thanks to the synergistic effects. This hydrogel also displayed notable biocompatibility in vitro and in vivo for 14 days, presenting great promise for highly sensitive biosensor applications (Fig. 3A–D). Since the study demonstrated promising results in vitro and in vivo, further validation in diverse physiological conditions and long-term biocompatibility studies are essential to assess its suitability for clinical applications.

In another study, a covalent biofunctionalization strategy using PDA as a nano-bio interface was introduced to enhance the stability and performance of MoS_2 nanosheets for intracellular biosensing [72]. Monolayer MoS_2 nanosheets were prepared via an ultrasonication-assisted lithium intercalation approach, followed by PDA coating to form MoS_2@PDA nanosheets (MP NSs). Thiol-terminated polyethylene glycol (PEG-SH) was then conjugated to MP NSs to form MoS_2@PDA-PEG (MPP) NSs. Subsequently, fluorescein-labeled substrate peptide (P1) and cell-penetrating peptide (P2) were covalently conjugated to MPP NSs, forming MoS_2@PDA--PEG-Peptide (MPPP) biosensors via Michael addition reactions. The MPPP biosensor demonstrated efficient caspase-3 detection, with a linear response of 2–360 ng/mL and a LOD of 0.33 ng/mL. The cytotoxicity of the biosensor was assessed on human cervix carcinoma (HeLa) cells using a lactate dehydrogenase (LDH) assay after 24 h of exposure. Results showed cell viability exceeding 95 % across 4–128 μg/mL concentrations, confirming good biocompatibility. Future studies may focus on in vivo applications and further optimizations for enhanced sensitivity and multiplexed detection capabilities.

4. Functionalized pioneering 2D materials in biosensors and bioelectronics

After the remarkable success of graphene, various newly arisen 2D materials, including g-C_3N_4, TMDCs, MOFs, BP, and MXene NSs, have captured considerable attention in materials science and bioelectronics. Due to their exceptional physicochemical properties, these materials, including the graphene family, can be effectively functionalized with polymers to achieve impressive qualities such as outstanding flexibility, adjustable electrical conductivity, diverse functionalities, stability, and high biocompatibility. Table 1 shows a detailed overview of each class, with a comprehensive discussion in the following sections.

4.1. 2D graphitic carbon nitrides

A non-metallic semiconductor, g-C_3N_4 in sheet form, shares similarities with graphite [73–75]. It has garnered significant attention due to its easy synthesis from C- and N-rich precursors like melamine in aqueous media [76,77] (Fig. 4A). Compared to their bulk counterparts, 2D g-C_3N_4 nanostructures offer enhanced attributes, including improved biocompatibility, adjustable bandgap, enhanced electrical conductivity, greater surface area, reduced electron-hole pair recombination rate, and superior optical absorption with high quantum yield [76,78]. These semiconductor properties, such as electrochemiluminescence (ECL), photo-electrochemistry, and photoluminescence (PL), along with their electron-donating capability, make g-C_3N_4 a promising nanoplatform for diverse applications, including hydrogen production, biosensing,

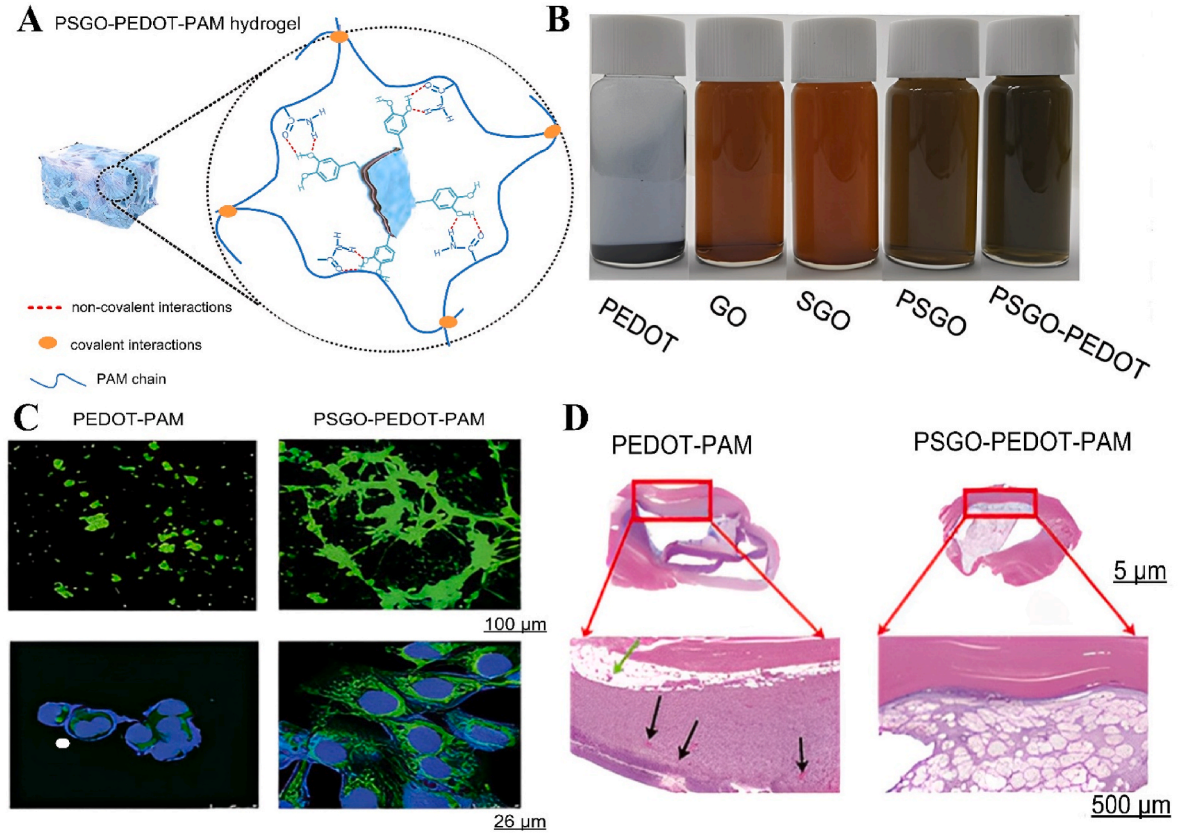

Fig. 3. A) Non-covalent interactions in PSGO-PEDOT-PAM hydrogel. **B)** Various nanosheet dispersibility after 24h in water. **C)** In vitro biocompatibility of PEDOTPAM and PSGO-PEDOT-PAM hydrogels, with cell morphologies (up) and focal adhesion staining (down). **D)** Histologic images of hydrogel implanted in rabbit muscle after 14 days, indicating inflammation (black arrow) and edema (green arrow). Reproduced from Ref. [71]. with permission from *Wiley*. (For interpretation of the references to colour in this figure legend, the reader is referred to the Web version of this article.)

Table 1
Polymer-functionalized 2D materials in biosensor design: Overview of physiochemical interaction between polymers and 2D materials, analytical performance, advantages, and challenges.

Biosensor designs	Interactions	Analytes	Linear range	LOD	Advantages	Challenges	References
2D Graphitic carbon nitride							
DexP- g-C_3N_4	π–π stacking	Con A	500–100 ng/mL	17 pg/Ml	Excellent ECL behavior, large surface area, biocompatibility, specificity, long-term storage stability (up to 15 days)	Experimental conditions optimization, low sensitivity	[93]
C-g–C_3N_4–PEI	Covalent bonding	OPs	0.001–5000 nM	0.3 pM	Simple and sensitive analysis	Low luminous efficiency and stability, AChE immobilization	[94]
g-C_3N_4/chitosan	Electrostatic attraction	Hg^{+2}	1.00 − 80.0, 0.1 − 5 μmol L^{-1}	0.01 μmol L^{-1}	Improved mechanical, electrochemical activity, electron transfer, selective, and sensitivity	Limited linear range	[230]
2D Graphene family							
hemin/RGO-CMF	–	H_2O_2	0.06–540.6 μM	~16 nM	Cost-effective, eco-friendly, high electro-reduction ability, superior selectivity, sensitivity (0.51 μAμA^{-1} cm^{-2}) at S/N = 3, rapid response (4 s)	Hemin stabilization, experimental conditions optimization	[231]
Graphene-PANI	–	HPV type 16 DNA	10–200 nM	2.3 nM	Cost-effective, high selectivity, reproducible inkjet printing, scalable mass production, enhanced electroactive surface area	Excess Agglomeration of G-PANI layers, complicated and time-consuming covalent probe immobilization	[232]
ChOx/PEI-rGO	Electrostatic attractions	Cholesterol	0.10×10^{-6} – 9.331×10^{-3} mol L^{-1}	0.021 μmol L^{-1}	Excellent dispersion of PEI-r GO in water, biocompatible, increased enzyme immobilization, direct electron transfer, anti-interference ability, stability (99 % over 50 cyclic scans)	Optimization of fabrication conditions, electrode stability	[233]
Graphene-Nafion	Physical adsorption	HIV-1	1×10^{-13} – 1×10^{-10} M	2.3×10^{-14} M	Simple method, label-free, high sensitivity, specific surface area	Limited LOD detection	[114]
PANI/graphene	Electrostatic attraction	HIV-1	5.0×10^{-16} – 1.0×10^{-10}	1.0×10^{-16} M	High sensitivity, electrical conductivity, selectivity, and stability	DNA immobilization, specificity, sensitivity optimization	[111]
rGO/PEI	Electrostatic attraction	E. coli	1.0×10^{1}–1.0×10^{4} cfu mL^{-1}	~10 cfu mL^{-1}	Sensitive and selective detection in aqueous and serum samples	Adaptability, specificity optimization, matrix variability in real samples	[118]
2D MXenes nanostructure							
TiO_2(G) NW@EPNS/Cyt C	–	NO_2^-	0.5–9000 mM	0.225 mM	Enhanced photocatalytic oxidation, electron transfer, sensitivity (201.79 μA $μM^{-1}$ cm^{-2}), selectivity, reproducibility, biocompatibility, and reusability	Cyt C stability in TiO_2(G) NW@EPNS matrix, optimization of detection conditions, EPNS stability	[117]
PPy@$Ti_3C_2T_x$/PMo_{12}	–	OPN biomarker	500–10 ng/mL	0.98 fg mL^{-1}	Strong binding ability towards RNA aptamer, high sensitivity, selectivity, stability, and reusability	Hindered electron transfer, complex fabrication procedure	[136]
GOx/Au/Ti_3C_2/Nafion/GCE	–	Glucose	0.1 mM–18 mM	5.9 μM	Improved electron transfer kinetics, selectivity, sensitivity (4.2 μAmM−1cm−2) at S/N = 3, and storage stability	Uniform and stable film coating on GCE	[133]
CIPs/AuNPs/$Ti_3C_2T_x$/GCE	–	Yeast cells	1×10^{2}–1×10^{9} cells per mL	20 cells per mL	Enhanced electron transfer rate, surface area, sensitivity, selectivity, reproducibility, and repeatability (up to 7 times)	Dependent electron transfer rate on polymer thickness, optimization of illumination time, and monomer to cross-linker ratio	[234]
AuNPs/MXene@PAMAM	Covalent bonding	cTnT	0.1–0.001 ng/mL	0.069 ng/mL	Enhanced loading capacity, conductivity, sensitivity, stability, large specific surface areas, in vitro biocompatibility	Irreversible oxidation of MXene under anodic potentials, limited LOD	[235]
2D Black phosphorous							
Ca^{2+}-doped BP@PDA	–	Protein, DNA	P: 0.1–25 nM, D: 1.0–10 nM	P: 0.02 nM, D: 0.52 nM	Resistance to non-specific displacement by other biological ligands, simple preparation, highly stable, and biocompatible	Short biostability, selectivity, and sensitivity in complex bio-samples	[236]
CuNPs-Chit-BP	Electrostatic attraction	H_2O_2	10 μM–10.3 mM	0.390 μM	Enhanced BP dispersion, increased surface area, electro-catalytic activity, and selectivity	Partial oxidation of BP over time	[237]
Poly-L-lysine-BP	Non-covalent electrostatic attraction	H_2O_2	10 μM–700 μM	–	High direct electron transfer and electrocatalytic activity	Careful synthesis control process to maintain the native structure and activity of Hb	[159]
BP/polyallylamine	Electrostatic attraction	Interleukin-6	0.003–75 ng/mL	1 pg/mL	Economical fabrication, enhanced stability, charge transfer rate, binding sites, and selectivity	Optimization of PAMI ratios for stable BP encapsulation	[160]

(*continued on next page*)

Table 1 (*continued*)

Biosensor designs	Interactions	Analytes	Linear range	LOD	Advantages	Challenges	References
Poly-L-lysine/BP-TFG	Electrostatic attractions	NSE	0.01–100 ng/mL	1 pg/mL^{-1}	Label-free, ultrahigh sensitivity, specificity, real-time monitoring	Efficient layer-by-layer (LbL) technique, BP stable and uniform coating on fiber surface	[161]
Polyethyleneimine-BP	Electrostatic adsorption	Cu^{2+}	0.25–177 μM	0.02 μM	Excellent electrochemical reduction, surface area, mechanical stability, flexibility, sensitivity (0.05–0.1 μA μM^{-1} cm^{-2}) and selectivity, rapid response (1.5 s)	Short-term stability, optimization of PEI to BP ratio	[238]
2D Transition metal dichalcogenides							
WS_2/B-PVA	–	HbA1c	3.3 × 10^{-8} M	–	Specific recognition of HbA1c achieved through reversible bonds with boronic acid moiety	Challenging exfoliation and functionalization of WS_2 NSs in water	[171]
MoS_2/WS_2@PDA	Electron transfer	5 fC-DNA	0.005–200 nM	3.7 pM	Improved photoactivity, sensitivity, selectivity, and specificity, applicable for RNA formylation detection	Steric-hindrance effects and electrostatic repulsion caused by 5 fC-DNA	[172]
SPAN-MoS_2	π–π* interaction	CAP	0.1–1000 μmol L^{-1}	0.65 × 10^{-8} mol L^{-1}	Enhanced electrocatalytic activity, reproducibility, long-term stability, and sensitivity	Optimization of mass ratio and ultrasonication time, pH sensitivity, alkaline interference	[239]
PANI-MoS_2	Electrostatic attraction	DNA	1.0 × 10^{-15} – 1.0 × 10^{-6}	2.0 × 10^{-16}	High electrochemical activity, efficient DNA immobilization, and hybridization	Optimization of MoS_2 dosage and reaction time	[240]
pDNA/PANI-MoS_2/ITO	Electrostatic attraction	CML	10^{-6} M – 10^{-17} M	3 × 10^{-18} M	Large electroactive surface area, improved electron transfer, catalytic activity and conductivity, uniform growth of nanocomposite, high stability (up to 42 days)	Template removal, optimization of experimental conditions, specific detection	[241]
PIn6COOH/WS_2	Physical adsorption	DNA	1 × 10^{-17} – 0.1 × 10^{-12} mol L^{-1}	0.23 × 10^{-19} mol L^{-1}	Label-free, large specific surface area, high stability (up to 10 days), and selectivity.	Steric hindrance from ssDNA probe, specificity	[242]
WS_2-PEDOT/GO-SWCNTs/GCE	–	VB_2	0.002–0.9 μM	0.7 nM	Improved response and electron transfer, specificity via imprinting, good anti-interference ability, and storage stability	Optimization of thickness, molar ratios, pH, and incubation time	[243]
2D Metal-organic frameworks							
Co–Ni (Fe)-MOF/PPy	-	Glucose	0.002–3.0 mM	1.13 μM	Superior electrochemical activity, sensitivity (1805 μA mM^{-1} cm^{-2}), and selectivity	Low reproducibility and stability	[191]
MIP/Au@PANI/SeS_2@Co MOF	-	PT	0.001–100 nM	0.66pM	Higher electrocatalytic activity, improved surface area, active sites, and sensitivity.	Electrochemical signal stability, steric hindrance due to PT imprinting	[244]
PFO- H_2*dtoa*Cu	Adsorption	MMP-2	0.1–2.5 pg/mL	–	High specificity and selectivity, PFO dots as ultrasensitive luminophore, good stability	Optimization of reaction conditions	[245]
ZIF-L/PEDOT	Electrostatic attraction	DA	25 nM – to 500 μM	7 nM	High conductivity, catalytic activity, and sensitivity (381.3 μA mM^{-1} cm^{-2}) at S/N = 3, long-term storage stability (up to 28 days)	Detachment of ZIF-L/PEDOT particles from electrode surface over time	[192]
Ab/$Cu_3(BTC)_2$-PANI/ITO	–	*E. coli*	2–2 × 10^8 cfu/mL	2.0 cfu mL^{-1}	Quick response (2 min), large surface area, high stability (up to 60 days), and selectivity	Biosensor stability during fabrication and use, specificity in complex sample matrices	[246]

EDC: 1-ethyl-3-(3-dimethylaminopropyl) carbodiimide; NHS: N-hydroxy succinimide; CMF: Cellulose microfiber; ChOx: Cholesterol oxidase; EPNS: Electroconductive polymer nanosponge; GCE: Glassy carbon electrode; CIPs: Cell imprinted polymers; PAMAM: Poly(amidoamine); cTnT: Human cardiac troponin T; PDA: polydopamine; HbA1c: Glycated hemoglobin; SPAN: self-doped polyaniline; CAP: Chloramphenicol; ITO: Indium tin oxide; CML: Chronic myelogenous leukemia; VB_2: vitamin B_2; PT: Patulin; PIn6COOH: Poly(indole-6-carboxylic acid); PFO: Poly(9,9-dioctylfluorenyl-2,7-diyl).

bioimaging, photocatalysis, and more [79–81]. Furthermore, due to these characteristics, ultrathin 2D g-C_3N_4 materials have demonstrated minimal cytotoxicity and strong tissue compatibility, suggesting their suitability for applications in bioelectronics and biosensors [60,82]. They have effectively detected various substances, such as antibiotics, harmful metal ions, organic molecules, enzymes, nucleic acids, and chemical substances, leveraging their diverse electronic and semiconductor features [83].

Despite its potential, g-C_3N_4 suffers from some limitations, like low conductivity [84], structural disorder [85], poor dispersibility [86], and limited processability [87]. Natural ligands like –N/–NH/–COOH and –NH_2 present on carboxyl-g-C_3N_4 exhibit strong chelate bonding capabilities with metal complexes or can be linked to biomolecules using carbodiimide coupling chemistry [88]. This process entails chemical modifications like oxidation/reduction, amidation, and polymer grafting, improving stability at the expense of introducing defects in the material's sp^2 framework that can impact electrical properties but can be advantageous in applications like catalysis and composites when the defect density is carefully controlled [85]. One promising approach to enhancing g-C_3N_4 properties involves combining it with polymers via non-covalent and covalent modifications, offering unique functionalities such as biodegradability, stimulus responsiveness, self-healing, and electrical conductivity [89]. Combining traditional polymers with innovative metal-free sheets like g-C_3N_4 holds significant potential. This fusion harnesses the strength of both material classes. g-C_3N_4 contributes to improved photocatalytic and photoluminescent properties and

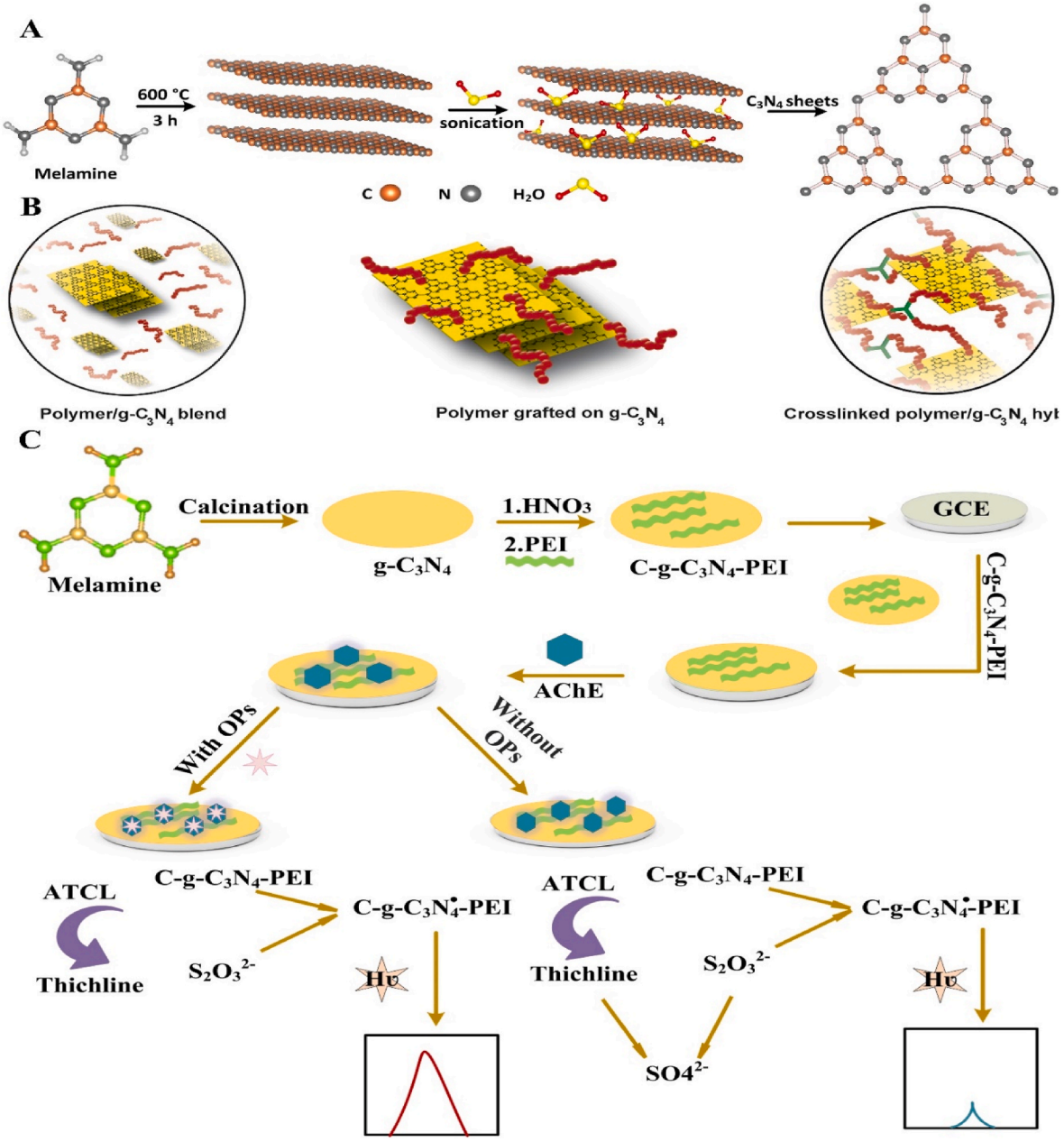

Fig. 4. A) Synthesis and structure of C_3N_4 (g-C_3N_4) sheets. Reproduced from Ref. [77]. with permission from *American Chemical Society*. **B)** Methods for g-C_3N_4/polymer modification: techniques involving the incorporation of g-C_3N_4 into polymers through blending, grafting, and grafting/crosslinking processes. Reproduced from Ref. [87]. with permission from *Royal Society of Chemistry*. **C)** Illustrative depiction of the synthesis procedure for C-g–C_3N_4–PEI and the construction of modified biosensor, including insights into the response mechanism. Reproduced from Ref. [94]. with permission from *Elsevier*.

improves mechanical and physical characteristics, whereas polymers enhance processability and conductivity [90]. Various techniques can be employed to create g-C_3N_4/polymer composite materials [87], including (i) "physical absorption or deposition" (typically in a liquid phase), (ii) the "grafting from" method involving polymerization from g-C_3N_4 surface, and (iii) the "grafting to" process that relies on chemical bonding between active polymer end groups and reactive sites on g-C_3N_4 (Fig. 4B).

ECL, also known as electrogenerated chemiluminescence, is a widely employed method for generating light from ECL emitters that are excited electrochemically through efficient electron transfer. ECL has gained prominence in biosensing due to its rapid response, high sensitivity, simplified setup, broad detection range, flexibility, cost-effectiveness, and compatibility with miniaturized instrumentation [91]. Since the revelation of g-C_3N_4 nanosheets' cathodic ECL characteristics, they have become a focal point for ECL biosensors. While g-C_3N_4 has its advantages, researchers are exploring the integration of polymers to enhance the sensitivity and specificity of ECL sensors [87,92]. A signal-on ECL biosensor was fabricated by combining BSA and phenoxy dextran (DexP) with g-C_3N_4 for detecting concanavalin A [93]. The dexP-g-C_3N_4 nanocomposite was bound to Con A binding sites via a specific carbohydrate-Con A interaction, forming a sandwiched structure with GOx and Con A during electrode fabrication. Increased Con A concentration led to more DexP-g-C_3N_4 binding, enhancing the ECL signal for quantitative Con A detection. DexP- g-C_3N_4 was an ECL signal probe and facilitated specific Con A binding, enabling a novel sandwich-like ECL detection strategy. The biosensor showed remarkable sensitivity (LOD of 17 pg/mL for Con A) and a broad linear detection range (0.05–100 ng/mL), with stable performance over successive scans (RSD of 2.2 % for ten cycles), long-term storage (maintaining 91.5 % of the initial

response after 15 days), and reproducibility (RSD of 5.7 %). Additionally, it demonstrated practicality for detecting Con A in real biological samples, with recoveries ranging from 94.2 to 104 %. The critical contribution of this work was preparing the DexP- g-C_3N_4 hybrid and its application in constructing a signal-on sandwiched ECL biosensor. Although the biosensor had a longer preparation time, combining 3D-GR-AuNPs nanocomposites and GOx in advance can shorten the total assay time by avoiding prolonged GOx incubation on the electrode. In a different investigation, Wang and colleagues developed an ECL biosensor using a hybrid material, denoted as C-g–C_3N_4–PEI, along with acetylcholinesterase (AChE) for susceptible detection of organophosphate pesticides (OPs) [94]. This nanocomposite was synthesized by establishing a covalent amide connection between the amino unit of polyethyleneimine (PEI) and the carboxylic group of carboxylated-g-C_3N_4 using EDC/NHS coupling. In the absence of OPs, AChE catalyzed the hydrolysis of ATCl to produce thiocholine, consuming $S_2O_8^{2-}$ co-reactant and decreasing the ECL signal. In the presence of OPs, inhibition of AChE by OPs hindered thiocholine generation, leading to increased ECL response (as shown in Fig. 4C). The resulting functionalized biosensor for detecting OPs achieved an impressive LOD of 0.3 pM. Still, it was limited to standard OP solutions under optimal conditions, necessitating adaptation for real-life samples. Recovery experiments showed 97.4–102 % recoveries, affirming the biosensor's potential for sample analysis, while stability and reproducibility tests revealed an R.S.D. of 0.32 % and 2.36 %, respectively, indicating excellent stability and acceptable reproducibility.

The limited ability to disperse in organic and aqueous environments of pure g-C_3N_4 is one of the main challenges in utilizing it for practical applications, as solid van der Waal (π–π stacking) interactions cause accumulation [95]. However, there are two methods to enhance its dispersibility in the aqueous phase. One approach involves adding charged groups to promote stability through electrostatic repulsion in aqueous environments. Another method is to attach hydrophilic polymers, which use steric repulsion to stabilize g-C_3N_4 dispersion in water. As polymers have been the preferred choice for enhancing dispersibility, various methods exist for incorporating polymers. One straightforward approach to achieving dispersible g-C_3N_4 involved initiating polymerization using g-C_3N_4 through photoinitiation [96]. This involved adding *N*, *N*-dimethylacrylamide (DMA) to a dispersion of g-C_3N_4 in ethylene glycol/water and exposing it to visible light. This process led to the development of a gel with a loose structure, characterized by high viscosity and composed of PDMA-grafted g-C_3N_4, making it readily dispersible in water. In addition, these dispersions demonstrated excellent stability, lasting up to two months, thanks to the steric stabilization of g-C_3N_4 colloids. Furthermore, pH-responsive solubility can be achieved by using allylamine, resulting in solubility in acidic solutions and precipitation in alkaline conditions. A recent development involved grafting allylamine to g-C_3N_4 [97], notably enhancing its dispersion at an acidic pH of 4 through amino group protonation. Conversely, raising the pH to 9 resulted in rapid particle precipitation due to amino group deprotonation. Re-acidifying the solution restored uniform dispersion, indicating reversibility. In biosensor applications, the improved sensitivity and selectivity provided by polymer-functionalized g-C_3N_4 can be credited to improved dispersion and better accessibility to the sensing site.

Despite polymers offering new possibilities for g-C_3N_4 usage, there are still notable challenges to address. Limitations arise from the dependence on physical blending methods and employing environmentally unfriendly organic solvents in synthesis processes. To pave the way for large-scale production, future research should emphasize solvent-free and eco-friendly approaches [87]. Additionally, a comprehensive understanding of the electronic and lattice systems of polymer/g-C_3N_4 composites is crucial for unraveling their sensor mechanisms. Despite initial hurdles, advancements in polymer compatibility and dispersibility with g-C_3N_4 have been observed, marked by favourable interactions such as hydrogen bonding and π–π interactions. Overall, g-C_3N_4 holds promise as an affordable and sustainable semiconductor. With careful adjustments to its properties and polymer design, it could significantly impact academia and various industries, particularly bioelectronic devices.

4.2. 2D graphene family

Since the groundbreaking isolation of high-quality graphene, this single-atom-thick layer of sp^2 hybridized C atoms has been spotlighted as the most extensively studied 2D material in material science [98,99] (Fig. 5A). 2D graphene, with its hexagonal patterns, boasts exceptional properties, including outstanding electrical conductivity, a high specific surface area, robust mechanical strength, rapid electron mobility, and ambipolar transfer abilities [100–102]. These distinctive features make graphene suitable for diverse applications, including bioelectronic devices and biosensors [103]. Moreover, its chemical surface modification has led to the creation of reduced graphene oxide (rGO) and graphene oxide (GO) as cutting-edge innovative materials [104]. Being hydrophilic, GO possesses numerous oxygenated functional groups like –OH, –C═O, and –COOH, enabling it to capture water molecules from the surroundings, making it an ideal biosensing nanomaterial due to its affinity towards aromatic rings and hydrophobic bio-molecules, good water dispersibility, and fluorescence properties [105,106].

Oxygenated groups on both the basal and edge planes of rGO create defect sites, enhancing its electrocatalytic activity more than graphene. This increased activity is observed towards various electroactive species, including H_2O_2, glucose, etc. [107]. Hence, graphene and its derivatives have made strides in applications like biosensors and bioelectronics due to their exceptional properties like high absorptivity, superior conductivity, and stability, making them excellent materials for electrodes with swift carrier mobility [108,109]. For instance, a biosensor was innovatively crafted using GO as an efficient fluorescent marker and Au NPs as a fluorescence quencher for detecting DNA-DNA interactions. This study highlighted the potential of large-scale, cost-effective GO nanomaterials in various bio-applications, such as biosensors and molecular imaging [110]. However, the LOD of approximately 0.1 pmol of target DNA limits its applicability in scenarios requiring detection at lower concentrations. Moreover, the experimental conditions and protocols do not fully reflect real-world complexities, potentially affecting the biosensor's performance in practical applications.

Hence, in spite of their outstanding physiochemical and biological advantages, that regard them as ideal materials for developing biosensors, graphene-based nanomaterials suffer from some limitations. This includes aggregation due to weak van der Waals attractions, limited biorecognition capabilities, and varying levels of biotoxicity, particularly in the case of GO, where the extent of toxicity is contingent on concentration and exposure time [43,111,112]. To address these issues, enhancing graphene and its derivatives through biological or chemical functionalization is crucial to improving recognition and biocompatibility. This improvement is possible because functional moieties, as seen in rGO and GO, permit surface functionalization with appropriate components, facilitating the attachment of biomolecules, metal oxides, and polymers to enhance biosensors' performance [6].

Various strategies, categorized as non-covalent and covalent functionalization, are employed to functionalize graphene nanomaterials with substances like polymers. These strategies resemble those used for other 2D materials [43,113]. In the non-covalent method, negative rGO/GO (carry negative charges due to their oxygenated groups) or functionalizing polymers like PEI, PEG, chitosan, PANI, etc., can positively charge-neutral graphene, facilitating electrostatic cross-linking with biomolecules carrying a negative charge, For instance, a susceptible DNA sensor for detecting the HIV-1 gene was created using a GCE modified by graphene-Nafion nanocomposite film through π–π* stacking interactions [114]. The biosensor operated by adsorbing ssDNA onto the modified surface of a GCE, which then interacted with the target DNA to form dsDNA. This interaction induced changes in electron transfer

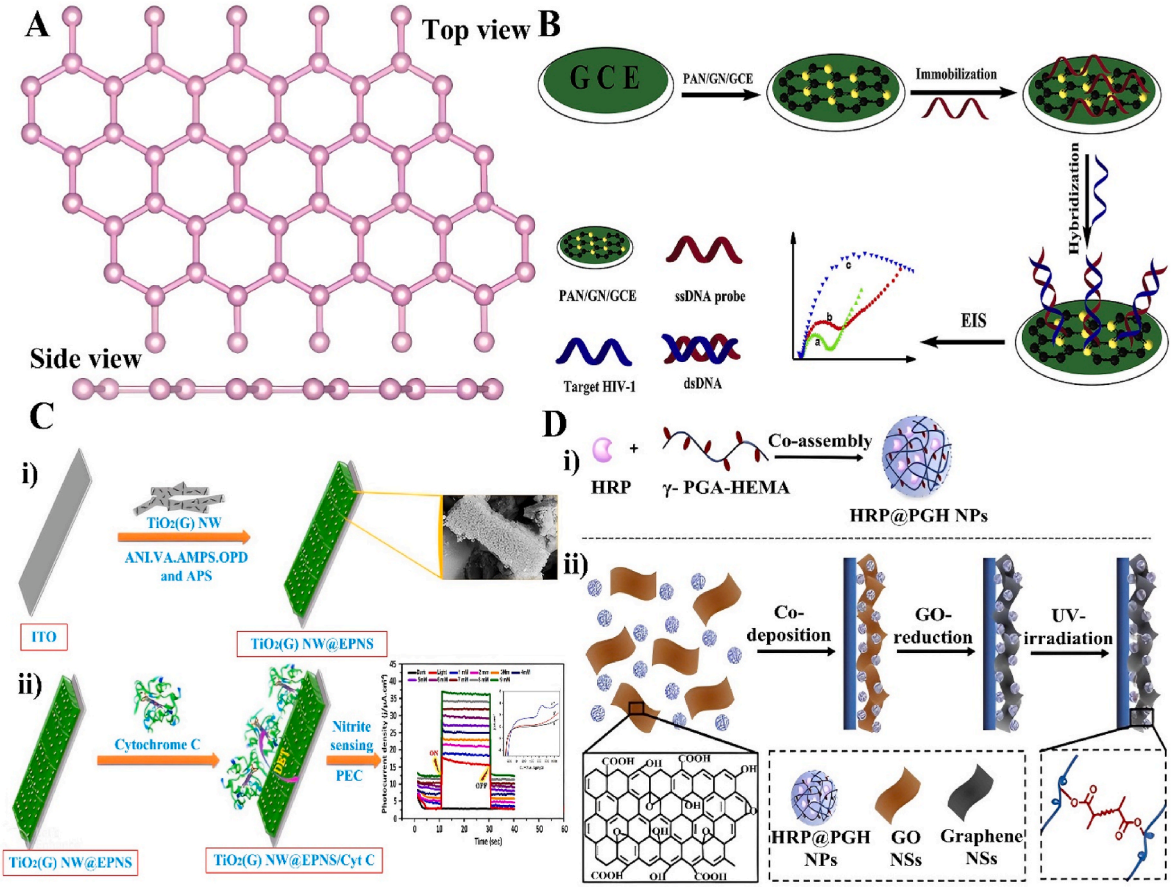

Fig. 5. A) Structure of 2D graphene (top and side view). **B)** Illustration of the detection process for the HIV-1 gene, accompanied by the sequential synthesis steps and the performance evaluation of the DNA sensor. Reprinted from Ref. [111]. with permission from *Elsevier*. **C) i)** Synthesis of EPNS coated with TiO_2(G). **ii)** Immobilization of Cyt C to create a biosensor using TiO_2(G) NW@EPNS, followed by photoamperometric biosensing. Reproduced from Ref. [117]. with permission from *Elsevier*. **D)** Schematic representation of enzymatic biosensor, **i)** Formation of enzyme-polymer nanoparticles (HRP@PGH NPs) through the co-assembly of HRP and γ-PGA-HEMA. **ii)** Construction of integrated HRP@PGH/GNS sensing film by electrophoretic co-deposition of 0D HRP@PGH NPs and 2D GO NSs. Reproduced from Ref. [120]. with permission from *Elsevier*.

resistance, allowing for the detection of the HIV-1 gene. Notably, Nafion stabilized graphene and enhanced its dispersion, enabling sensitive detection of a target gene over a wide concentration range with a LOD of 0.23×10^{-15} M. The biosensor also exhibited good selectivity, stability, and reproducibility, making it a promising tool for HIV-1 gene detection. However, further discussion on biosensor specificity in actual samples, particularly in distinguishing between complementary and mismatched DNA sequences, would strengthen the evaluation of its performance.

Considering the robust stability associated with covalent bonding, methods involving covalent modification play a key role in functionalizing graphene-based nanomaterials with polymers [115]. Oxygenated functional moieties like hydroxyl and carboxyl groups on rGO and GO surfaces provide optimal platforms for immobilizing polymers/biopolymers with multiple functional groups [108]. The –COOH moieties in GO and rGO are particularly advantageous for achieving higher biomolecule loading through robust amide bond formation with aminated groups present in polymers like PEI, PANI, and biopolymers such as proteins, enzymes, antibodies, and peptides, assisted by EDC and NHS interactions [116]. In 2019, Xiang and coworkers addressed the agglomeration issue of graphene materials by developing a novel DNA sensor using ssDNA/PANI/graphene nanocomposites through reverse-phase polymerization [111]. This biosensor was designed for detecting HIV-1 and featured a covalently immobilized ssDNA probe on a PAN/GN/GCE (Fig. 5B). Results indicated that PANI introduction not only improved graphene dispersion in N, N-dimethylformamide (DMF) but also enhanced the stability and conductivity of the modified electrode for HIV-1. The DNA biosensor demonstrated high sensitivity to HIV-1 gene concentrations (5.0×10^{-16} M to 1.0×10^{-10} M) with an LOD of 1.0×10^{-16} M (S/N = 3), attributed to graphene and PAN synergy. In addition, it exhibited selective hybridization with complementary DNA sequences, showing stable reproducibility (standard deviation of 4.7 %) and storage stability for two weeks at 2 °C. The study suggests its clinical utility for HIV-1 diagnosis. But it overlooks key practical challenges like sample handling, assay time, and cost-effectiveness, which are pivotal for real-world deployment.

An innovative PEC biosensing platform was created to improve the biocompatibility and photoactivity of 2D graphene. The electroconductive polymer nanosponge (EPNS), containing graphene (G) and TiO_2 nanowires (NW) with cytochrome C (Cyt C) immobilization, served as the foundation for constructing a highly selective and sensitive PEC biosensor for detecting NO_2^- [117]. The proposed biosensing mechanism involved light-induced electron transfer from TiO_2 to G that facilitated the transformation of heme-Fe (III) to heme-Fe (II) in immobilized Cyt C, where NO interacted with heme-Fe (II) sites to form N_2O, elucidating the role of NO rather than NO_2 in heme-protein interactions. The biosensor enhanced performance at low bias potential (−0.11 V). It offered advantages such as sound sensitivity (201.79 μA μM^{-1} cm^{-2}), rapid response (~5s), a wide linear range from 0.5 to 9000 mM, stability, and selectivity for detecting NO_2^- in actual samples (Fig. 5C). The fabrication process involved multiple steps in this study, which may hinder scalability and reproducibility. Additionally, environmental factors like light intensity and pH can affect the sensitivity and reliability of PEC

biosensors. Moreover, graphene-based materials are employed to detect microorganisms. A gold electrode modified using thin active layers of rGO/PEI was developed through electrophoretic deposition (EPD) for detecting uropathogenic *E. coli* [118]. The electrochemical analysis showed improved redox current upon rGO/PEI electrode functionalization, suggesting enhanced electron transfer kinetics. However, the electrode's specificity towards *E. coli* UTI89 was limited, especially at lower concentrations, posing challenges for accurate detection, particularly in complex samples. Anti-fimbrial E. coli antibodies were immobilized on the electrodes using NHS/EDC coupling chemistry to improve specificity. The sensor exhibited a linear range from 10^1–10^4 cfu mL^{-1} and an LOD below 10 cfu mL^{-1} for UTI89 detection with a promising sensitivity. Notably, the biosensor also performed well in various media, including aqueous, urine, and serum, demonstrating its potential for diagnosing pathogenic viruses. However, exploring additional strategies, such as optimizing antibody immobilization density, may further enhance specificity.

The integration of polymers with graphene is also a keen area of study because it enhances the sensitivity of biosensors due to their unique structural and compositional sophistication [119]. A robust enzymatic biosensing platform was fabricated by depositing 0D enzyme-loaded biopolymeric NPs onto 2D GO NSs, which acted as conductive nano-supports (Fig. 5D). This platform demonstrated outstanding performance for H_2O_2 due to a synergistic effect from material design and the hierarchical 0D-2D nanostructure [120]. The photo-cross-linkable polypeptide γ-PGA-HEMA played a pivotal role in developing a biocompatible microenvironment and enhancing the bioactivity and structural stability of the HRP enzyme through photo-induced cross-linking. Concurrently, the conductive graphene NSs facilitated electron flow across the sensing interface, elevating sensitivity. The HRP@PGH/GNSS sensor demonstrated rapid H_2O_2 detection within 3s, with a linear range of 1.0–340 μM and a LOD of 0.27 μM, offering enhanced sensitivity and stability. It exhibited high anti-interference ability and excellent reproducibility, making it suitable for practical applications in biomedical fields with recoveries ranging from 96.80 % to 104.46 % in human serum samples. However, the study faces challenges in ensuring long-term stability and preventing enzyme leakage due to the complex synthesis process and potential interactions between components.

Although the potential of polymer-functionalized graphene for biosensors is promising, several hurdles persist. Challenges lie in effectively applying 2D graphene-based biosensors, especially for real sample analysis, which necessitates the creation of highly selective sensors that excel in complex conditions [58]. Moreover, non-covalent functionalization methods may lead to false positive signals due to the adsorption capacity of graphene for non-target substances. Conversely, covalent strategies, while effective, are complex and require precise control. Last but not least, ensuring the uniformity of these materials in terms of thickness, size, the number of surface functional moieties, and biocompatibility is a significant hurdle [43]. This uniformity not only impacts the efficiency of surface functionalization but also has a profound impact on the reproducibility and performance assessment of the developed biosensors. There is an optimistic anticipation that ongoing research efforts will overcome these issues, leading to a more sophisticated graphene biosensor system.

4.3. 2D MXenes nanostructures

MXenes represent an innovative class of 2D materials characterized by layered structures of metallic nitrides, carbides, or carbonitrides. The formation of MXenes involves selectively removing "A" layers from MAX phases with the general formula "$M_{n+1}AX_n$", where "M" signifies transitional metals like V, Ti, Mo, "A" signifies main-group elements from IIIA or IVA, "X" signifies carbonitrides, nitrogen, or carbon, and "n" represents the number of layers linked by van der Waals forces and does not exceed 3. MAX phases exhibit hexagonal layering, where X atoms occupy the octahedral positions within tightly packed M layers, with A atoms interspersed between neighbouring layers (Fig. 6A). During synthesis, "M" and "X" remain unchanged from their MAX predecessors. At the same time, "A" groups are introduced during the etching stage to signify terminated groups like chlorine (–Cl), fluorine (–F), hydroxyl (–OH), and oxygen (–O) [121,122], as illustrated in Fig. 6B. This process makes them hydrophilic, near-infrared (NIR) absorption capable, metallic conductive, size-adjustable, biocompatible, and opens up opportunities for surface modifications [42,123]. However, the etching process significantly impacts their suitability for biomedical purposes due to a lack of controlled drug release, instability in physiological environments, and the potential harm to healthy cells or tissues due to limited target specificity [42]. Even tiny illustrations of remnants of HF in biological devices can trigger cell death within living organisms [124].

To overcome these limitations, researchers have enhanced MXenes by introducing surface modifications. This process involves incorporating various materials such as polymers like PVP [125], polyvinyl alcohol (PVA) [126], cellulose [127], soybean phospholipid (SP) [128], PEG [129], or inorganic nanoparticles like mesoporous silica nanoparticles (MSNs) [130] and polyoxometalates (POMs) [131]. Biocompatible polymers are particularly favoured due to their non-toxic nature, compatibility with biological fluids, and the absence of a need for surgical removal after treatment [132]. Surface modifications using polymers like SP, PEG, PVA, PVP, and PLGA enhance the physical and chemical stability of MXenes and make them biocompatible. These modifications can be achieved through surface adsorption or electrostatic interactions [42]. Furthermore, MXenes can detect different analytes by altering their conductivity through charge transfer while attaching various molecules. This attachment makes MXenes highly adaptable for sensing applications with varying surface terminations. Rakhi and his colleagues developed an innovative biosensor called GOx/Au/Ti_3C_2/Nafion/GCE, designed for glucose detection [133]. In this system, the enzyme glucose oxidase (GOx) was crucial in reducing glucose to gluconolactone and H_2O_2. The high reduction/oxidation potential of H_2O_2 led to GOx immobilization on MXene/GCE for glucose sensing. Including Nafion, improved enzyme adhesion to GCE, elimination of interfering signals, and enhanced biosensor selectivity.

To maintain enzyme activity and promote direct electron transfer, gold nanoparticles (Au) were employed during adsorption, reducing insulating effects and increasing electrical conductivity between GOx and GCE. MXenes, with their expansive surface area, facilitated charge accumulation, thereby boosting sensor sensitivity and linearity. The GOx comprised one flavin adenine dinucleotide (FAD) molecule and two protein units, explaining the glucose-sensing mechanism (Eqs. (1)–(3)),

$$\mathrm{GOx\,(FAD) + Glucose \;\rightarrow\; GOx\,(FAD_2) + Glucono - d - lactone} \quad (1)$$

$$\mathrm{GOx\,(FADH2) + O2 \;\rightarrow\; GOx\,(FAD) = H2O2} \quad (2)$$

$$\mathrm{Glucose + O_2 \xrightarrow{GOx} Glucono - d - lactone + H_2O_2} \quad (3)$$

This MXene/GCE biosensor exhibited outstanding storage stability, a good sensitivity (4.2 μA $mM^{-1}cm^{-2}$), a wide detection range (0.1–18 mM), and a low LOD (5.9 μM). Yet, evaluating the biosensor's performance with real biological samples, such as blood or urine, would validate its practical utility and reliability in clinical or point-of-care testing (POCT). Recently, a cutting-edge biosensing patch designed for personal wearable bioelectronics was introduced. This advanced patch is constructed using a unique combination of materials, including MXene/fluoropolymer nanofiber-derived hierarchical porous TiO_2 and 3D fibrous carbon nanohybrid electrodes, which resulted in numerous active edges to facilitate efficient electron transmission, remarkable electrical conductivity (with a sheet resistance of 15.6 Ω sq^{-1}), and ample surface area for enzyme immobilization [134]. Three complementary effects contribute to these exceptional attributes: first, the

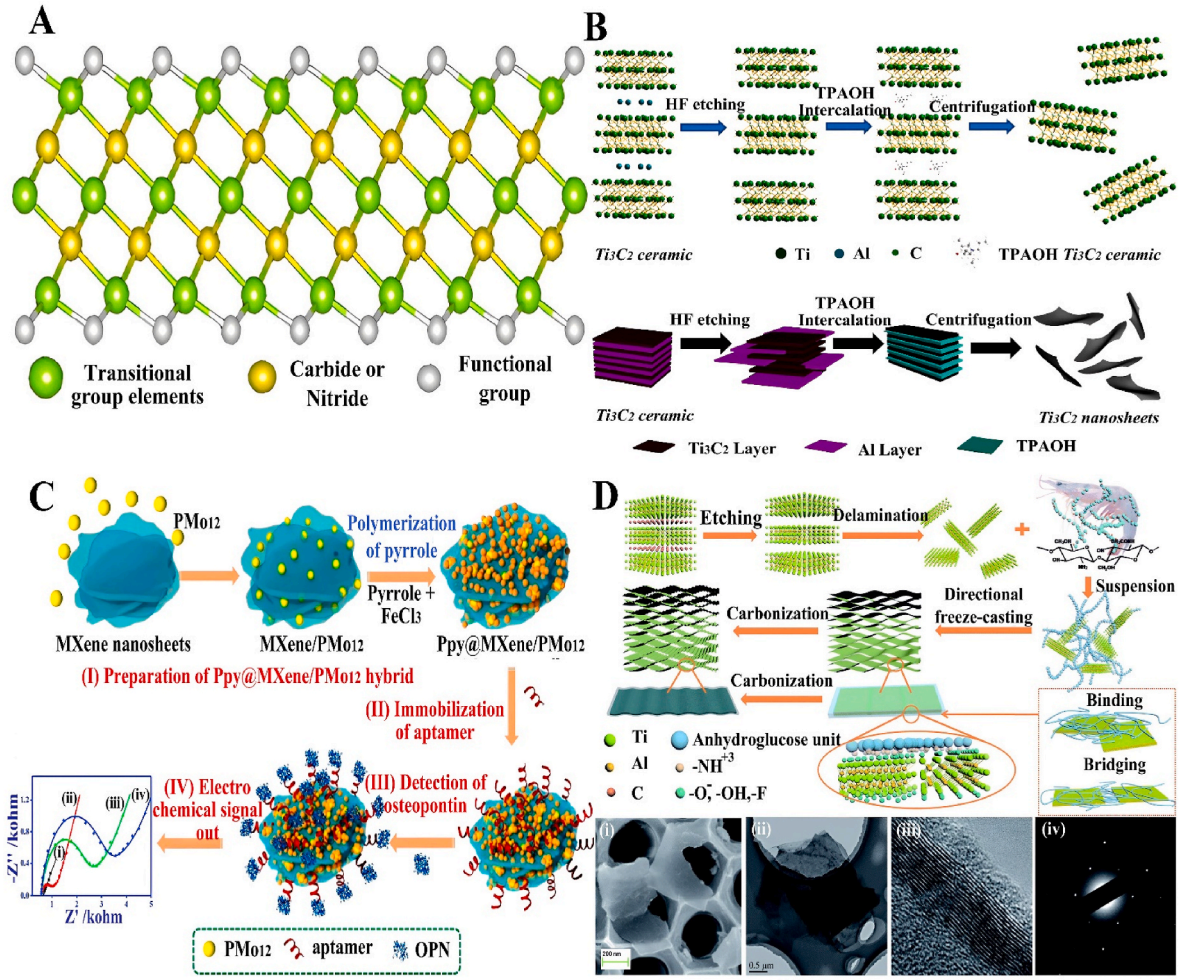

Fig. 6. A) Structure of 2D MXene. **B)** Diagram depicting the two-step exfoliation process for producing Ti_3C_2 nanosheets. Reproduced from Ref. [128]. with permission from *Wiley*. **C)** Schematic illustration detailing the assembly of the aptasensor for OPN detection via PPy@$Ti_3C_2T_x$/PMO_{12} hybrid. The process involves **i)** the synthesis of the PPy@$Ti_3C_2T_x$/PMo_{12} hybrid, **ii)** immobilization of the aptamer, **iii)** OPN detection, and **iv)** the subsequent output of the electrochemical signal. Reprinted from Ref. [136]. with permission from *Elsevier*. **D)** Process depiction for creating MXene and CS_x/MXene-C aerogels. **i)** SEM depiction of MXene sheets on the AAO template. **ii)** TEM image showcasing the MXene sheet. **iii)** Close-up view of the MXene sheet in TEM. **iv)** Patterns of SAED for the MXene. Reprinted from Ref. [137]. with permission from *Royal Society of Chemistry*.

conductivity of the inner, unoxidized MXene layers; second, the rapid electron transfer facilitated by the exterior TiO_2 NPs; and third, electron "bridge" effects provided by the porous disordered carbon structure. When incorporated into textiles, this modified biosensing patch precisely monitors sweat glucose levels while adjusting pH (exhibiting a sensitivity of 77.12 μA mm^{-1} cm^{-2} within physiological levels ranging from 0.01 to 0.2 × 10^{-4} m and recording electrocardiogram signals (with a S/N of 37.63 dB). Overall, this study represents a significant advancement in wearable biosensing technology. However, further research is needed to address scalability, long-term stability, and compatibility with diverse physiological conditions. Moreover, Wang and his colleagues developed a biosensor for H_2O_2 detection by anchoring hemoglobin (Hb) onto TiO_2-modified Ti_3C_2 [135]. This enhances conductivity and surface area by promoting direct electron transport between the electrode and protein. Nafion usage eliminated interference, enhanced selectivity, and improved enzyme adhesion to the electrode. Adding TiO_2 nanoparticles enhanced protein stability and bioactivity, improving biosensor performance. They proposed an electrocatalytic mechanism for the Hb-based electrode, as mentioned in Eqs. (4) and (5).

$$Hb\left(Fe^{+3}\right) + e^{-} \rightarrow Hb\left(Fe^{+2}\right) \quad (4)$$

$$Hb\left(Fe^{+2}\right) + H_2O_2 + 2H^{+} \rightarrow Hb\left(Fe^{+3}\right) + 2H_2O \quad (5)$$

This biosensor exhibited rapid response time (<3 s), with a broad detection range of 0.1–380 mM, a sensitivity of 447.3 μA mM^{-1} cm^{-2}, and a LOD of 14 mM for H_2O_2 detection. Additionally, it showed excellent stability (97.5 % retention after 30 days) and reproducibility (R.S.D of 2.1 %) for practical applications. However, achieving uniform TiO_2 nanoparticle distribution on Ti_3C_2 layers is crucial for consistent biosensor performance; variations may lead to heterogeneous enzyme immobilization, impacting sensitivity and reproducibility. In 2019, a PPy@$Ti_3C_2T_x$/PMo_{12}-based electrochemical aptasensor was devised to detect the cancer biomarker OPN (osteopontin) by employing a combination of phosphomolybdic acid (PMo_{12}) nanoparticles and $Ti_3C_2T_x$ NSs within a polypyrrole (PPy) matrix (Fig. 6C). This aptasensor demonstrated remarkable sensitivity to OPN, achieving an impressively low LOD (0.98 fg mL^{-1}) and a more comprehensive detection range (0.05–10.0 ng/mL) [136]. The exceptional detection efficiency of this aptasensor can be credited to several critical factors, including the unique structure of the PPy layer with a π-π conjugated electron system, which enhances both electrochemical activity and OPN aptamer immobilization. Additionally, the aptasensor benefited from a π-π conjugated carbon nanostructure, good electron transport capabilities, and abundant TiO_2 and $Ti_3C_2T_x$, preventing dense PPy stacking and aiding

aptamer anchoring. Lastly, the strong binding affinity between polyoxometalates and biomacromolecules was primarily due to electrostatic interactions. Real sample analysis using human serum spiked with OPN confirmed the applicability of the aptasensor for OPN detection, with recoveries ranging from 96.61 % to 104.09 %. A discussion on the practical implications and potential challenges of deploying the aptasensor in real-world clinical settings would be valuable.

MXenes, with their adaptable hydrophilicity and surface characteristics, also hold significant promise for use in biomedical contexts. An example of this potential is evident in the nanosheets of Ti_3C_2 integrated into chitosan-based aerogels (depicted in Fig. 6D). These nanosheets exhibited impressive qualities, including flexibility, remarkable compressibility (up to 150,000 cycles), structural stability, and elasticity, enabling them to endure extreme strain (up to 99 %), and repetitive bending [137]. Also, the unique lamellar structure of aerogel boasted an extensive linear range (0.5–70 % strain) and an extraordinarily high sensitivity (measuring 80.4 kPa^{-1}). These advantageous features position the aerogel as a promising material for flexible wearable devices that detect biological signals. However, the study does not extensively discuss the potential impact of environmental factors, like humidity or temperature, on the performance of the aerogels, which could be relevant for real-world applications.

Several significant challenges hinder the practical utility of utilizing polymer-functionalized 2D MXenes in bioelectronics. These obstacles include issues related to chemical stability (such as degradation in humid or high-temperature environments, particularly during storage

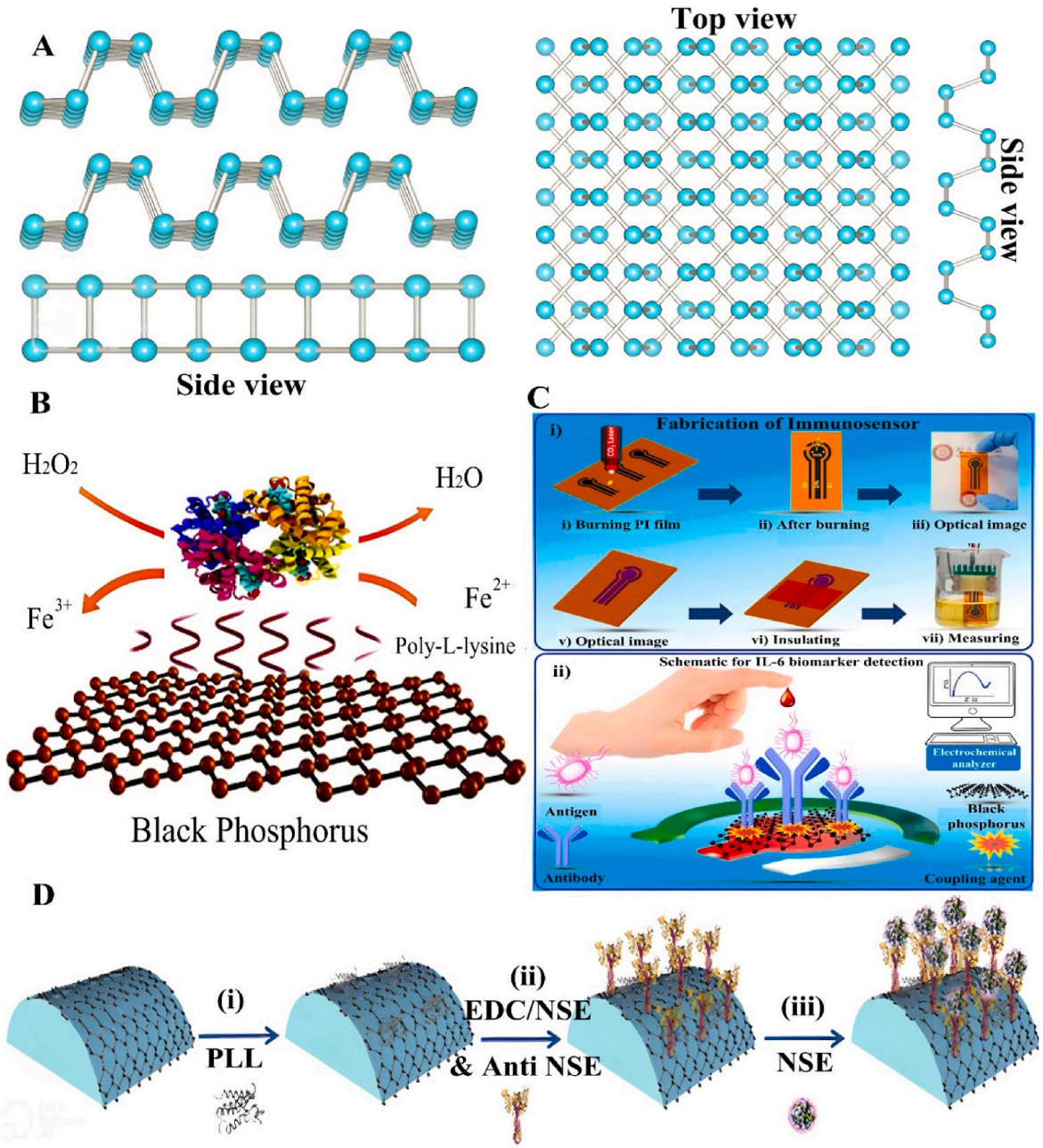

Fig. 7. A) Structure of 2D BP with top and side views. **B)** Poly-L-lysine/BP hybrid with detection mechanism. Reprinted from Ref. [159]. with permission from *American Chemical Society*. **C) i)** Steps involved in creating the IL-6 immunosensor, and **ii)** Diagram illustrating the detection process of the IL-6 biomarker. Reprinted from Ref. [160]. with permission from *Elsevier.* **D)** Functionalizing and linking BP-TFG: **i)** Incorporation of biocompatible PLL for biofunctionalization, **ii)** Fixation of anti-NSE through EDC/NHS bioconjugation, **iii)** Establishment of bio-affinity binding between anti-NSE and target NSE biomarkers. Reprinted from Ref. [161]. with permission from *Elsevier*.

and use), precise composition control, in vivo retention, mass production, and long-term biosafety [138,139]. Current methods, like hydrophilic polymers, enhance the water dispersity of MXenes in biosensors, but stability issues arise in extreme conditions. Future efforts should prioritize stable covalent modifications and dynamic bonding methods for biosensors. Additionally, research on functionalized 2D MXene biocompatibility remains nascent, particularly concerning cell uptake and toxicity [140]. Addressing these gaps requires developing novel surface modification techniques for biosensors and assessing the toxicity of polymer-functionalized 2D MXenes. The utilization of MXene-polymer combinations in biotechnology is in its early stages, and investigating polymer-based MXenes for bioelectronic applications is essential.

4.4. 2D black phosphorus

BP, also known as phosphorene in its monolayer form, has garnered significant interest since being rediscovered as a single-element 2D material in 2014, when liquid-phase-exfoliated BP demonstrated its effectiveness as a FET [141,142]. Unlike graphene, BP has a distinct puckered honeycomb orthorhombic lattice structure where each phosphorous atom covalently bonds with three neighbouring P atoms, resulting in a layer-to-layer spacing of about 5 Å [143,144], as depicted in Fig. 7A. This unique structure imparts BP with remarkable electronic characteristics, including high mobility (~1000 cm^2Vs^{-1}), layer-dependent fluorescence, an adjustable direct band gap (bulk, 0.3 eV; monolayer, 2 eV), anisotropic electrical and thermal conductivities, and excellent optical response [55,145]. These distinctive electronic and optoelectronic properties position phosphorene as an ideal candidate for diverse applications, like optoelectronic devices, bioelectronic devices, solar cells, biosensors, and thermoelectric devices [146,147]. Also, the biocompatibility and low toxicity of 2D BP materials make it an attractive choice for biosensor and bioelectronic applications [148]. Its biocompatibility stems from its essential role in the human body, where phosphorus and phosphate constitute roughly 20 % of bones and teeth [149].

Additionally, by manipulating the bandgap of BP, its photodetection range can be adjusted when employed in fluorescence biosensors as photosensitizers. The 2D structure of BP allows for compact photodetectors in fluorescence biosensors, facilitating the development of portable biosensors [149]. These approaches may also apply to emerging 2D materials in the future. For the first time in 2017, Teng Yew and his team used 2D BP as a nanoscale fluorescent marker to fabricate a sensor for detecting DNA. This method relied on the varying affinities of labeled ssDNA and dsDNA fragments to self-assemble with BP nanoparticles [150]. The resulting nano-biosensor had a detection range of 4.0–4000 pM, showing high linearity ($r = 0.91$) and the ability to differentiate triple nucleotide differences. Additionally, it exhibited good sensitivity, with a LOD of 5.9 pM. The researchers suggested that 2D BP holds substantial promise for diverse biosensing applications, particularly in DNA nano biosensors, with potential applications for detecting enzymes, proteins, and inorganic ions using fluorescence-based methods. However, the study involved the following limitations: the complex synthesis process of BPNPs and the need for further assessment of selectivity, sensitivity, biocompatibility, and compatibility with real sample matrices.

Despite the promising research conducted on pristine 2D BP for applications such as photodetection, biosensors, and biomedicine, further progress is hindered by the inherent properties of pure BP [151,152]. Firstly, few-layer BP are vulnerable to oxidation in water and oxygen presence, which limits their practical applicability. This oxidation occurs because of the lone-electron pairs carried by surface P atoms [153]. Secondly, there is currently no effective method for preparing large-area single-crystal BP. Current top-down procedures like mechanical milling and liquid-phase exfoliation result in minor areas or create diminutive BP flakes. At the same time, bottom-up methods need high pressure and heat to convert red phosphorus into BP [154–157]. Lastly, the poor solubility of BP in common organic solvents complicates its solution-based fabrication [158]. To address these limitations and enable diverse applications of BP, it is crucial to explore modification methods that can transform its unfavourable properties into desirable ones.

Considering the progress made by materials like 2D graphene and MXenes, combining 2D BP with biocompatible materials seems promising to create a more stable and sensitive biosensing platform [159]. Scientists have demonstrated that modifying BP with polymers maintains its transport properties and enhances stability, making it more suitable for ambient conditions [55]. Polymer surface modifications can also improve BP chemical properties, including biocompatibility, and address issues like solubility in organic solvents [149]. Two main strategies for polymer-based surface modifications to enhance BP stability are covalent functionalization, which forms covalent bonds between polymer functional groups and BP surface lone-electron pairs. Non-covalent functionalization relies on interactions like hydrophobic and electrostatic forces between the two materials [15]. For example, a straightforward method involving non-covalent modifications was suggested to produce a hybrid material called pLL-BP through water-based exfoliation in aqueous conditions [159]. In this process, pLL is attached to the BP surface via hydrophobic interactions with butyl chains and electrostatic interactions with protonated amino groups on pLL and deprotonated phosphate (P_xO_y) groups on 2D BP (Fig. 7B). This resulting pLL-BP hybrid served as an excellent framework for immobilizing hemoglobin. It facilitated direct electron transport due to BP's remarkable conductivity and biological compatibility, preserving hemoglobin's natural structure and bioactivity. The enzymatic electrochemical biosensor, incorporating Hb-pLL-BP, demonstrated impressive catalytic efficiency in reducing oxygen and H_2O_2. Its electrochemical response to the concentration of H_2O_2 was within the 10 μM–700 μM range, making it a promising component for new biosensors and bioelectronics. While the study focused on the electrochemical performance of biosensors, it did not extensively study the analytical parameters like selectivity, stability, reproducibility, etc. Understanding these parameters could provide valuable insights into the biosensor's performance and stability in real sample analysis.

A different study developed an immunosensor for detecting the IL-6 biomarker by incorporating BP with a versatile cationic polymer called polyallylamine (PAMI) through electrostatic interaction [160]. This study was the first to address the BP degradation issue, improve charge transfer, and introduce $–NH_2$ groups for attaching target biomolecules. It was noted that the cationic properties of PAMI enhanced the stability of immobilized biomolecules by creating a saline environment (Fig. 7C). Also, the PAMI-coated BP platform provided abundant binding sites, resulting in exceptional stability, cost-effective production, and the potential for point-of-care (POC) analysis of cancer. The developed immunosensor showed linear responses for detecting IL-6 biomarkers from 0.003 to 75 ng/mL with a 1 pg/mL LOD, demonstrating high selectivity and reproducibility, with a recovery range of 93.1–98.4 % in spiked serum samples. Significantly, the researchers believed that BP-PAMI could be employed to recognize various disease biomarkers following treatment with respective biomolecules. Still, clinical validation using a larger sample size and comparison with established methods is necessary to evaluate its accuracy and reliability in real-world clinical settings. Apart from depositing functionalized BP onto an electrode, an optical biosensor using a three-step in-situ layering process is devised to apply BP onto a tilted fibre grating (TFG) to diagnose cancer [161]. Initially, they functionalized –OH groups on the optical fibre through an alkaline treatment. Subsequently, –OH groups on the fibre interacted with APTES, forming Si–O–Si bonds that created a positively charged surface. Finally, a few layers of BP attached to the fibre via the coulombic attraction between the positively charged APTES bonds and the BP surface (as shown in Fig. 7D). To facilitate cancer diagnosis, poly-L-lysine was integrated with the BP-TFG and acted as a connector

to connect with anti-NSE to target NSE biomarkers. The BP-TFG biosensor demonstrated an excellent linear response (0.01–100 ng mL^{-1}) with a 1.0 pg/mL^{-1} LOD. The expressed sensitivity is 100 times more significant than GO and AuNP-based biosensors. However, the long-term stability and durability of the BP nanosheets deposited on fibre optic devices must be investigated. Environmental conditions, mechanical stress, and chemical exposure may affect the integrity and performance of the biosensor over time.

Although the promise of BP modification is significant, this research area is still in its early stages. Polymer-functionalized BP has promising applications in biosensors, enabling the attachment of biomarkers, but challenges remain [55]. Firstly, the preparation methods for BP/polymers need refinement, focusing on simplifying processes and achieving precise component additions in conventional single-crystalline methods. This characteristic becomes particularly crucial in disease diagnostics, such as tumor detection. Secondly, the judicious selection and utilization of polymers, encompassing factors like polymer type, functionalization procedures, and polymer thickness, are vital for enhancing BP/polymer stability. Adjustable stability is valuable for practical applications, especially in electronics. Lastly, comprehensive research on the biocompatibility of BP/polymers, particularly their effects on the nervous, reproductive, and immune systems, is essential for their application in various fields, especially biomedicine.

4.5. 2D transition metal dichalcogenides

Layered TMDCs, considered one of their foremost graphene counterparts, have attracted substantial attention in recent decades due to their chemical adaptability and outstanding physicochemical attributes, including impressive mechanical features, good optical absorption efficiency, expansive surface areas, noteworthy electronic conductivity, robust chemical stability, high catalytic activities, an energy band gap

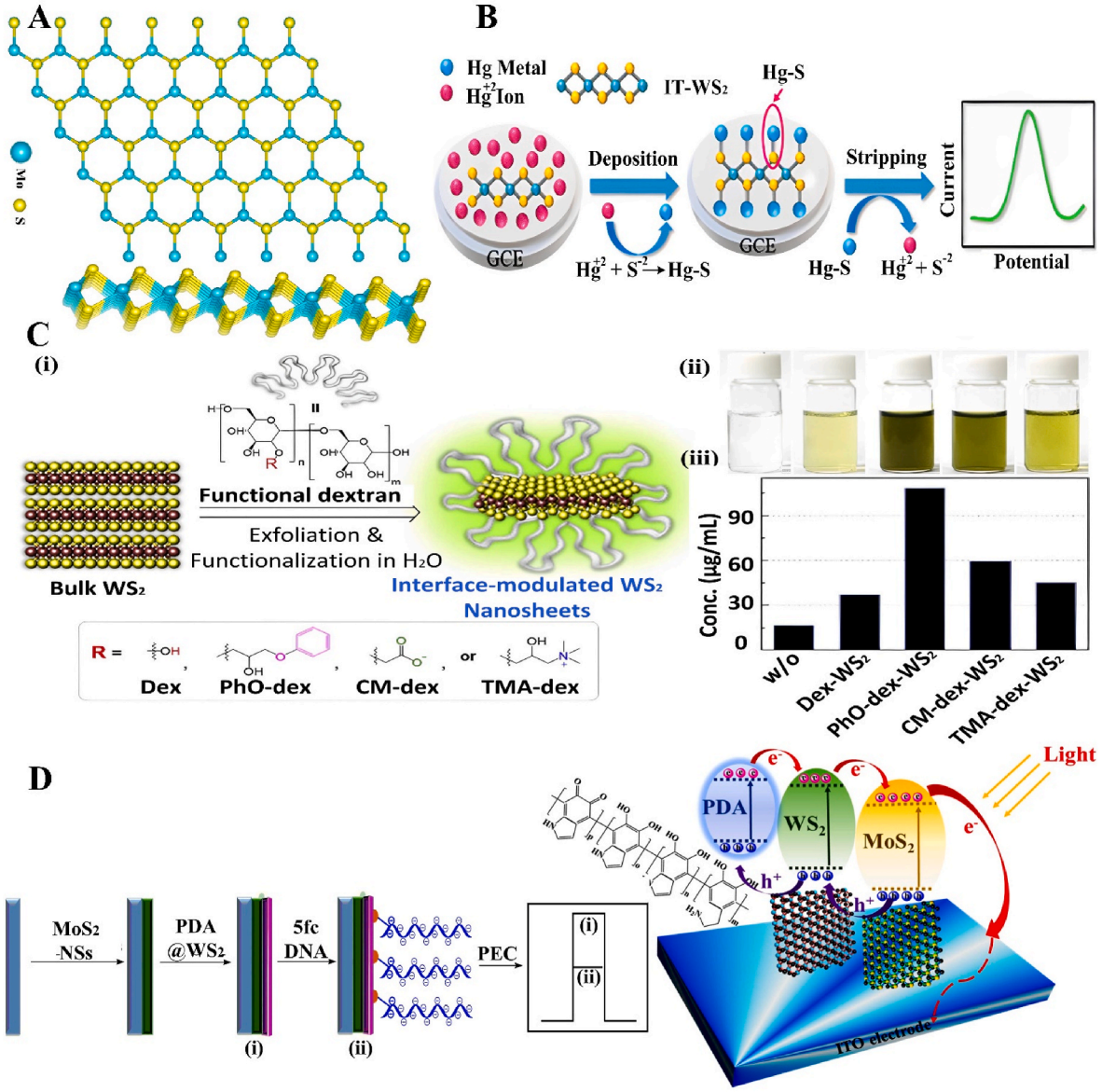

Fig. 8. A) Top and side views of 2D MoS_2 structure. **B)** Illustration depicting the sensing mechanism of Hg^{2+} utilizing 1T-WS_2, along with experimental results highlighting the S–Hg interaction. Reproduced from Ref. [168]. with permission from *Wiley*. **C)** Liquid-phase exfoliation of WS_2 nanosheets using various functionalized polymers (dextran, phenoxy-modified dextran, carboxymethyl dextran, and tri-methyl ammonium-modified dextran) in water. **i)** Schematic illustration of the process. **ii)** Photographs showcasing the exfoliated WS_2 nanosheets. **iii)** Concentrations of the nanosheets with different polymeric interfaces. Reproduced from Ref. [170]. with permission from *Elsevier*. **D)** Diagram depicting the PEC biosensor platform designed to detect 5 fC. Reproduced from Ref. [172]. with permission from *Elsevier*.

(0.2–2.1 eV) and straightforward synthesis methods [162,163]. These qualities hold promising potential for advancing high-performance biosensing applications [164,165]. TMDCs are layered materials composed of stacked planar crystals denoted by the general formula MX_2; here, M represents the transitional metallic atom, and X signifies the neighbouring chalcogen atoms, e.g., S, Mo, Se [166]. This structure, depicted in Fig. 8A, involves covalent bonding within the hexagonal lattice of the same layer and weak van der Waals forces between adjacent layers, facilitating easy thinning of the stack [167]. Examples of extensively researched TMDCs include WSe_2, WS_2, MoS_2, and $MoSe_2$. The electronic characteristics of these materials vary based on the elements and structural arrangements, providing flexibility for diverse applications [166]. Rahman and coworkers developed a straightforward hydrothermal method to prepare metallic 1T-WS_2 microflowers for detecting trace Hg^{2+} levels [168]. The diagram illustrates the sensing process, where Hg^{2+} ions form strong adsorption and deposition on the 1T-WS_2 surface, creating a Hg–S covalent bond (Fig. 8B). The oxidization of mercury during stripping generated a current response proportional to the levels of Hg^{2+} in solution. The modified GCE exhibited a broad linear response to Hg^{2+} within the range of 1–1 μM and 0.1–1 mM, with an impressive LOD as low as 79.8 pM. While the 1T-WS_2 performance in tap water analysis showed promising results, its stability in real environmental conditions, such as varying pH levels, temperatures, and exposure to different substances, is not thoroughly investigated.

As discussed earlier, atomically thin TMDCs exhibit various advantageous properties like high photothermal response, fluorescence, and moderate conductivity, making them valuable for biosensor applications. However, these materials lack intrinsic biocompatibility and necessitate additional functionalization for integration into biological systems [164]. Moreover, further modification may be essential to improve sensitivity because most 2D TMDCs struggle to maintain a stable suspension in typical polar solvents like H_2O, posing challenges for in vivo applications [164,169]. Due to their significant surface-to-volume ratio, one approach involves non-covalently incorporating biocompatible polymers into TMDC materials to create polymer/TMDC composites, facilitating their use in biosensing [164]. For example, a PEC sensing platform for detecting glutathione (GSH) was developed using PANI and nanoMoS_2 composites as optoelectronic materials [61]. The PEC response increased with an increasing dose of PANI/nanoMoS_2, up to a certain point beyond which it decreased due to excessive weight hindering light transmission. The pH of the solution was also found to affect PEC intensity, with pH 6.0 identified as the ideal pH for subsequent studies. At this pH, the biosensor demonstrated a linear response (1.0×10^{-10}–1.0×10^{-4} mol L^{-1}) for GSH concentrations, achieving a LOD of 0.31×10^{-12} mol L^{-1}. It displayed long-term stability, retaining over 90 % of its initial photocurrents after four weeks of storage. The method proved reliable for detecting intracellular GSH levels in human cell lines and GSH concentrations in human serum samples, with recoveries between 95.9 % and 103.3 %. The biosensor's performance was optimized at pH 6.0, which may not be suitable for all sample types or clinical scenarios, potentially impacting sensitivity and accuracy in samples with varying pH levels. In another study, dextran-polymer-functionalized WS_2 NSs were created through liquid-phase exfoliation, resulting in four distinct WS_2 interfaces [170]. These interface variations significantly influenced the thermodynamics and adsorption kinetics of a fluorescein-labeled DNA (FAM-DNA) probe. Compared to pristine dextran-WS_2, (tetramethylammonium-modified dextran) TMA-dex-WS_2 and (carboxymethyl-modified dextran) CM-dex-WS_2 demonstrated a 3.6-fold increase in the adsorption rates for the FAM-DNA probe. Notably, the adsorption ability of FAM-DNA on CM-dex-WS_2 exceeded its hybridization energy for miR-29a, preventing favourable desorption (Fig. 8C). Contrary to this, TMA-dex-WS_2 displayed an appropriate adsorption strength, allowing for favourable desorption with miR-29a after hybridization. This interface modulation enabled sensitive and selective recognition of miR-29a (the Alzheimer's disease biomarker) in human serum, highlighting its potential for bioassays. While the LOD of 745 pM in human serum is impressive, its reliability for detecting miR-29a in clinical samples is uncertain. Clinical samples may exhibit lower miRNA concentrations or background noise levels, potentially challenging sensitive detection.

To harness the fluorescence characteristics of 2D TMDs in water, a method for simultaneous functionalization and exfoliation of WS_2 NSs with B-PVA (boronic acid-modified poly(vinyl alcohol)) in water through pulsed sonication was devised [171]. The resultant B-PVA-WS_2 nanosheets were employed to detect glycated hemoglobin (HbA1c). B-PVA-WS_2 NSs displayed fluorescence quenching due to HbA1c presence, providing a clear distinction from PVA-WS_2. Based on specific fluorescence quenching, B-PVA-WS_2 selectively detected HbA1c at low levels of 3.3×10^{-8} M. Although the biosensor showed selectivity for HbA1c in glucose presence, potential interference from other biomolecules in biosamples must be thoroughly evaluated to avoid false-positive or false-negative results. Li and his group enhanced the photoresponse of MoS_2 by using the WS_2@PDA composite [172]. This composite, characterized by the solid electron donor and matched energy band properties of PDA, effectively reduced electron-hole pair recombination (depicted in Fig. 8D). By utilizing the improved photoactivity of WS_2@PDA and MoS_2, they crafted a sensitive and straightforward PEC biosensor for detecting 5-formylcytosine (5 fC-DNA) formation, with a broad linear range from 5000 to 200 nM and an LOD of 3.7 pM. It demonstrated a stable photocurrent response (RSD 2.26 %) upon repeated irradiation every 20 s, indicating long-term detection stability. Additionally, six parallel biosensors showed good reproducibility with an RSD of 1.87 %. The biosensor could also selectively discriminate between 5-hydroxymethylcytosine, 5-methylcytosine, and cytosine, increasing its specificity. Biological variability, like genetic diversity and sample heterogeneity, along with dynamic DNA modifications under different physiological conditions, may affect the detection of 5 fC-DNA. Standardizing sample preparation protocols and validating them across diverse biological contexts are crucial steps to mitigate this limitation.

Although the unique physicochemical properties of polymer-functionalized 2D TMDCs have demonstrated their effectiveness in biosensing [164,173], the synthesis of these materials lacks consistency. There is no standardized technique to ensure well-controlled dispersity, thickness, dimensions, and uniform functionalization. Current large-scale synthesis methods result in varied size and thickness distributions, while bottom-up synthesis faces difficulties in achieving well-functionalized nanosheets with controlled thickness. The cytotoxicity of such TMDCs in biosystems appears relatively low, but toxicity in non-targeted areas remains poorly studied and is crucial for potential clinical trials. Regardless of being in the early stages, the functionalization of TMDCs for biomedical use holds promise for highly sensitive biosensing, offering advantages over existing biodegradable materials. However, further research and development are necessary to establish polymer-functionalized 2D TMDCs as a viable nanomaterial for biomedical applications.

4.6. 2D metal-organic frameworks

Metal-organic frameworks (MOFs) are a novel category of porous coordinate materials with properties similar to 2D materials. At the same time, they also possess distinctive features like significant porosity (ranging from 0.5 to 2.5 nm) [174], high adjustability in structure [175], and biodegradability [68], making them suitable for diverse biomedical uses. The fundamental framework of MOFs mainly comprises transitional metal ions connected to negatively charged organic components through various functional links like cyanide, glutamate, formates, triazole, and sulfonates, forming a network through coordination bonds, hydrogen bonding, electrostatic interactions, or π-π stacking [176,177], Fig. 9A. This versatility in metal coordination and organic linkers allows MOFs to create well-organized pores of

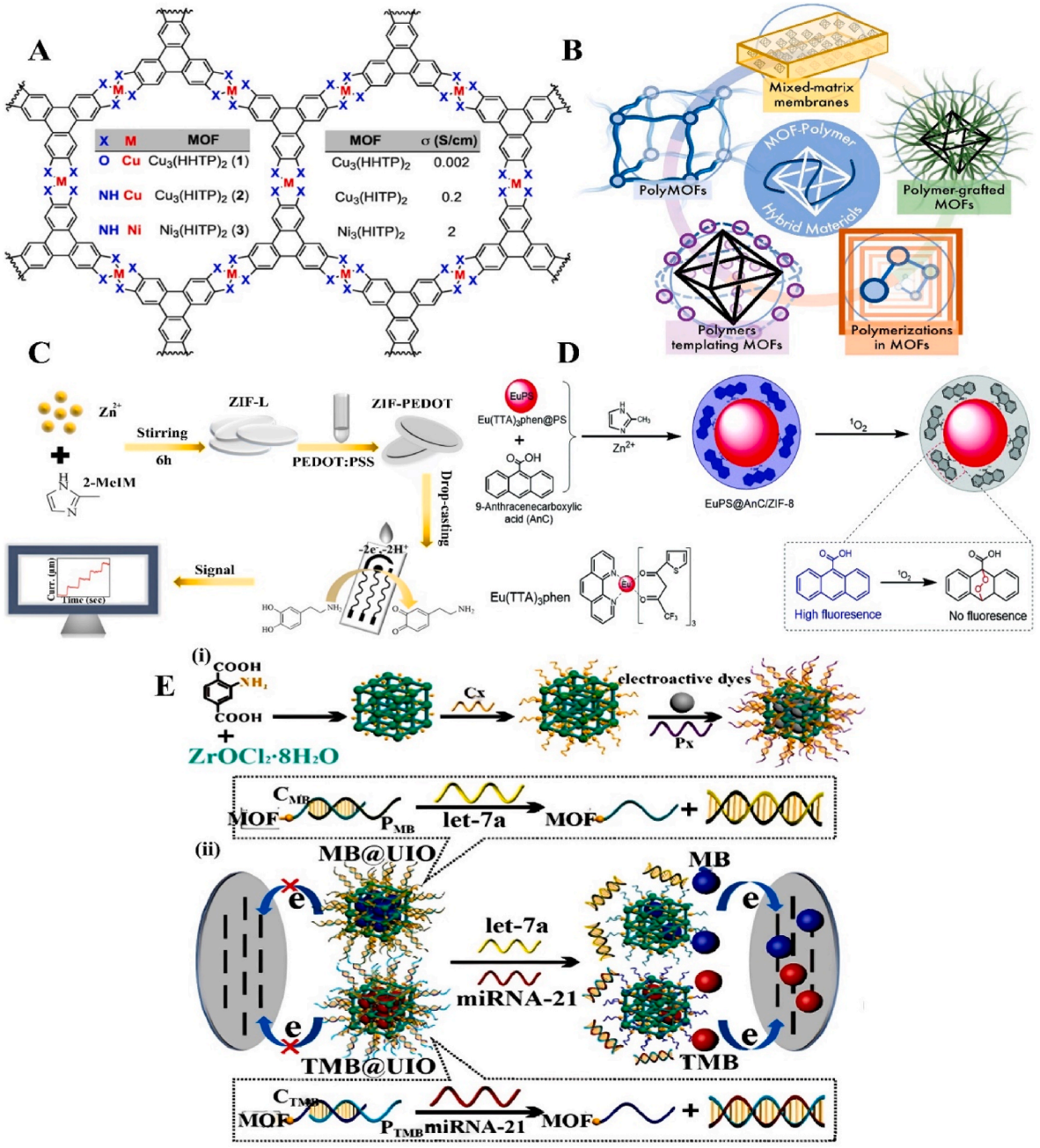

Fig. 9. A) Chemical structure of conductive 2D MOFs ($Cu/Ni_3[HHTP/HITP]_2$). Reprinted from Ref. [177]. with permission from *American Chemical Society*. **B)** Systematic depiction of MOF-polymer hybrids focusing on mixed-matrix membranes (MMMs), polymer-grafted MOFs, polymerization in MOFs, polymer templating in MOFs, and polyMOFs. Reprinted from Ref. [189]. with permission from *American Chemical Society*. **C)** Fabrication of ZIF-L/PEDOT biosensor and the electrochemical detection mechanism for dopamine. Reprinted from Ref. [192]. with permission from *Royal Society Chemical*. **D)** Synthesis process of EuPS@AnC/ZIF-8 and its operational concept in ratiometric sensing of $^1O_2$. Reprinted from Ref. [193]. with permission from *Royal Society Chemical*. **E) i)** Procedure for fabricating nucleic acid-functionalized MOFs, **ii)** Explaining the principle behind MOF-based homogeneous electrochemical biosensor for multiple miRNA detection. Reprinted from Ref. [196]. with permission from *American Chemical Society*.

customized sizes and functionality, offering vast potential across numerous technological fields [178,179]. MOFs have gained recognition as a potential sensing material due to their excellent mass transfer capabilities within their carefully designed porous structure [180]. One illustrative case involves zeolitic imidazolate frameworks (ZIFs), which, owing to their substantial porosity and expansive surface area, are thought to enhance the concentration of dehydrogenase enzymes for in vivo electrochemical monitoring of neurochemicals like glucose [181]. Nevertheless, the limited conductivity, reduced selectivity, absence of customizable modification sites, and instability in aqueous environments constrain the broader utilization of MOFs in biosensor applications [182].

One effective strategy to overcome these challenges involves combining MOFs and conductive polymers to create a single nanostructure with advantageous characteristics of both material categories [183–185]. MOFs offer distinct benefits such as precise porosity, well-defined crystal structures, and controlled metal content. In contrast, conductive polymers contribute qualities like environmental durability, excellent compatibility with biosystems, large surface area, ease of processing, robust mechanical and chemical resilience, and

suitability for biosensor applications [186,187]. Research groups have explored a broad range of approaches to create MOF-polymer composites, such as polymer-templated MOF growth, polymer-grafting particles, and MOF preparation with polymer ligands (polyMOFs, as shown in Fig. 9B). The controlled incorporation of MOFs and polymers frequently results in the creation of composite materials that possess either novel characteristics or a combination of properties that surpass those of a mere physical blend of individual components [188]. Due to the synergistic interaction of MOFs and other active elements, these composites are suitable for diverse applications, encompassing storage and separation processes, heterogeneous catalysis, energy devices, biosensing technologies, and biomedical applications [189,190].

To expand the conductivity and utility of MOFs in biosensors, an efficient approach to integrating Co–Ni(Fe)-MOF NSs with conductive PPy for detecting glucose through non-enzymatic electrochemistry was devised [191]. The modified electrode with Co–N(Fe)-MOF/PPy nanocomposite offered exceptional sensitivity (1805 $\mu AmM^{-1}cm^{-2}$) and a LOD of 1.13 μM for glucose detection, attributed to its synergistic active sites and excellent electron transfer capabilities. The glucose sensor also exhibited high selectivity for glucose over various interferences, with excellent reproducibility and stability. It is a promising platform for sensitive glucose detection in actual samples, achieving recoveries between 103.7 % and 109.5 %. The researchers suggested that this approach opens possibilities for creating various composites of MOFs and conducting polymers to enhance electrochemical biosensing. Yet, the study lacks a comprehensive analysis of nanocomposite's long-term stability and reproducibility in real-world conditions. While short-term stability is demonstrated, further investigation into durability under varied environmental conditions, such as temperature fluctuations and exposure to different analytes, is needed to assess practical applicability thoroughly.

To address issues such as poor stability, poor catalytic activity, and low conductivity in the water dielectric medium of leaf-shaped ZIF, Liu and colleagues introduced the conductive polymer (PEDOT: PSS) into the ZIF-L for sensitive sensing of DA [192]. The resultant ZIF-L/PEDOT composite not only maintained the ZIF-L surface structure but also displayed impressive electrochemical properties due to improved electron transport at the ZIF-L and PEDOT: PSS interface (Fig. 9C). The established biosensor exhibited a LOD of 7 nM and a broad linear range from 25 to 500 μM for DA. Furthermore, the biosensor demonstrated excellent long-term storage stability, retaining approximately 90.52 % of its original current after 28 days of repeated testing. These findings highlighted the latent effect of ZIF-L/PEDOT on disease detection. The study mentioned a slight decrease in sensitivity over time due to the detachment of excess ZIF-L/PEDOT particles from the electrode surface during prolonged immersion. Developing strategies to enhance the stability of the electrode and prevent particle detachment could improve long-term performance. Additionally, fluorescent MOFs with the polymer can detect ions, gases, and vapors. For instance, the combination of 2-methylimidazole, 9-anthracenecarboxylic acid (AnC), zinc nitrate, and europium chelate-doped polystyrene (EuPS) spheres in a methanol solution can result in the creation of EuPS@AnC/ZIF-8, a dual-emissive material with excellent fluorescence [193]. The fabrication process of the sensor involved the self-assembly of EuPS, AnC, and ZIF-8, resulting in a core-shell structure where EuPS served as a reference signal emitter. At the same time, AnC acted as a response signal emitter for singlet oxygen ($^1O_2$) detection (Fig. 9D). The integration of AnC and EuPS within the ZIF-8 host not only retained their original fluorescence properties but also prevented the leakage of AnC, enhancing the sensor's stability and performance. This biosensor detected $^1O_2$ due to its ability to emit different fluorescent signals of Eu^{3+} and AnC to $^1O_2$. It is sensitive, ranging from 0.5 to 200 μM and having a LOD of 43 nM (S/N = 3). It could distinguish $^1O_2$ from other reactive oxygen species. Notably, the color change of the sensor in response to stimuli is readily observable with the naked eye under a UV lamp. The biocompatibility test performed using HeLa cells is an excellent initial step. Additional studies on various cell types and tissues would provide a more comprehensive understanding of the sensor's behaviour in biosystems. Furthermore, long-term stability studies, particularly under physiological conditions, are crucial. This research offers new insights into designing multifunctional composites using MOFs.

Functionalizing MOFs with natural biopolymers, such as proteins, nucleic acid (dsDNA, ssDNA, and aptamer), and cellulose, has been a significant area of recent research. MOF-based nucleic acid biosensors offer distinct advantages over biosensors based on graphene, GO, and AuNP [194]. These advantages include a conjugated π-electron system, open metal sites, flexible porosity, and high loading capacity, making them well-suited for detecting biomolecules, bacteria, and cells [195]. An innovative electrochemical biosensor capable of susceptible detection of two miRNAs was developed, showing potential as valuable cancer biomarkers for diagnosing and treating tumors [196]. They achieved this by attaching functionalized dsDNAs onto MOF surfaces through adsorption and encapsulating electroactive dyes (MB and TMB) within MOF cavities. When target miRNAs hybridized with probe DNAs, the electroactive dyes released from the MOFs, enabled the concurrent analysis of miRNA-21 and Let-7a, both classified as miRNAs (Fig. 9E). The biosensor exhibited high sensitivity, with LODs of 3.6 fM for let-7a and 8.2 fM for miRNA-21 in the ranges of 0.01–10 pM and 0.02–10 pM, respectively. Real sample analysis of serum from breast cancer patients further validated the biosensor's potential for accurate and early cancer diagnosis, detecting concentrations of 19.68 nM for let-7a and 23.24 nM for miRNA-21. However, the synthesis process described for preparing the dsDNA-capped MOFs involves several steps and reagents, which may limit its scalability and practicality for large-scale production. Simplifying the synthesis protocol could enhance the feasibility of widespread adoption.

Polymer integration with MOFs facilitates solvent interactions, improving dispersion, assembly, and processability while enhancing biocompatibility and conductivity for biosensing applications. However, challenges remain. Optimizing polymer loading while preserving porosity is essential, as is understanding the homogeneity of polymer guests within MOF templates. Factors such as MOF crystal size and polymerization rate affect composite performance but lack systematic study. Additionally, the influence of polymers on mass transport within microporous MOFs needs clarification. Understanding MOF-polymer interactions, polymer arrangement in pores, and structural impacts is crucial for performance optimization [197]. Advanced characterization techniques, like solid-state NMR and computational modelling, offer insights into MOF-polymer interactions and arrangement, guiding synthetic procedures for enhanced composite performance. Integrating experimental studies with computational methods holds promise for addressing experimentally challenging questions, such as MOF stability and polymer arrangements within pores. Lastly, future research should focus on scaling up the production of polymer-functionalized 2D MOFs using low-cost synthesis methods while maintaining control over their size, shape, and porosity [198].

5. Emerging functionalized 2D materials for biosensor and bioelectronics applications

Biosensors and bioelectronics that utilize polymer-functionalized 2D materials have found diverse applications across several domains, such as food quality and safety, environmental monitoring, disease biomarkers, and electronic skin. These applications demonstrate the immense potential of such materials in advancing healthcare, environmental protection, and safety. Table 2 presents a detailed comparison of biosensors based on functionalized 2D materials in spiked real samples.

5.1. Food safety and quality monitoring

Food consumption is a fundamental human need, and ensuring its quality and safety is vital for maintaining a healthy life. The ongoing

Table 2
Comparison of biosensors utilizing polymer-functionalized 2D materials in real samples: Polymer functionality, analytical performance, advantages, and challenges.

Biosensor designs	Role of polymer	Analytes	Linear range	LOD	Real samples/ Recovery	Advantages	Challenges	Suitability	References
Food safety and quality monitoring									
Au NPs/ NCPDs@FLBP/ SPE	Act as a conductive matrix, improved transmission path, carrier mobility, surface area, and molecular adsorption	*E. coli* O157: H7	1.0×10^{-19} – 1.0×10^{-6} mol/L	3.33×10^{-20} mol/L	Chicken meat	Portable electrochemical system, smartphone control, reasonable specificity, sensitivity, and reproducibility, long term stability (up to 30 days)	Optimization of experimental conditions, sensitivity to environmental conditions, and interference	In vitro	[200]
CTAB-MoS_2-NSs	Stabilization of exfoliated MoS_2, prevented restacking, facilitated smooth film formation	S. typhimurium	10^1–10^7 CFUmL^{-1}	10 CFU mL^{-1}	–	Superior electron transport, sensitivity, and specific binding	Insufficient incubation time, limited sensitivity for low concentrations	In vitro	[201]
MNPs/CS/g-C_3N_4	Provided a biocompatible surface for enzyme immobilization, enhanced stability, and reusability	Lactose	0.9–100 mm	0.3 mm	Dairy products spiked/un-spiked	Cost-effective, highly active site, homogeneity, metal-free composition, good magnetism, high specificity, short-term stability (up to 7 days), and sensitivity (4.4 μA mM^{-1})	Uniform dispersion of nanoparticles, optimization of conditions, short long-term stability	In vitro	[205]
PPy-GO-AuNPs	Immobilized GO and Au NPs on electrode surface, enhanced electrocatalytic activity and sensitivity	H_2O_2	2.5 − 25 mM	5 μM	Milk/96.0–100.6 %	Fast electrocatalytic activity, rapid response (2 s), high sensitivity (41.35 μA μM^{-1} cm^{-2}) at S/N = 3, stability (up to 30 days)	pH effect on electrochemical oxidation, limited LOD	In vitro	[207]
NiONSs/PANiNW/ GO	Enhanced homogeneity, active surface area, electrical conductivity, selectivity, and sensitivity	Glucose	2 μM–5.560 mM	0.5 μM	Fetal bovine serum/ 99.2–100.4 %	High selectivity, sensitivity (376.22 μA mM^{-1} cm^{-2} at S/N = 3, and electrocatalytic activity	Complex fabrication process	In vitro	[206]
PDA-coated Cu-MOF	Acted as a signal amplification marker, enhance sensitivity	AFB_1	0.05–2 ng/mL	0.01 ng/mL	Lotus seed, maize/ 80.3–104.6 %	Improved sensitivity, cost-effective, simple, avoidance of mAbs loss, excellent hydrophilicity, and biocompatibility, stability at room temperature (up to 90 days) and at 45 °C (up to 7 days)	Stability and bioconjugation capacity of hybrid, optimization of concentration and pH of DA solution		[203]
$Ti_3C_2T_x$/PVDF	Acted as an efficient electrochemical redox probe, improved binding sites	OTA	1.0 fg mL^{-1} – 1.0 ng/mL	2.15 fg mL^{-1}	Grape juice/92–104 %	Excellent electroactive surface sites, selectivity, reproducibility, and stability (up to 7 days)	Optimization of experimental parameters	In vitro	[204]
Environmental monitoring									
graphene/PANI	Improved electron transfer kinetics, surface-to-volume ratios	Zn^{2+}, Pb^{2+}, Cd^{2+}	1–300 μg L^{-1}	Zn^{2+}: 1.0 μg L^{-1}, Cd^{2+}, Pb^{2+}: 0.1 μg L^{-1}	Human serum/ 93.8–109.7 %	Low cost, disposable, enhanced sensitivity, and electrical conductivity	Agglomeration of graphene at higher concentrations, low stability	In vitro	[211]
PM/g-C_3N_4	Improved electron transfers, electrocatalytic activity, and sensitivity	Cd^{2+}, Pb^{2+}	0.1–1.0 μM	Cd^{2+}: 0.02 μM, Pb^{2+}: 0.008 μM	Real water/ 92.5–106.4 %, 90–102.6 %,	Low-cost, efficient adsorption, sensitivity, and stability (up to 7 days)	Selective detection, limited LOD	In vitro	[212]
Fe_3O_4@Au-PPy/ GO	Enhanced electron transfer rate and stability	Triclosan	1.0×10^{-8} – 1.0×1.0^{-6} M	2.5×10^{-9} M	Urine/98.0 %, Toothpaste/101.0 %, Shampoo/96.6 %, Liquid soap/101.6 %	Enhance effective surface area, electrochemical reaction, and storage stability (up to 14 days)	Complex fabrication process, optimization of nanocomposite film	In vitro	[213]
AChE/Con A/ PDA/RGO-GNP	Reduced GO and GNP under alkaline conditions, improved electrical conductivity and protein immobilization	Carbofuran	5–40 mg/kg	0.012 mg/kg	Tomatoes/101 %	Simple approach, low cost, specific binding affinity, improved electrochemical activity, surface area, and sensitivity	Balance between enzyme binding size and pesticide, blockage of AChE active sites	In vitro	[216]
g-C_3N_4/CMCS/ ZnCdS/ZnS QDs	Acted as ligand, improved biocompatibility, and fluorescence	Mn^{2+}	1.961×10^{-6} – 1.667×10^{-5} mol/L	–	Real water/90–107 %	Simple approach, eco-friendly, long-term stability, and reproducibility	Stability of nanocomposites to surrounding environment	In vitro	[247]
Detection of disease biomarkers									

(*continued on next page*)

Table 2 (*continued*)

Biosensor designs	Role of polymer	Analytes	Linear range	LOD	Real samples/ Recovery	Advantages	Challenges	Suitability	References
MXenes-Apt2/ exosomes/Apt1/ PNIPAM-AuNPs	Enhanced aptamer immobilization and catalytic ECL signals	MCF-7	5×10^2–5×10^6 particles μL^{-1}	125 particles μL^{-1}	Serum/95–104 %	High sensitivity, specific recognition, amplification strategy, surface area, and conductivity	Complex fabrication process	In vitro	[219]
Prussian blue-polythiophene-GO	Enhanced electronic transmission capacity and electrocatalytic performance	H_2O_2	1.0 − 100.0 μM	0.32 μM	Milk/95.0–105.0 %	Large specific surface area, high conductivity, selectivity, and sensitivity (0.1066 μA/μM) at S/N = 3	Experimental parameters optimization	In vitro	[220]
$TiO_2/Ti_3C_2T_x$/NUF	Acted as electrochemical active sites	DA, UA	DA: 0.002–100 μM, UA: 0.001–60 μM	DA: 0.2, UA: 0.18 nM	Urine/98.4–100.9 %.	Large electrode effective area, catalytic activity, anti-fouling property, anti-interference ability	Heterojunction stability, electrode microstructure optimization	In vitro	[248]
PPY/MXene	Increased electroactive surface area, conductivity, and sensitivity	*M. tb*	100 fM − 25 nM	11.24 fM	Human sputum/ 90.52–100.8 %.	Cost-effective, high electrochemical activity, sensitivity (21.92 μA nM^{-1} cm^{-2}), selectivity, rapid response (10 s)	DNA probe immobilization, hybridization optimization, limited selectivity	In vitro	[249]
Wearable bioelectronics and E-Skins									
PANI-doped F–$Ti_3C_2T_x$	Enhanced ion-to-electron charge transfer, conductivity, and electrochemical stability	H_3O^+	pH ≈ 1−11	–	Human sweat	Highly selective sensitivity, electrochemical stability, fast response, anti-interference ability	$Ti_3C_2T_x$ oxidation, potential drift in $Ti_3C_2T_x$/ PANI electrodes	In vivo	[224]
WS_2/PDMS/G	Acted as a flexible membrane substrate, improved repeatability and stretchability	Water moisture	–	–	Human breath	Sensitivity up to 2357 (for 90 % humidity), fast response time, repeatable moisture sensing properties, transparency, flexibility, stretchability, and real-time monitoring	Optimization of electrode structure, improvement of sensitivity	In vivo	[225]
rGO/PET/textile hybrid	Maximize electrical conductivity, durability, and biocompatibility, mitigate polarization effects, and limit ion intercalation	Various biopotentials (EEG, ECG, EMG)	–	–	–	Exceptional biocompatibility, robust, washable textile-based structure, reduced electrode polarization	Laser power optimization, precise integration of rGO into PET, variations in laser power	In vivo	[250]

NCPDs*:* N-doped carbonized polymer dots; *E. coli*: *Escherichia coli* O157: H7; S. typhimurium*: Salmonella* typhimurium; MNPs: Magnetic nanoparticles; PVDF: Polyvinylidene fluoride; OTA: Ochratoxin A; GNP: Gold Nanoparticles; PANIPAM: Poly (N-isopropylacrylamide); NUF: Covalent organic polymers; *M. tb*: *Mycobacterium tuberculosis*; CMCS: Carboxymethyl chitosan; EEG: electroencephalography; ECG: electrocardiography; ECG: electromyography.

globalization of markets is diminishing the prevalence of foods being processed and consumed locally where they are produced. This global integration of the food supply chain necessitates novel approaches to guarantee food safety and quality, as various biotic and abiotic factors compromise food quality during multiple stages. Consequently, routine food safety and quality monitoring at different points in the supply chain becomes imperative. Recently, biosensors have been designed to detect harmful analytes in foods, with sensitivity significantly boosted by the use of 2D materials [199]. Polymer-functionalized 2D materials, with their exceptional physiochemical properties, are ideally suited for incorporation into biosensors and other tools employed in food quality analysis.

For instance, a new portable DNA biosensor was fabricated using NCPDs grown onto a few BP sheets as electrode modifiers, combining methylene blue (MB) as a chemical indicator and Au NPs for immobilizing thiolated ssDNA probes for sensing the specific DNA sequence of *E. coli* O157: H7 [200], (Fig. 10A). The biosensor exhibited a broader linear range (1.0×10^{-19} to 1.0×10^{-6} mol L^{-1}), a low LOD (3.33×10^{-20} mol L^{-1}, three σ), and high sensitivity, validated by detecting *E. coli* genomic DNA in spiked samples of chicken meat with good reproducibility, RSD values of 2.60 % and 4.03 % for two different concentrations of target DNA sequence. It also exhibited long-term stability when stored in a refrigerator at 4 °C for up to 30 days. Real-world application potential is highlighted, but challenges like sample complexity and device integration into portable systems need further exploration for practical field use. Addressing power consumption, miniaturization, and user interface design would enhance the feasibility of on-site detection. In another study, CTAB functionalized-MoS_2 nanosheets were produced to detect *S. typhimurium* on a microfluidics electrode [201]. The nanosheets were fabricated through exfoliation assisted by CTAB, and CTAB-MoS_2-NSs acquired a positive charge, with subsequent deposition on a patterned hydrolyzed ITO microelectrode using electrostatic forces (Fig. 10B). This integrated setup was then combined with a PDMS microfluidic device, resulting in the formation of a lab-on-a-Chip system designed explicitly for *S. typhimurium* recognition. The device exhibited a high sensitivity of 1.79 kΩ/CFU^{-1} mL cm^{-2} and an LOD of 1.56 CFU mL^{-1} in a broad linear range from 10^1 to 10^7 CFU mL^{-1}. However, the stability of the immunochip decreased significantly after the 3rd week of storage, with a 14.2 % decrease in impedance signal observed by the end of the 7th week. This limitation could affect the long-term reliability and practical application of the device.

Besides pathogens, these 2D materials are actively utilized for precise mycotoxin detection in food. Mycotoxins are toxic compounds produced by certain fungi on agricultural commodities, such as nuts, grains, and fruits. These toxins contaminate food and feed, posing health risks when ingested [202]. A recent development includes a strip lateral flow immunoassay (SLFIA) designed for on-site analysis of AFB_1 in food samples. This innovative approach used PDA-coated Cu-MOF as a signal amplification marker [203]. Under optimal conditions, the modified SLFIA demonstrated a low LOD of 0.01 ng/mL and a broad concentration range of 0.05–2 ng/mL for AFB1. Its application in lotus seed and maize samples yielded reasonable recoveries of 80.3 %–104.6 %, confirming its accuracy in real-world scenarios. Furthermore, stability tests revealed that the SLFIA strips remain effective for up to 90 days at room temperature and tolerate storage at 45 °C for seven days, highlighting their suitability for field use without cold chain transport. However, the cost of materials and equipment required for the SLFIA method, like

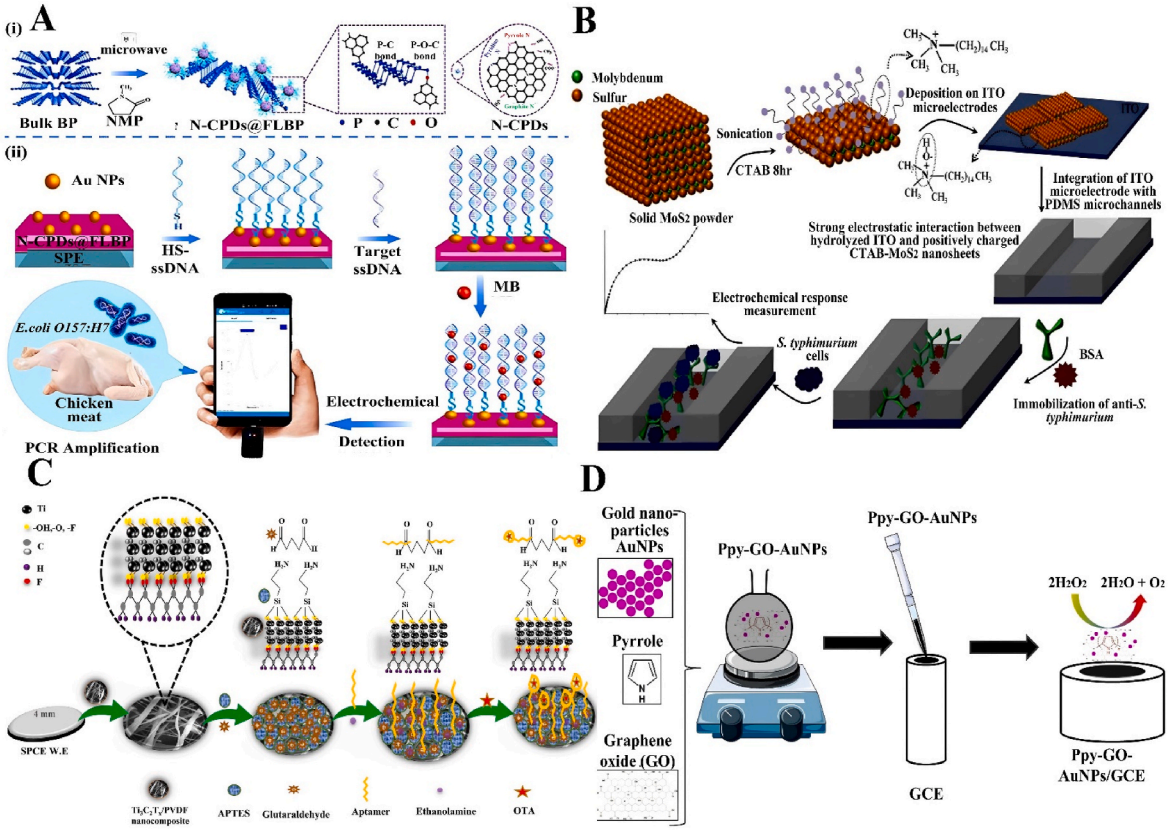

Fig. 10. A) i) One-step synthesis of N-CPDs@FLBP heterostructure, **ii)** Schematic illustration of a portable intelligent electrochemical DNA biosensor for detecting E. coli O157: H7. Reproduced from Ref. [200]. with permission from *Elsevier*. **B)** Diagram illustrating the sequential process of crafting a microfluidic biosensor for detecting S. typhimurium. Reprinted from Ref. [201]. with permission from *Elsevier*. **C)** Systematic depiction of fabrication and working mechanism of aptasensor. Reprinted from Ref. [204]. with permission from *Elsevier*. **D)** Synthesis process of PPy-GO-AuNPs nanocomposites. Reprinted from Ref. [207]. with permission from *Elsevier*.

MOFs, PDA, and monoclonal antibodies, may limit its accessibility, particularly in resource-limited regions or for small-scale food producers. Here, a very sensitive electrochemical aptasensor was fabricated using electrospun $Ti_3C_2T_x$/PVDF nanocomposite on a screen-printed carbon electrode to detect OTA accurately [204]. Structural and electrochemical analyses revealed enhanced electroactive sites due to the synergistic effect between β-phase PVDF and $Ti_3C_2T_x$, along with redox probe effective covalent bio-functionalization with aptamer (Fig. 10C). This synergy amplified signal strength and transduction, notably increasing sensitivity with a low LOD of 2.15 fg mL^{-1} and a broad dynamic range from 1.0 fg mL^{-1} to 1.0 ng/mL. It had the potential to detect fg mL^{-1} concentrations of OTA in grape juice, outperforming HPLC with recoveries ranging from 92 % to 104 % and RSDs from 2.99 % to 6.89 %, highlighting its practical applicability and precision in the food industry. Further validation using a broader range of food matrices and comparison with established analytical methods (e.g., HPLC) would strengthen the credibility and reliability of the proposed sensor for real-world applications.

Recent biosensor advancements have also made assessing lactose and glucose levels in food samples easy. For example, an efficient lactose sensor was developed using an MNPs/CS/g-C_3N_4 composite to support cellobiose dehydrogenase immobilization and as a modifier for GCE [205]. The sensor exhibited excellent performance for detecting lactose with a low LOD (0.3 mm), wide range (0.9–100 mm), and high sensitivity (40.8 μA mm^{-1}). Moreover, it demonstrated a rapid response time of 5s. It also proved effective in quantifying lactose in real dairy products, demonstrating its capability for real samples. Although it revealed promising short-term stability over a week, the observed decrease in response after four weeks suggested potential enzyme loss during storage. Enhancing the long-term stability of biosensors would be crucial for their practical utility in real-world applications where extended storage may be required. Zhuang and his team introduced a new glucose biosensor using a hybrid composite of NiONPs, PANi nanowires, and GO on a GCE [206]. Electrochemical studies revealed the superior electrocatalytic activity of NiONSs/PANiNW/GO modified electrodes for glucose oxidation in an alkaline solution, attributed to the presence of PANi. The biosensor demonstrated high sensitivity (376.22 μA mM^{-1} cm^{-2}), a wide linear range (2 μM–5.560 mM), low LOD (0.5 μM), and excellent selectivity of glucose against interfering reagents (AA, DA, UA). Real sample analysis of fetal bovine serum showed accurate glucose determination with high recovery rates (99.2 %–100.4 %) and low RSD (1.3 %–1.9 %), highlighting its potential in various practical applications, including clinical diagnosis and food analysis. An extensive investigation of the long-term stability and durability of the sensor can determine its practical utility.

Biosensors can also detect H_2O_2, which is paramount in signalling processes associated with diverse diseases. The ability to accurately analyze H_2O_2, qualitatively and quantitatively, is crucial in sectors ranging from healthcare to industrial processes and food applications. A research group successfully engineered an extremely sensitive electrochemical biosensor to recognize H_2O_2 in food samples. They fabricated the sensor by employing PPy-GO-AuNPs nanocomposites prepared via in-situ polymerization with $FeCl_3{\cdot}6H_2O$ as an oxidizing agent [207] (Fig. 10D). The resulting PPy-GO-AuNPs/GCE exhibited significant electrocatalytic activity for detecting H_2O_2, with an LOD of 5 μM and a superior sensitivity of 41.35 μA/mM within a linear range (2.5 μM–25 10^{-3} Mm). The practical utility of this nanocomposite was verified in actual milk samples with up to 100.6 % recovery, showcasing its potential for wide-range and sensitive H_2O_2 detection in healthcare and food analysis. The study also investigated the effect of pH on H_2O_2 determination, with pH 7 identified as the optimal condition for electrochemical analysis with maximum sensor performance. However, exploring the sensor's response across a broader pH range could provide additional insights into its pH sensitivity and applicability in diverse environments.

5.2. Environmental monitoring

Ensuring the safety and well-being of humans and the environment on our planet is fundamentally dependent on continuously monitoring our surroundings, safeguarding human health, overseeing chemical processes, and upholding air and water quality. It also entails the detection of gases, infrared radiation, contaminants like organic and inorganic compounds, pesticides, heavy metals, antibiotics, poisonous gases, bacteria, and more, whether they are present in water or the atmosphere. The existence of these harmful substances poses a substantial risk to both the environment and human well-being. Monitoring and managing these dangerous and toxic elements, radiation, and microorganisms has significantly challenged the scientific community. Regarding this, adopting 2D materials as the basis for sensors has proven highly efficient and is well-suited to modern manufacturing techniques [208,209]. Materials like MOF, BP, and others possess unique properties that make them attractive for producing exceptionally sensitive sensors. These properties are a result of the inherent structures of these materials. When 2D materials are modified with various polymers, their sensitivity, selectivity, biocompatibility, and other characteristics are significantly amplified, as Zhang's team devised a nanohybrid called rGO/PEI/Pd [210]. This nanohybrid demonstrated peroxidase-simulated activity due to 3,3′,5,5′-tetramethylbenzidine (TMB) oxidation. The Hg^{2+} addition significantly enhanced the peroxidase-like activity, leading to intensified TMB oxidation and a deep blue colour in the solution. Utilizing nanohybrid, their Hg^{2+} sensing platforms achieved an LOD of 0.39 nM in a concentration range of 0.1–25 nM for double-distilled water and approximately 1 nM for actual water samples through spectrographic analysis. Importantly, this approach enabled the visual detection of 10 nM Hg^{2+} in serum and wastewater samples, showcasing potential applications in portable and straightforward environmental sample analysis for low concentrations of Hg^{2+}. Although the LOD for Hg^{2+} is reported to be low (0.39 nM), it is essential to consider the potential impact of the sample matrix and interference from other substances, which may affect the sensitivity and accuracy of detection in real-world samples.

The global problem of heavy metal ions (HMIs) pollution is a persistent concern. Consequently, the surveillance of HMIs in natural water sources is crucial and demands efforts to safeguard both environmental well-being and human safety. To address this issue, it is essential to identify these HMIs first. A graphene/PANI-modified electrode was developed using drop casting and electrospray techniques [211]. This electrode was an electrochemical sensor capable of detecting Zn^{2+}, Pb^{2+}, and Cd^{2+} simultaneously. Compared to the unmodified electrode, the modified electrode exhibited enhanced peak anodic current and electrochemical conductivity (Fig. 11A). It exhibited a linear detection range of 1–300 μg L^{-1}, with an LOD of 1.0 μg L^{-1} and 0.1 μg L^{-1} for Zn^{2+}, Cd^{2+}, and Pb^{2+}, respectively. Notably, this modified electrode displayed careful identification of the target analytes in the existence of other metal ions, i.e., Fe^{2+}, Mn^{2+}, Fe^{3+}, Co^{3+}, Ni^{2+}, and Cu^{2+}. It also effectively detected Zn^{2+}, Cd^{2+}, and Pb^{2+} in human serum at levels consistent with typical healthy adult concentrations. With recoveries between 93.8 % and 109.7 % and RSD below 9.0 %, the method demonstrated high accuracy and reproducibility, showcasing its analytical reliability for clinical applications. While the study showed the effectiveness of electrodes in human serum, their biocompatibility is not explicitly addressed. Additional research uncovered the distinctive sensitivity of poly(melamine)/graphitic-carbon nitride in detecting Pb^{2+} and Cd^{2+} (Fig. 11B). It comprised an innovative, cost-effective, and highly efficient nano-engineered PM/g-C_3N_4 nanonetwork coated on a pre-activated screen-printed carbon electrode (ASPE) [212]. This modified electrode was designed for the selective, sensitive, and concurrent electrochemical detection of toxic HMIs in environmental water sources. The created PM/g-C_3N_4/ASPE is an environmental sensor for the selective and concurrent electrochemical detection of Cd^{2+} and Pb^{2+} ions via the differential pulse voltammetry (DPV) technique. This sensor

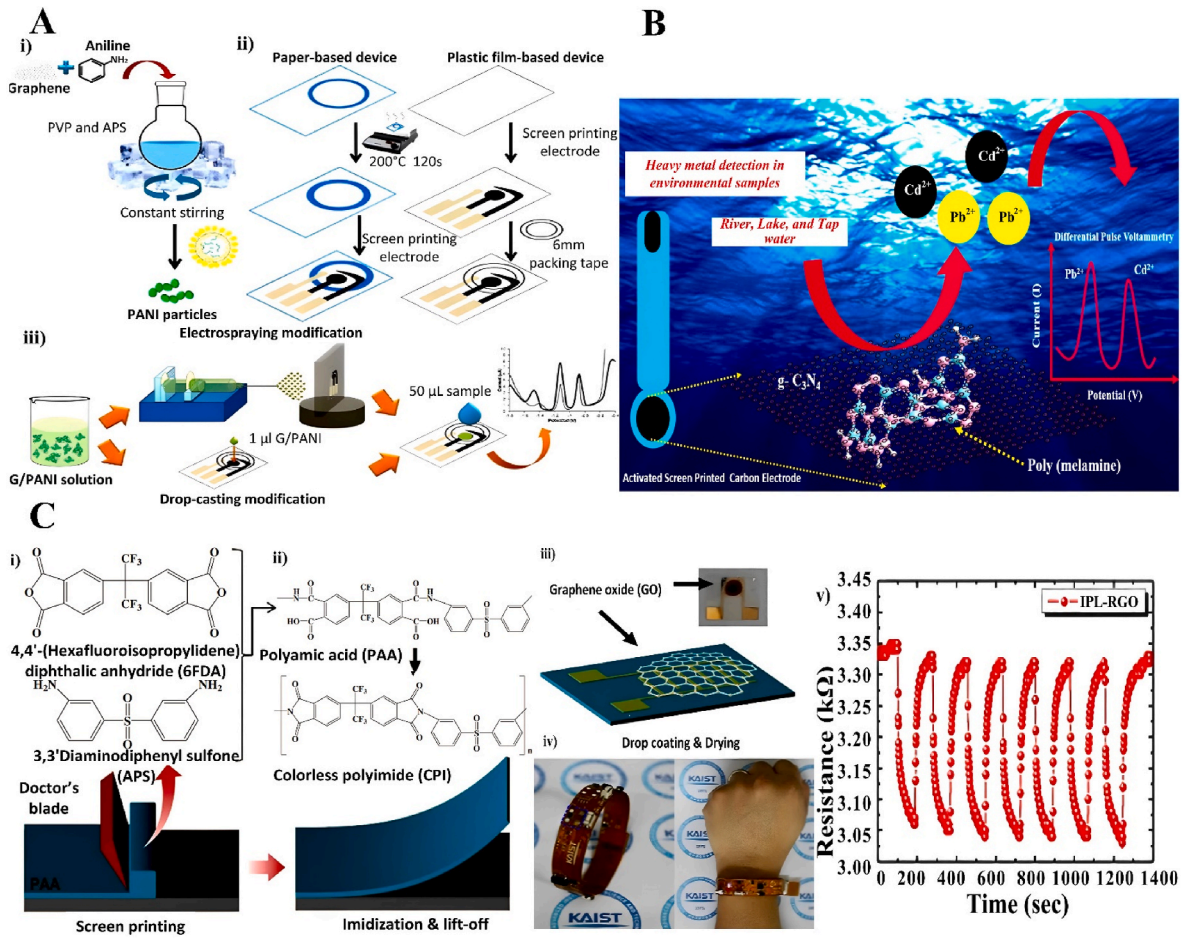

Fig. 11. A) Diagram illustrating **i)** the synthesis of G/PANI nanocomposite, **ii)** the assembly of the electrochemical sensor on plastic film/paper, and **iii)** the drop-casting and electrospray methods. Reproduced from Ref. [211]. with permission from *Elsevier*. **B)** Overview of the process and interaction mechanisms of ASPE-PM/g-C_3N_4 with HMIs in environmental water samples. Reprinted from Ref. [212]. with permission from *Elsevier*. **C)** Illustrations depicting **i)** the synthesis of polyamic acid (PAA), followed by screen printing on a glass substrate with a doctor's blade. **ii)** Subsequent imidization of PAA forms a CPI film, which can be lifted off the glass substrate. **iii)** GO sheets are coated on CPI film with an interdigitated electrodes (IDEs) pattern. **iv)** Optical images of a wearable sensor module with IPL-RGO sensor (blue dotted box). **v)** Resistance changes of the IPL-RGO sensor on the module in response to 20 p.p.m. H_2S at room temperature. Reproduced from Ref. [214]. with permission from *Nature*. (For interpretation of the references to colour in this figure legend, the reader is referred to the Web version of this article.)

exhibited outstanding selectivity and sensitivity, with an LOD of 0.02 μM for Cd^{2+} and 0.008 μM for Pb^{2+}. Interference studies revealed selective detection, while analysis of environmental water samples confirmed precise detection within the linear range (0.1–1.0 μM) with recoveries of 92.5–106.4 % for Pb^{2+} and 90–102.6 % for Cd^{2+}, indicating its potential as a reliable electrochemical sensor for HMIs. However, the sample preparation process, such as filtration and pH adjustment, may introduce errors or variability, impacting the accuracy and reliability of the analytical results.

There are not only HMIs in the environment but also a reservoir of multiple substances. One of them is bacteria, which can lead to severe illnesses. Saljooqi and co-workers introduced a sensitive biosensor utilizing a GCE enhanced with a magnetic Fe_3O_4@Au-PPy/GO nanocomposite to detect an antibacterial agent, triclosan [213]. This biosensor exhibited improved electron transfer, sensitivity (747.8 μA^{-1} μM^{-2}), linear range (0.01–1.0 μmol mL^{-1}), and a low LOD (2.5 nM) for triclosan. It also showed excellent precision (RSD 4.9 %) and stability (3.25 % decrease after 14 days at 4 °C), making them promising for triclosan detection. While the study reports acceptable sensitivity for triclosan detection, the LOD should be further optimized to meet the requirements of specific applications, especially in trace-level detection scenarios. Moreover, various hazardous gases present in the environment require effective control to prevent potential harm. Optically reduced GO NSs were introduced and fabricated on a highly thermally stable, transparent, colourless polyimide (CPI) substrate. This result was achieved by subjecting a GO-coated CPI film to intense pulsed light (IPL) irradiation (Fig. 11C). These flexible RGO sheets were gas-sensing layers suitable for wearable systems [214]. The ultrafast IPL irradiation process created RGO NSs on the CPI film in just 4 ms without damaging a plastic substrate. These IPL-RGO sheets displayed significantly enhanced chemical detection capabilities for gases like H_2, H_2S, and C_2H_5OH, with detection ranges and limits of 1–20 ppm and 20 ppm, respectively. In contrast, the original GO sheets showed no response to these gases. These sensing properties remained consistent after subjecting the IPL-RGO NSs on the polymer film to mechanical deformation through 104 bending cycles. While the study demonstrated the IPL-RGO sensor's stability under controlled bending conditions, its performance in real-life situations where the sensor may undergo repeated and unpredictable mechanical stress remains unclear. Assessing its durability in various environmental conditions, such as temperature fluctuations, humidity, and mechanical vibrations, would provide a more comprehensive understanding of its practical utility.

Contamination from pesticides, especially organo-phosphorus ones, is very harmful to people and animals. These pesticides can be found in water bodies and accumulate on fruits and vegetables, posing a potential risk to consumers by affecting the functions of the human body and even causing harm through the inhibition of AChE activity. That is why finding effective ways to detect, identify, and measure pesticides for

human well-being is essential. Electrochemical sensors, using 2D materials and their devices, have been effectively employed to detect pesticides [215]. For instance, Li and colleagues detected carbofuran in tomatoes using an electrochemical biosensor that immobilized AChE on an electrode modified with a con A/PDA-rGO-GNP composite. The biosensor demonstrated a broad detection range of 5–200 mg/kg, with a low LOD of 0.012 mg/kg [216]. Recovery measurements on tomato samples achieved a 101 % recovery for 10 mg/kg and 90 % recovery for 100 mg/kg, with an analysis time of 15–20 min, indicating accurate and rapid determination. Additionally, it demonstrated good repeatability (3.1 % RSD) and stability, retaining 80 % of the initial current after four weeks of storage at 4 °C. However, its specificity to carbofuran in the presence of other compounds commonly found in tomatoes must be thoroughly evaluated.

5.3. Detection of disease biomarkers

A biomarker is a biological signal to predict clinical outcomes, offering a more practical and cost-effective alternative to directly observing challenging endpoints or intermediate outcomes. Clinical biomarkers, applied in disease screening, diagnosis, and monitoring, serve diverse roles, such as prognostic indicators, supporting personalized therapies, anticipating adverse drug reactions, distinguishing cell types, and contributing to pharmacodynamic studies [217]. Achieving highly selective and sensitive detection of biomarkers using bioreceptor-free sensors has proven to be a significant challenge. To address this issue, 2D materials with exceptional properties are utilized, and their integration with polymers enhances their sensitivity, selectivity, and biocompatibility in disease biomarker detection. For example, early detection of cancer cells can be done by electronic biosensors. Joshi and co-workers developed a portable biosensor for instantaneous sensing of a cancer biomarker called carcinoembryonic antigen (CEA) at room temperature [218]. This biosensor utilized an innovative poly[(1,4-phenylene)-alt-(3,6-(1,2,4,5-tetrazine)/3,6-(1,2,4,5-dihydrotetrazine))] (PhPTz) as a matrix and rGO as a conducting layer for immobilizing CEA antibodies. The nitrogen-rich semiconducting PhPTz offered advantages such as efficient immobilization of anti-CEA and transportation of charge density variations to the rGO layer (Fig. 12A). As a result, the device displayed a response of 2.75–33.7 μA across a wide range from 0.25 pg/mL to 0.08 ng/mL for CEA concentrations. Using a modest algorithm, a portable read-out circuit with a voltage divider circuit and an Arduino UNO achieved 100 % prediction accuracy for classifying CEA concentrations. This technology holds potential for POC cancer treatment and diagnosis. The focus on detecting only CEA limits the biosensor's broader applicability. Further refinement and validation of the algorithm for predicting other analytes are needed to ensure accurate real-time monitoring in diverse clinical settings.

By adsorbing MXene on exosome-cultured AuNP/poly (N-isopropyl acrylamide)/GCE biosensors, it is fabricated to detect breast cancerous cells (MCF-7). Initially, these exosomes were grown on AuNP/PNIPAM/GCE by integrating an aptamer with an amino-functionalized layer [219]. Subsequently, MXene-based nanoprobes were synthesized after modifying the surface of MXene electrostatically with many aptamers

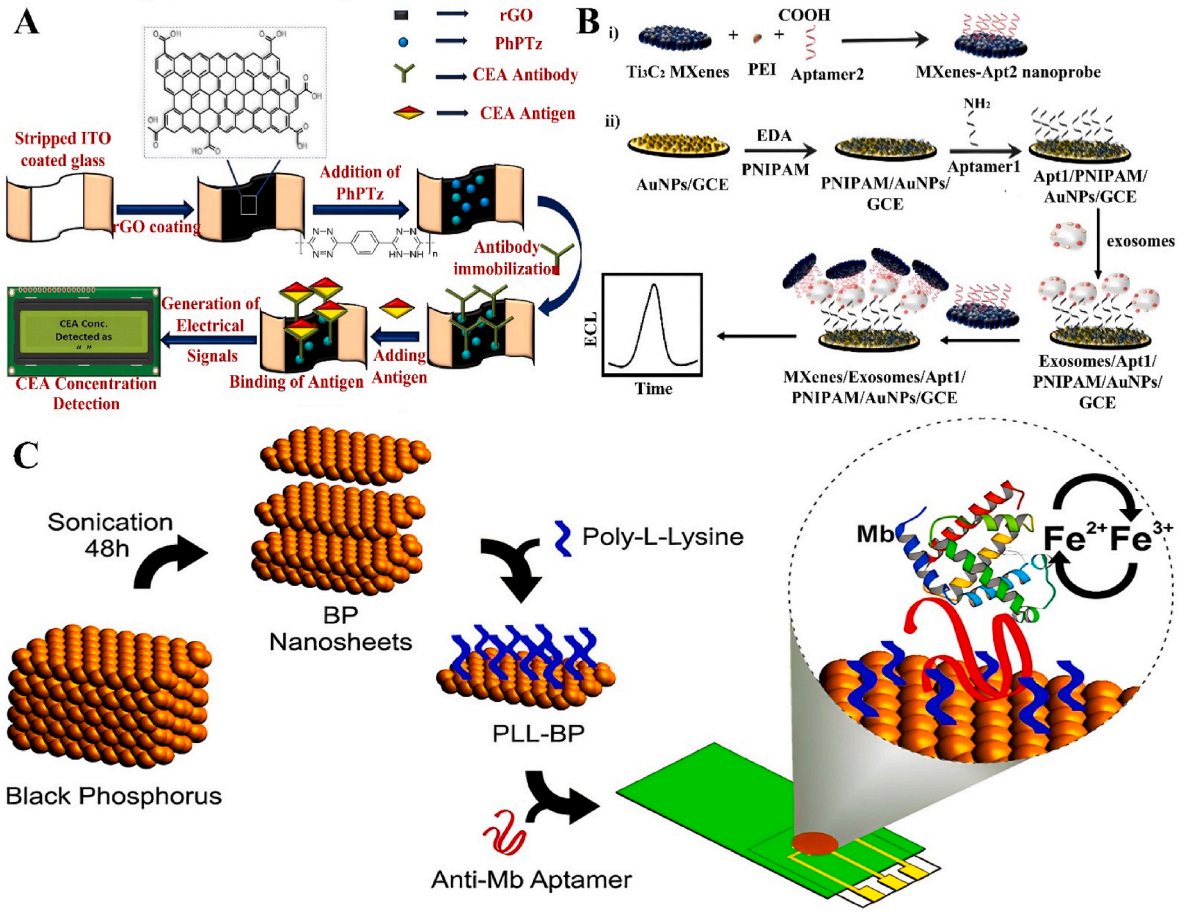

Fig. 12. A) Diagram illustrating the sequential fabrication stages of the electronic biosensor. Reproduced from Ref. [218]. with permission from *Nature*. **B)** Principle behind the signal amplification strategy in the ECL biosensor for detecting exosome activity. Reprinted from Ref. [219]. with permission from *Elsevier*. **C)** Illustrated workflow for liquid-phase exfoliation of BP nanosheets and their surface modification to develop a biointerface on an electrode for Mb detection. Reproduced from Ref. [221]. with permission from *American Chemical Society*.

and PEI (as shown in Fig. 12B). Research results specified that the PL intensity of the luminol solution is five times higher for the manufactured nanoprobe compared to pure GCE, supporting the usage of MXene-based aptamer nanoelectrodes for exosome sensors. This system exhibited a detection range of 500 to 5,000,000 particles per microliter and an LOD of approximately 125 particles per microliter. Its reproducibility (RSD: 3.2 %–4.5 %) and stability showcased its potential for clinical serum sample assays. In this study, MXene nanosheets served a dual purpose by catalyzing the ECL process of luminol due to their outstanding catalytic properties and conductivity and offering an increased surface area to efficiently load the aptamer Apt2, thereby facilitating the capture of exosomes. However, the scalability and cost-effectiveness of the biosensor fabrication process need to be considered for widespread adoption in clinical settings. Costly materials or complex fabrication procedures may hinder large-scale production and accessibility.

Several biomarkers cause oxidative stress, which is the root cause of several diseases like neurodegenerative diseases, cardiovascular diseases, kidney diseases, lung diseases, bone, blood, and liver disorders, and many other infectious diseases. Oxidative stress (OS) is defined as a situation in which there is an imbalance between the formation of ROS and the presence of antioxidants that can neutralize them. The degree of OS can be assessed by examining the levels of different biomarkers [19]. According to one study, using an electrochemical technique, a Prussian blue-polythiophene-GO membrane biosensor was prepared to detect the level of one primary OS-causing biomarker, such as H_2O_2, in a range of 1.0–100 μM [220]. In the case of cardiovascular disease, numerous cardiac biomarkers have shown great interest due to their ability to serve as indicators of cardiovascular incidents. Among these markers, serum cardiac biomarkers, with myoglobin (Mb) particularly noteworthy, hold significant importance in clinical diagnosis. An elevated level of myoglobin signifies myocardial injury and has now established itself as the gold standard for diagnosing acute myocardial infarction (AMI), often known as a heart attack. To address this problem, Vinod and his colleagues reported the electrochemical analysis of the redox-active cardiac biomarker Mb with nanostructured BP electrodes functionalized with aptamers. This process involved the direct measurement of electron transfer [221]. The few-layer BP nanosheets, synthesized for this purpose, were treated with pLL to enhance their interaction with anti-Mb DNA aptamers generated on the nanostructured electrode (Fig. 12C). The resulting biosensor platform showcased an exceptional LOD of 0.524 pg mL^{-1} and high sensitivity of 36 μA pg^{-1} mL cm^{-2} for Mb. It covered a dynamic response range of 1.0 pg mL^{-1} to 16 μg mL^{-1} in serum samples, setting the stage for forming POC systems for multiplexed cardiovascular disease diagnosis in complex human samples. Still, the biocompatibility and potential cytotoxic effects of BP nanosheets, PLL, and the functionalized aptasensor need thorough investigation before clinical translation.

5.4. Wearable bioelectronics and E-skins

Wearable bioelectronic devices incorporating 2D materials have been extensively researched. This section explores notable examples of such devices, particularly in skin monitoring, which is an essential application for 2D material-based biosensors. These sensors display a capacity for secure and personalized attachment to the skin, ensuring sustained sensitivity over extended durations. The distinctive interface with human skin presents a valuable research domain for monitoring temperature, pressure, touch, and diseases [15]. Consequently, due to their unique physicochemical advantages, a skin-sensing device (E-skin) incorporating 2D nanomaterials has been developed for detecting various human body indicators, presenting a significant advancement over traditional materials-based E-skins in the past decade [222,223].

The growing focus of today's society on personal health has led to the thriving development of wearable physiological and physical signal monitoring medical devices for treating, diagnosing diseases, and assessing daily health. By utilizing functionalized 2D materials, these wearable electronic devices can offer high sensitivity, softness, and versatility, enabling precise detection of indicators like sweat acidity, alkalinity, blood glucose concentration, etc. Here, a novel and practical electrochemical sweat pH biosensor was designed to continuously track hydrogen-ion levels in human sweat [224]. A flexible electrode on a PET substrate was crafted using screen-printing technology by incorporating fluoroalkyl silane functionalized $Ti_3C_2T_x$ and PANI membrane. PANI-doped F–$Ti_3C_2T_x$ enhanced responsiveness, pH sensitivity (−41.91 mV per pH), and reversibility due to its superhydrophobic characteristics. When the resulting pH sensor was used to monitor human sweat pH in real-time during exercise, it demonstrated accurate detection on curved surfaces and pH values above 8 for both genders, indicating its versatility and applicability in health monitoring and environmental sensing (Fig. 13A). This study presented a practical solution for online monitoring the pH of human sweat using a reliable MXene-based mini pH sensor. In addition to sweat sensing, polymer-functionalized 2D materials are extensively valuable for humidity sensing. The WS_2 film was a robust high humidity sensor, demonstrating remarkable sensitivity (up to 2357) for 90 % humidity and repeatability in flat and mechanically flexible states when exposed to periodic saturation with moisture gas [225]. Moreover, when integrated into a PDMS membrane, the sensor flexibility allowed for repeatable water moisture sensing even under bent curvature down to 5 mm and withstands up to 40 % elastic stretch without significant performance degradation. Furthermore, a transparent, flexible, and stretchable sensor is developed using graphene electrodes and a thinner PDMS membrane as a substrate. When laminated onto the skin, this sensor showed repeatable humidity responses under compressing, stretching, and relaxing states. Also, real-time monitoring of human breathing revealed its effectiveness in tracking fast (1 s) and slow (5 s) breathing patterns, showcasing significant potential for healthcare applications like real-time dynamic monitoring of human breath. However, further optimization of electrode structures may be required for improved sensitivity, as current levels achieved by rigid and flexible devices are low (nA and pA levels, respectively).

Furthermore, these materials enable the visualization of various physical signals, like pressure and strain. Pressure sensors have been successfully developed using 2D materials with capacitive, triboelectric, and piezoresistive effects. For example, a very flexible, repeatable, and highly sensitive self-powered tactile biosensor based on triboelectric effects was developed with wrinkled PDMS/MXene composite films [226]. The resulting composite film, generated through UV ozone treatment, introduced –OH groups and surface wrinkles on PDMS, while MXene addition introduced –F and O-containing groups, collectively contributing to superior sensitivity of 0.06 V/Pa during 80–800 Pa and 0.18 V/Pa during 10–80 Pa. The results suggested that this sensitivity is higher compared to other self-powered tactile sensors and has the potential for monitoring complex human physiological indications and replicating human touch sensations in E-skin technology (Fig. 13B). Yet, the potential impact of factors such as temperature, humidity, and exposure to contaminants that may influence the performance and sensitivity of sensors needs to be addressed.

From prior research, it is evident that various compressible and elastic carbon aerogels (CECAs) composed of CNTs, graphene, and 2D nanomaterials have demonstrated effective piezoresistive behaviour. These materials are highly suitable for sensitive sensors in wearable E-skins and bioelectronics. A light CECA was developed to address challenges related to insufficient interaction between nanomaterials by employing bacterial cellulose (BC) as a nano-binder to link Ti_3C_2 nanosheets [227]. The resulting CECAs exhibited excellent elasticity and compressibility (up to 99 % strain for over 10,000 cycles), as shown in Fig. 13C. In contrast, the device demonstrated high sensitivity (12.5 kPa^{-1}) over a broad working pressure range (0–10 kPa) and good linearity, reaching 95 % workable strain. Notably, the sensor displayed sensitivity to subtle pressure and strain changes, making it capable of

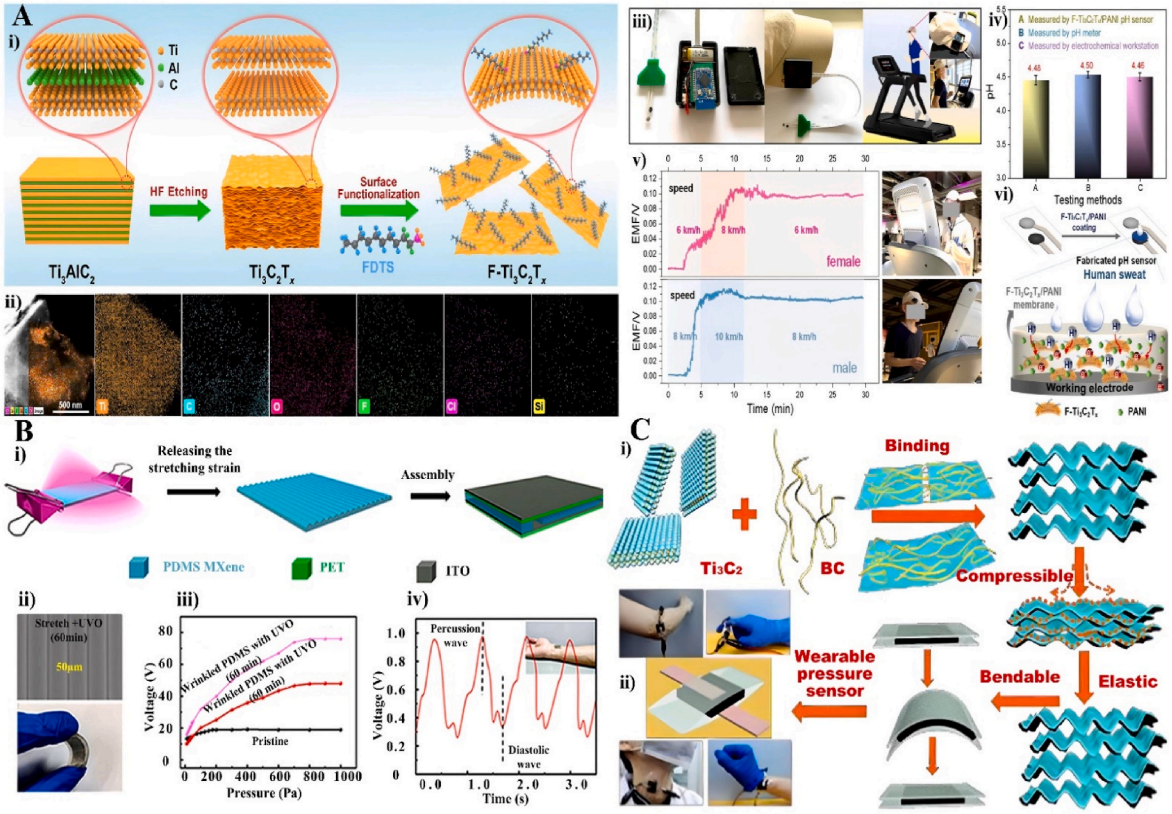

Fig. 13. A) i) Preparation and surface modification of F–$Ti_3C_2T_x$ NSs. **ii)** TEM image and element mappings of uniform Ti, C, O, F, Cl, and Si distribution in NSs. **iii)** Wearable pH-sensing device image with a Li-ion battery, mini potentiometer, F–$Ti_3C_2T_x$/PANI pH sensor, and sports cap for immobilization. **iv)** pH sensor for continuous real-time monitoring of sweat pH. **v)** Comparison of human sweat pH measured by different methods. **vi)** F–$Ti_3C_2T_x$/PANI compound systematic functioning as an H_3O^+-selective membrane and intermediate solid contact layer in SC-ISEs for sensing human sweat pH. Reproduced from Ref. [224]. with permission from *American Chemical Society*. **B) i)** Fabrication of wrinkled PDMS/MXene composite film. **ii)** SEM images of PDMS surface and cross-section and flexibility demonstration (PDMS/MXene). **iii)** Performance between PDMS/MXene and PDMS. **iv)** Real-time V-t curve of tactile sensor demonstrating pulse in action. Reproduced from Ref. [226]. with permission from *Elsevier*. **C) i)** C-MX/BC-x carbon aerogel synthesis with bendable ability. **ii)** C-MX/BC-2 applications in biosignals detection, plus the assembly of a sensor (center). Reproduced from Ref. [227]. with permission from *Elsevier*.

recording variations in human speech when attached to the throat. When placed on the human throat, the sensor captured electrical changes while uttering words like “carbon” and “super.” Scientists anticipated that these sensors on CECA, with their ultra-high linear sensitivity, superior mechanical properties, and low LOD (1.0 Pa), hold significant promise for future applications in wearable sensing devices. Although it demonstrated remarkable fatigue resistance and structural stability under cyclic compression, its long-term durability under real-world conditions, such as exposure to moisture, temperature variations, and mechanical wear, needs further investigation.

6. Challenges and future directions

Recent advancements in 2D materials have found widespread use, especially in biosensors and bioelectronics. Numerous studies have shown that new 2D materials with polymer functionalities can be used in bioelectronic devices. However, there is still a long way to go before they can be used in real life.

The primary challenge lies in optimizing the synthetic process of polymer-functionalized 2D materials for practical applications, where factors like uniformity, morphology, pore diameter, and surface area significantly impact their properties. Complex synthetic methods for bioelectronic devices pose a risk of uncontrollability during production expansion, hindering ideal structural features and specialized functions. The stability of materials prepared through such methods raises concerns, potentially causing structural decomposition and collapse in complex environments. Moreover, for the successful commercialization of bioelectronic devices, it is essential to have cost-effective manufacturing methods that allow for high throughput and large-scale customization. Traditional manufacturing approaches like etching processes, photolithography, and high-vacuum deposition require expensive equipment and are time-intensive, leading to higher product costs. Advanced techniques like printing offer the potential for mass production, uniform nanosheet sizes, and reduced manufacturing expenses. Additionally, achieving favourable biocompatibility requires that the fabrication process avoid using toxic materials or solvents. Innovative manufacturing technologies are crucial to ensuring that polymer-functionalized 2D materials are compatible with processing parameters.

Second, the interactions between biological entities and polymer-functionalized 2D nanomaterials are less covered. Understanding how these materials influence signal pathways and control biological processes, including interactions with structural proteins and genetic materials, can open various opportunities to discover biosensing applications and enhance the current LOD. This knowledge deepens our understanding of how functionalized 2D material characteristics, such as size, shape, and chemical composition, impact specific biological responses, biocompatibility, and cytotoxicity. Although the endocytosis pathways and biological activities of specific nanosheets in cancerous cells have been explored, such studies are in their infancy, and more endeavours are required to delve into the interactions of various polymer/2D materials with biomolecules. For instance, Tao et al. [228] introduced a doxorubicin hydrochloride-loaded delivery platform utilizing BP nanosheets. Their work innovatively uncovered the endocytosis pathways as well as the biological functions of PEGylated BP

nanosheets, illustrating the transportation route via 'micropinocytosis,' 'late endosomes,' and 'lysosomes.' with autophagy playing a role in the breakdown of PEGylated BP nanosheets.

Third, the long-term stability of polymer-functionalized 2D materials and their application in sensing platforms have been underexplored in existing research. Stability is crucial in developing sensing devices, particularly those intended for continuous and extended analyte monitoring. Achieving long-term stability necessitates a combination of characteristics such as high skin compatibility, environmental resilience, strong binding properties, mechanical robustness, and flexibility. Although efforts have been made to enhance the functionality of 2D materials with polymers to meet these requirements, the stability of these composites tends to diminish over time, an aspect that remains inadequately investigated. Addressing this challenge involves a strategic approach to polymer selection and utilization, encompassing factors such as polymer type, functionalization methods, and thickness. The ability to tailor the stability of polymer and 2D materials is crucial for their diverse applications. For instance, reusable devices must endure repeated attachment and detachment cycles to ensure consistent performance. Therefore, future research endeavours should prioritize investigating the long-term stability of these materials to develop durable sensing platforms with extended lifespans.

Fourth, each emerging 2D material possesses unique advantages, yet its limitations cannot be overlooked. While polymers have significantly enhanced the properties of 2D materials for biosensing applications, their widespread application in clinical diagnosis, particularly for POCT, remains challenging. Challenges include miniaturization of instruments, efficient and stable loading between nano-carriers and targets, and probe cytotoxicity or interference. Given the suitability of simple and convenient biosensors for POCT, the design of automated sample devices and portable instruments is crucial. Hence, novel approaches leveraging nanotechnology and signal amplification strategies are imperative for practical and accurate clinical applications. For example, creating hybrid nanomaterials with diverse materials, including but not limited to 2D materials, proves effective in avoiding inherent shortcomings. Combining the benefits of $Ti_3C_2T_x$ NSs with efficient charge transfer and WSe_2 NSs with abundant active sites, a $Ti_3C_2T_x/WSe_2$ hybrid biosensor for volatile gas sensing is meticulously engineered [229]. The resulting hybrid material forms numerous heterojunction interfaces, significantly increasing the adsorption of oxygen species and consequently releasing more electrons back to the channel, thereby improving the detection sensitivity of oxygen-containing volatile organic compounds by over 12 times. Moreover, material hybridization can yield intriguing material interfaces, enhancing recognition ability and signal amplification while mitigating material defects. Furthermore, recent years have also seen remarkable advancements in nanotechnology, with numerous 2D materials being employed in modified signal amplification strategies and sensitivity, such as nucleic acid signal amplification, multivalent aptamer, and dual-signal probes. These methods significantly enhance signal throughput, speed, sensitivity, and simplicity and reduce sample consumption, enabling the detection of biomolecules at the single-cell or single-molecule level, with promising potential for practical applications.

Lastly, getting functionalized 2D material-based biosensors to find biological or chemical molecules on the market is much harder than getting activity-tracking devices or regular lab-based biosensors on the market. This complexity arises from the need for continuous biosensing and accurate measurement of these molecules. Here's a detailed breakdown of the key considerations and potential solutions:

1. A reliable power supply is crucial for the robust performance of bioelectronics. However, conventional power sources tend to be bulky and rigid, and they may contain hazardous materials that are not ideal for soft, curvilinear, and limited-space biological organisms. Solutions such as lithium-ion and lithium-polymer batteries, harvesting methods, biofuel cells, kinetic solar cells, and wireless power transfer methods are viable for meeting energy needs.
2. Biosensor devices generate massive amounts of data during experimental testing. Future compatibility with cloud technology and AI could enable medical professionals to monitor patients remotely, allowing them to recuperate at home. Advanced wireless communication technologies like Wi-Fi, NFC, Zigbee, Bluetooth, body area networks, and new protocols such as LBE and 6LoWPAN can also enhance sensor accuracy and timeliness.
3. Thin, soft-skin bioelectronics are compliant and can withstand high-cycle fatigue tests with repetitive mechanical deformations. However, their durability under long-term, dynamic skin movements such as stretching, compressing, and twisting requires robust adhesion and device configuration. Developing ultrathin biocompatible adhesives with good mechanical robustness is one approach. Still, these devices often suffer from limited stretchability and mechanical durability due to the trade-off between thinness and robustness. A thorough understanding and investigation of materials and rigid-soft interface design are necessary to prevent interface failure over long-term use.
4. Ensuring biofouling safety, longevity, and prevention is critical for overall performance and practicality. Wearable sensing devices must undergo rigorous testing to ensure stability and detection accuracy. Surface contamination, which reduces detection accuracy, poses a significant challenge. We should strengthen anti-fouling and effective calibration mechanisms to ensure stability during long-term use. Nonspecific binding of proteins, cells, or macromolecules can cause bioaccumulation, which can lead to sensing drift, especially in wearable oral biosensors operating in high protein environments like saliva. Protective coatings can minimize the impact of fouling and eliminate interference from electroactive substances.
5. To manage overall costs for successfully commercializing functionalized 2D materials-based biosensors, optimizing production processes, exploring specialized equipment and personnel, and utilizing cost-effective materials are essential. Additionally, joint efforts from materials and device engineers, data scientists, and medical professionals are required for technical progress. Closer involvement of users and caregivers is necessary before addressing common biosensor design issues such as bioreceptor selection, material biocompatibility, and sample matrix challenges. Sensor design teams must prioritize understanding the performance requirements of various users, including food consumers, environmental monitors, citizens using public services, healthcare workers, and regulatory agencies. Establishing key performance indicators in advance is vital to ensuring the biosensor's performance aligns with the desired quality of service (QoS) based on biosensor data.

In summary, integrating polymer-functionalized 2D materials with flexible circuit systems yields bioelectronic devices with versatile sensing capabilities, making them valuable for human body signal detection. Technological advancement and material performance are expected to enhance these devices, enabling high-quality disease monitoring. A profound understanding of emerging polymer-based 2D materials and innovative technologies promises to achieve biocompatible and highly effective bioelectronics and biosensors. It is expected that 2D nanomaterials will soon progress to the stage of clinical research and practical application.

7. Conclusion

The exploration of bioelectronics traces its roots back to the 18th century when Luigi Galvani conducted experiments on the electrical response of detached frog legs. On the other hand, research on 2D materials is still in its early stages, presenting opportunities and challenges for their integration into bioelectronic devices. This review delves into the recent advancements in utilizing 2D materials in bioelectronics,

examining the progress in fundamental research and device development. 2D materials, owing to their atomic thinness, high transparency, large specific area, distinctive optoelectrical properties, and biocompatibility, play a crucial role in the construction of biosensors and wearable bioelectronic devices. However, addressing significant challenges, particularly those associated with using 2D nanomaterials in biomedical science, is crucial before their therapeutic application. Key biomedical challenges include biological compatibility, adaptability, functionality, biocompatibility, and nano bio-surface characteristics. Polymers and 2D nanomaterials are essential to addressing biological issues within the human body. Polymer-functionalized 2D materials are more pliable and chemically attack-resistant than other 2D materials, offering advantages. Polymers can be easily functionalized or combined to form composites through covalent and non-covalent functionalization methods, surpassing conventional 2D materials. After the literature review, the authors can suggest that polymers are a promising choice for enhancing the traditional performance of 2D materials in biosensors and bioelectronics. This review paper closely examines how biocompatible polymers are added to the surfaces of 2D nanomaterials like g-C3N4, the graphene family, MXene, BP, MOF, and TMDCs. It focuses on their current state, physicochemical structures, synthesis methods, material properties, and uses in biosensors and bioelectronics.

CRediT authorship contribution statement

Tahreem Zahra: Writing – original draft, Conceptualization. **Umme Javeria:** Writing – review & editing, Conceptualization. **Hasan Jamal:** Writing – review & editing. **Mirza Mahmood Baig:** Writing – review & editing. **Farid Akhtar:** Writing – review & editing, Supervision. **Urooj Kamran:** Writing – review & editing, Supervision, Conceptualization.

Declaration of competing interest

The authors declare that they have no known competing financial interests or personal relationships that could have appeared to influence the work reported in this paper.

Data availability

No data was used for the research described in the article.

Acknowledgements

Urooj Kamran gratefully acknowledges the financial support provided by Luleå University of Technology, Luleå, Sweden, through the Excellent Postdoctoral Fellowship Program (grant number: 228121). Farid Akhtar acknowledges the funding support from Formas, The Swedish Research Council for Sustainable Development (grant number: 2022-01989). In addition, the authors also extend their gratitude to Korea University, Seoul, Republic of Korea; University of Narowal, Narowal, Pakistan; Daegu Gyeongbuk Institute of Science & Technology, Daegu, Republic of Korea; and University of Ulsan, Ulsan, Republic of Korea for their time, assistance, and guidance in completion of this review paper.

References

[1] Y. Fang, L. Meng, A. Prominski, E.N. Schaumann, M. Seebald, B. Tian, Recent advances in bioelectronics chemistry, Chem. Soc. Rev. 49 (2020) 7978–8035.
[2] H. Yuk, B. Lu, X. Zhao, Hydrogel bioelectronics, Chem. Soc. Rev. 48 (2019) 1642–1667.
[3] I. Jeerapan, J.R. Sempionatto, J. Wang, On-body bioelectronics: wearable biofuel cells for bioenergy harvesting and self-powered biosensing, Adv. Funct. Mater. 30 (2020) 1906243.
[4] J. Shi, Y. Fang, Nanowire Bioelectronics, Springer, Singapore, 2019, pp. 337–352.
[5] P. Kang, M.C. Wang, S. Nam, Bioelectronics with two-dimensional materials, Microelectron. Eng. 161 (2016) 18–35.
[6] A.Y.S. Tan, N.W. Lo, F. Cheng, M. Zhang, M.T.T. Tan, S. Manickam, K. Muthoosamy, 2D carbon materials based photoelectrochemical biosensors for detection of cancer antigens, Biosens. Bioelectron. 219 (2023) 114811.
[7] E. Macchia, F. Torricelli, P. Bollella, L. Sarcina, A. Tricase, C. Di Franco, R. Österbacka, Z.M. Kovács-Vajna, G. Scamarcio, L. Torsi, Large-area interfaces for single-molecule label-free bioelectronic detection, Chem. Rev. 122 (2022) 4636–4699.
[8] D. Jiang, C. Yang, Y. Fan, H.-M. Polly Leung, K. Inthavong, Y. Zhang, Z. Li, M. Yang, Ultra-sensitive photoelectrochemical aptamer biosensor for detecting E. coli O157:H7 based on nonmetallic plasmonic two-dimensional hydrated defective tungsten oxide nanosheets coupling with nitrogen-doped graphene quantum dots ($dWO_3 \bullet H_2O$@N-GQDs), Biosens. Bioelectron. 183 (2021) 113214.
[9] Y. Wang, H. Haick, S. Guo, C. Wang, S. Lee, T. Yokota, T. Someya, Skin bioelectronics towards long-term, continuous health monitoring, Chem. Soc. Rev. 51 (2022) 3759–3793.
[10] A. Zhang, J.-H. Lee, C.M. Lieber, Nanowire-enabled bioelectronics, Nano Today 38 (2021) 101135.
[11] G. Hong, X. Yang, T. Zhou, C.M. Lieber, Mesh electronics: a new paradigm for tissue-like brain probes, Curr. Opin. Neurobiol. 50 (2018) 33–41.
[12] X. Dai, G. Hong, T. Gao, C.M. Lieber, Mesh nanoelectronics: seamless integration of electronics with tissues, ACS Publ. 51 (2018) 309–318.
[13] S.K. Rastogi, A. Kalmykov, N. Johnson, T. Cohen-Karni, Bioelectronics with nanocarbons, J. Mater. Chem. B 6 (2018) 7159–7178.
[14] S. Arshavsky-Graham, N. Massad-Ivanir, E. Segal, S. Weiss, Porous silicon-based photonic biosensors: current status and emerging applications, Anal. Chem. 91 (2018) 441–467.
[15] F. Chen, Q. Tang, T. Ma, B. Zhu, L. Wang, C. He, X. Luo, S. Cao, L. Ma, C. Cheng, Structures, properties, and challenges of emerging 2D materials in bioelectronics and biosensors, InfoMat 4 (2022) e12299.
[16] S. Alwarappan, N. Nesakumar, D. Sun, T.Y. Hu, C.-Z. Li, 2D metal carbides and nitrides (MXenes) for sensors and biosensors, Biosens. Bioelectron. 205 (2022) 113943.
[17] M. Mohammadniaei, A. Koyappayil, Y. Sun, J. Min, M.-H. Lee, Gold nanoparticle/MXene for multiple and sensitive detection of oncomiRs based on synergetic signal amplification, Biosens. Bioelectron. 159 (2020) 112208.
[18] V. Chaudhary, V. Khanna, H.T. Ahmed Awan, K. Singh, M. Khalid, Y.K. Mishra, S. Bhansali, C.-Z. Li, A. Kaushik, Towards hospital-on-chip supported by 2D MXenes-based 5th generation intelligent biosensors, Biosens. Bioelectron. 220 (2023) 114847.
[19] M. Garg, A. Gupta, A.L. Sharma, S. Singh, Advancements in 2D materials based biosensors for oxidative stress biomarkers, ACS Appl. Bio Mater. 4 (2021) 5944–5960.
[20] N. Dwivedi, C. Dhand, P. Kumar, A.K. Srivastava, Emergent 2D materials for combating infectious diseases: the potential of MXenes and MXene–graphene composites to fight against pandemics, Mater. Adv. 2 (2021) 2892–2905.
[21] K. Deshmukh, T. Kovářík, S.K. Khadheer Pasha, State of the art recent progress in two dimensional MXenes based gas sensors and biosensors: a comprehensive review, Coord. Chem. Rev. 424 (2020) 213514.
[22] M. Marian, D. Berman, D. Nečas, N. Emami, A. Ruggiero, A. Rosenkranz, Roadmap for 2D materials in biotribological/biomedical applications – a review, Adv. Colloid Interface Sci. 307 (2022) 102747.
[23] P. Kumbhakar, C. Chowde Gowda, P.L. Mahapatra, M. Mukherjee, K.D. Malviya, M. Chaker, A. Chandra, B. Lahiri, P.M. Ajayan, D. Jariwala, A. Singh, C.S. Tiwary, Emerging 2D metal oxides and their applications, Mater. Today 45 (2021) 142–168.
[24] N. Rohaizad, C.C. Mayorga-Martinez, M. Fojtů, N.M. Latiff, M. Pumera, Two-dimensional materials in biomedical, biosensing and sensing applications, Chem. Soc. Rev. 50 (2021) 619–657.
[25] D. Jiang, Z. Liu, Z. Xiao, Z. Qian, Y. Sun, Z. Zeng, R. Wang, Flexible electronics based on 2D transition metal dichalcogenides, J. Mater. Chem. A 10 (2022) 89–121.
[26] M. Dadashi Firouzjaei, M. Karimiziarani, H. Moradkhani, M. Elliott, B. Anasori, MXenes: the two-dimensional influencers, Mater. Today Adv. 13 (2022) 100202.
[27] S. Yu, H. Tang, D. Zhang, S. Wang, M. Qiu, G. Song, D. Fu, B. Hu, X. Wang, MXenes as emerging nanomaterials in water purification and environmental remediation, Sci. Total Environ. 811 (2022) 152280.
[28] G. Liao, F. He, Q. Li, L. Zhong, R. Zhao, H. Che, H. Gao, B. Fang, Emerging graphitic carbon nitride-based materials for biomedical applications, Prog. Mater. Sci. 112 (2020) 100666.
[29] M. Ismael, A review on graphitic carbon nitride (g-C3N4) based nanocomposites: synthesis, categories, and their application in photocatalysis, J. Alloys Compd. 846 (2020) 156446.
[30] J. Yang, Z. Zeng, J. Kang, S. Betzler, C. Czarnik, X. Zhang, C. Ophus, C. Yu, K. Bustillo, M. Pan, J. Qiu, L.-W. Wang, H. Zheng, Formation of two-dimensional transition metal oxide nanosheets with nanoparticles as intermediates, Nat. Mater. 18 (2019) 970–976.
[31] M. Luo, T. Fan, Y. Zhou, H. Zhang, L. Mei, 2D black phosphorus–based biomedical applications, Adv. Funct. Mater. 29 (2019) 1808306.
[32] Y. Sui, J. Zhou, X. Wang, L. Wu, S. Zhong, Y. Li, Recent advances in black-phosphorus-based materials for electrochemical energy storage, Mater. Today 42 (2021) 117–136.
[33] S. Li, L. Ma, M. Zhou, Y. Li, Y. Xia, X. Fan, C. Cheng, H. Luo, New opportunities for emerging 2D materials in bioelectronics and biosensors, Curr. Opin. Biomed. Eng. 13 (2020) 32–41.

[34] Q. Wu, N. Li, Y. Wang, Y. liu, Y. Xu, S. Wei, J. Wu, G. Jia, X. Fang, F. Chen, X. Cui, A 2D transition metal carbide MXene-based SPR biosensor for ultrasensitive carcinoembryonic antigen detection, Biosens. Bioelectron. 144 (2019) 111697.

[35] J. Yoon, T. Lee, J.-W. Choi, Development of bioelectronic devices using bionanohybrid materials for biocomputation system, Micromachines 10 (2019) 347.

[36] O. Parlak, S. Beyazit, M.J. Jafari, B.T.S. Bui, K. Haupt, A. Tiwari, A.P.F. Turner, Light-triggered switchable graphene–polymer hybrid bioelectronics, Adv. Mater. Interfac. 3 (2016) 1500353.

[37] Q. Wang, X. Pan, C. Lin, H. Gao, S. Cao, Y. Ni, X. Ma, Modified Ti3C2TX (MXene) nanosheet-catalyzed self-assembled, anti-aggregated, ultra-stretchable, conductive hydrogels for wearable bioelectronics, Chem. Eng. J. 401 (2020) 126129.

[38] B. Wang, Y. Sun, H. Ding, X. Zhao, L. Zhang, J. Bai, K. Liu, Bioelectronics-related 2D materials beyond graphene: fundamentals, properties, and applications, Adv. Funct. Mater. 30 (2020) 2003732.

[39] G. Guan, S. Zhang, S. Liu, Y. Cai, M. Low, C.P. Teng, I.Y. Phang, Y. Cheng, K. L. Duei, B.M. Srinivasan, Y. Zheng, Y.-W. Zhang, M.-Y. Han, Protein induces layer-by-layer exfoliation of transition metal dichalcogenides, J. Am. Chem. Soc. 137 (2015) 6152–6155.

[40] A. Ghosh, S. Fathima Thanutty Kallungal, S. Ramaprabhu, 2D metal-organic frameworks: properties, synthesis, and applications in electrochemical and optical biosensors, Biosensors 13 (2023) 123.

[41] S. Vinoth, K.S. Devi, A. Pandikumar, A comprehensive review on graphitic carbon nitride based electrochemical and biosensors for environmental and healthcare applications, TrAC, Trends Anal. Chem. 140 (2021) 116274.

[42] S.M. George, B. Kandasubramanian, Advancements in MXene-Polymer composites for various biomedical applications, Ceram. Int. 46 (2020) 8522–8535.

[43] Z. Jiang, B. Feng, J. Xu, T. Qing, P. Zhang, Z. Qing, Graphene biosensors for bacterial and viral pathogens, Biosens. Bioelectron. 166 (2020) 112471.

[44] E. Toto, S. Laurenzi, M.G. Santonicola, Recent trends in graphene/polymer nanocomposites for sensing devices: synthesis and applications in environmental and human health monitoring, Polymers 14 (2022) 1030.

[45] A. Yadav, H. Kumar, R. Sharma, R. Kumari, Synthesis, processing, and applications of 2D (nano) materials: a sustainable approach, Surface. Interfac. 39 (2023) 102925.

[46] Z. Zhang, J. Du, J. Li, X. Huang, T. Kang, C. Zhang, S. Wang, O.O. Ajao, W.-J. Wang, P. Liu, Polymer nanocomposites with aligned two-dimensional materials, Prog. Polym. Sci. 114 (2021) 101360.

[47] Y. Xu, H. Cao, Y. Xue, B. Li, W. Cai, Liquid-phase exfoliation of graphene: an overview on exfoliation media, techniques, and challenges, Nanomaterials 8 (2018) 942.

[48] K. Lobo, P. Sahoo, R. Kurapati, V. Krishna K., V. Patil, A. Pandit, H.S.S.R. Matte, Additive-free aqueous dispersions of two-dimensional materials with glial cell compatibility and enzymatic degradability, Chem. Eur J. 27 (2021) 7434–7443.

[49] F. Lebre, D. Hanlon, J.B. Boland, J. Coleman, E.C. Lavelle, Exfoliation in endotoxin-free albumin generates pristine graphene with reduced inflammatory properties, Adv. Biosyst. 2 (2018) 1800102.

[50] Y. He, A.F. Andrade, C. Ménard-Moyon, A. Bianco, Biocompatible 2D materials via liquid phase exfoliation, Adv. Mater. (2024) 2310999.

[51] A. Gupta, T. Sakthivel, S. Seal, Recent development in 2D materials beyond graphene, Prog. Mater. Sci. 73 (2015) 44–126.

[52] A. Castellanos-Gomez, L. Vicarelli, E. Prada, J.O. Island, K.L. Narasimha-Acharya, S.I. Blanter, D.J. Groenendijk, M. Buscema, G.A. Steele, J.V. Alvarez, Isolation and characterization of few-layer black phosphorus, 2D Mater. 1 (2014) 025001.

[53] J.H. Jeong, S. Kang, N. Kim, R. Joshi, G.-H. Lee, Recent trends in covalent functionalization of 2D materials, Phys. Chem. Chem. Phys. 24 (2022) 10684–10711.

[54] U.G.K. Wegst, H. Bai, E. Saiz, A.P. Tomsia, R.O. Ritchie, Bioinspired structural materials, Nat. Mater. 14 (2015) 23–36.

[55] Y. Zhang, C. Ma, J. Xie, H. Ågren, H. Zhang, Black phosphorus/polymers: status and challenges, Adv. Mater. 33 (2021) 2100113.

[56] J. Yoon, S.N. Lee, M.K. Shin, H.-W. Kim, H.K. Choi, T. Lee, J.-W. Choi, Flexible electrochemical glucose biosensor based on GOx/gold/MoS_2/gold nanofilm on the polymer electrode, Biosens. Bioelectron. 140 (2019) 111343.

[57] M.-H. Wang, B.-W. Ji, X.-W. Gu, H.-C. Tian, X.-Y. Kang, B. Yang, X.-L. Wang, X. Chen, C.-Y. Li, J.-Q. Liu, Direct electrodeposition of Graphene enhanced conductive polymer on microelectrode for biosensing application, Biosens. Bioelectron. 99 (2018) 99–107.

[58] C. Deepa, L. Rajeshkumar, M. Ramesh, Preparation, synthesis, properties and characterization of graphene-based 2D nano-materials for biosensors and bioelectronics, J. Mater. Res. Technol. 19 (2022) 2657–2694.

[59] L. Zhou, C. Liu, Z. Sun, H. Mao, L. Zhang, X. Yu, J. Zhao, X. Chen, Black phosphorus based fiber optic biosensor for ultrasensitive cancer diagnosis, Biosens. Bioelectron. 137 (2019) 140–147.

[60] S.S. Low, Z. Chen, Y. Li, Y. Lu, Q. Liu, Design principle in biosensing: critical analysis based on graphitic carbon nitride (G-C3N4) photoelectrochemical biosensor, TrAC, Trends Anal. Chem. 145 (2021) 116454.

[61] X. Hun, Y. Li, S. Wang, Y. Li, J. Zhao, H. Zhang, X. Luo, Photoelectrochemical platform for cancer cell glutathione detection based on polyaniline and nanoMoS_2 composites modified gold electrode, Biosens. Bioelectron. 112 (2018) 93–99.

[62] C. Li, J. Xu, Y. Wu, Y. Zhang, C. Zhang, W. Lei, Q. Hao, g-C3N4 nanofibers doped poly(3,4-ethylenedioxythiophene) modified electrode for simultaneous determination of ascorbic acid and acetaminophen, J. Electroanal. Chem. 824 (2018) 52–59.

[63] Y. Xu, W. Lei, J. Su, J. Hu, X. Yu, T. Zhou, Y. Yang, D. Mandler, Q. Hao, A high-performance electrochemical sensor based on g-C_3N_4-E-PEDOT for the determination of acetaminophen, Electrochim. Acta 259 (2018) 994–1003.

[64] X. Li, J. Xu, Y. Jiang, Z. He, B. Liu, H. Xie, H. Li, Z. Li, Y. Wang, H. Tai, Toward agricultural ammonia volatilization monitoring: a flexible polyaniline/$Ti_3C_2T_x$ hybrid sensitive films based gas sensor, Sensor. Actuator. B Chem. 316 (2020) 128144.

[65] X. Zhao, Y. Li, J. Wang, Z. Ouyang, J. Li, G. Wei, Z. Su, Interactive oxidation–reduction reaction for the in situ synthesis of graphene–phenol formaldehyde composites with enhanced properties, ACS Appl. Mater. Interfaces 6 (2014) 4254–4263.

[66] B.K. Shrestha, R. Ahmad, S. Shrestha, C.H. Park, C.S. Kim, In situ synthesis of cylindrical spongy polypyrrole doped protonated graphitic carbon nitride for cholesterol sensing application, Biosens. Bioelectron. 94 (2017) 686–693.

[67] C.-X. Hu, Q. Xiao, Y.-Y. Ren, M. Zhao, G.-H. Dun, H.-R. Wu, X.-Y. Li, Q.-Q. Yang, B. Sun, Y. Peng, F. Yan, Q. Wang, H.-L. Zhang, Polymer ionic liquid stabilized black phosphorus for environmental robust flexible optoelectronics, Adv. Funct. Mater. 28 (2018) 1805311.

[68] A. Murali, G. Lokhande, K.A. Deo, A. Brokesh, A.K. Gaharwar, Emerging 2D nanomaterials for biomedical applications, Mater. Today 50 (2021) 276–302.

[69] J. Huang, Z. Li, Y. Mao, Z. Li, Progress and biomedical applications of MXenes, Nano Sel. 2 (2021) 1480–1508.

[70] Q. Zeng, J.-S. Cheng, X.-F. Liu, H.-T. Bai, J.-H. Jiang, Palladium nanoparticle/chitosan-grafted graphene nanocomposites for construction of a glucose biosensor, Biosens. Bioelectron. 26 (2011) 3456–3463.

[71] D. Gan, Z. Huang, X. Wang, L. Jiang, C. Wang, M. Zhu, F. Ren, L. Fang, K. Wang, C. Xie, X. Lu, Graphene oxide-templated conductive and redox-active nanosheets incorporated hydrogels for adhesive bioelectronics, Adv. Funct. Mater. 30 (2020) 1907678.

[72] X. Li, Y. Li, Q. Qiu, Q. Wen, Q. Zhang, W. Yang, L. Yuwen, L. Weng, L. Wang, Efficient biofunctionalization of MoS_2 nanosheets with peptides as intracellular fluorescent biosensor for sensitive detection of caspase-3 activity, J. Colloid Interface Sci. 543 (2019) 96–105.

[73] X. Zhu, Y. Hu, G. Wu, W. Chen, N. Bao, Two-dimensional nanosheets-based soft electro-chemo-mechanical actuators: recent advances in design, construction, and applications, ACS Nano 15 (2021) 9273–9298.

[74] Y. Li, M. Gu, X. Zhang, J. Fan, K. Lv, S.A.C. Carabineiro, F. Dong, 2D g-C_3N_4 for advancement of photo-generated carrier dynamics: status and challenges, Mater. Today 41 (2020) 270–303.

[75] X. Guan, Z. Li, X. Geng, Z. Lei, A. Karakoti, T. Wu, P. Kumar, J. Yi, A. Vinu, Emerging trends of carbon-based quantum dots: nanoarchitectonics and applications, Small 19 (2023) 2207181.

[76] N.A. Mohamed, A.F. Ismail, J. Safaei, M.R. Johan, M.A. Mat Teridi, A novel photoanode based on Thorium oxide (ThO_2) incorporated with graphitic Carbon nitride (g-C_3N_4) for Photoelectrochemical water splitting, Appl. Surf. Sci. 569 (2021) 151043.

[77] J.N. Tiwari, Y.-K. Seo, T. Yoon, W.G. Lee, W.J. Cho, M. Yousuf, A.M. Harzandi, D.-S. Kang, K.-Y. Kim, P.-G. Suh, K.S. Kim, Accelerated bone regeneration by two-photon photoactivated carbon nitride nanosheets, ACS Nano 11 (2017) 742–751.

[78] D. Zhu, Q. Zhou, Nitrogen doped g-C_3N_4 with the extremely narrow band gap for excellent photocatalytic activities under visible light, Appl. Catal. B Environ. 281 (2021) 119474.

[79] H. Zhang, D. Zheng, Z. Cai, Z. Song, Y. Xu, R. Chen, C. Lin, L. Guo, Graphitic carbon nitride nanomaterials for multicolor light-emitting diodes and bioimaging, ACS Appl. Nano Mater. 3 (2020) 6798–6805.

[80] Z. Fan, X. Guo, Z. Jin, X. Li, Y. Li, Bridging effect of S–C bond for boosting electron transfer over cubic hollow CoS/g-C_3N_4 heterojunction toward photocatalytic hydrogen production, Langmuir 38 (2022) 3244–3256.

[81] S. Ghattavi, A. Nezamzadeh-Ejhieh, A visible light driven AgBr/g-C_3N_4 photocatalyst composite in methyl orange photodegradation: focus on photoluminescence, mole ratio, synthesis method of g-C_3N_4 and scavengers, Composites, Part B 183 (2020) 107712.

[82] M. Xiong, Q. Rong, H. Meng, X. Zhang, Two-dimensional graphitic carbon nitride nanosheets for biosensing applications, Biosens. Bioelectron. 89 (2017) 212–223.

[83] N.S.K. Gowthaman, M. Amalraj, S. Kesavan, K. Rajalakshmi, S. Shankar, B. Sinduja, P. Arul, R. Karthikeyan, C. Loganathan, V. Mangala Gowri, J. Kappen, A. Ajith, W. Sea Chang, Zero-, one- and two-dimensional carbon nanomaterials as low-cost catalysts in optical and electrochemical sensing of biomolecules and environmental pollutants, Microchem. J. 194 (2023) 109291.

[84] L. Wang, W. Si, Y. Tong, F. Hou, D. Pergolesi, J. Hou, T. Lippert, S.X. Dou, J. Liang, Graphitic carbon nitride (g-C_3N_4)-based nanosized heteroarrays: promising materials for photoelectrochemical water splitting, Carbon Energy 2 (2020) 223–250.

[85] M. Majdoub, Z. Anfar, A. Amedlous, Emerging chemical functionalization of g-C_3N_4: covalent/noncovalent modifications and applications, ACS Nano 14 (2020) 12390–12469.

[86] Z. Chen, Y. Lan, Y. Hong, W. Lan, Review of 2D graphitic carbon nitride-based membranes: principles, syntheses, and applications, ACS Appl. Nano Mater. 5 (2022) 12343–12365.

[87] Q. Cao, B. Kumru, M. Antonietti, B.V.K.J. Schmidt, Graphitic carbon nitride and polymers: a mutual combination for advanced properties, Mater. Horiz. 7 (2020) 762–786.

[88] N. Gupta, K. Todi, T. Narayan, B.D. Malhotra, Graphitic carbon nitride-based nanoplatforms for biosensors: design strategies and applications, Mater. Today Chem. 24 (2022) 100770.

[89] Q. Zhang, Y. Liu, G. Yang, H. Kong, L. Guo, G. Wei, Recent advances in protein hydrogels: from design, structural and functional regulations to healthcare applications, Chem. Eng. J. 451 (2023) 138494.
[90] S.K. Gaddam, R. Pothu, R. Boddula, Graphitic carbon nitride ($g\text{-}C_3N_4$) reinforced polymer nanocomposite systems—a review, Polym. Compos. 41 (2020) 430–442.
[91] E. Sobhanie, F. Salehnia, G. Xu, Y. Hamidipanah, S. Arshian, A. Firoozbakhtian, M. Hosseini, M.R. Ganjali, S. Hanif, Recent trends and advancements in electrochemiluminescence biosensors for human virus detection, TrAC, Trends Anal. Chem. 157 (2022) 116727.
[92] Q. Cao, Q. Cui, Y. Yang, J. Xu, C. Han, L. Li, Graphitic carbon nitride as a distinct solid stabilizer for emulsion polymerization, Chem. Eur J. 24 (2018) 2286–2291.
[93] X. Ou, X. Tan, X. Liu, Q. Lu, S. Chen, S. Wei, A signal-on electrochemiluminescence biosensor for detecting Con A using phenoxy dextran-graphite-like carbon nitride as signal probe, Biosens. Bioelectron. 70 (2015) 89–97.
[94] B. Wang, X. Zhong, Y. Chai, R. Yuan, Ultrasensitive electrochemiluminescence biosensor for organophosphate pesticides detection based on carboxylated graphitic carbon nitride-poly(ethylenimine) and acetylcholinesterase, Electrochim. Acta 224 (2017) 194–200.
[95] J. Sun, R. Phatake, A. Azoulay, G. Peng, C. Han, J. Barrio, J. Xu, X. Wang, M. Shalom, Covalent functionalization of carbon nitride frameworks through cross-coupling reactions, Chem. Eur J. 24 (2018) 14921–14927.
[96] B. Kumru, V. Molinari, M. Hilgart, F. Rummel, M. Schäffler, B.V.K.J. Schmidt, Polymer grafted graphitic carbon nitrides as precursors for reinforced lubricant hydrogels, Polym. Chem. 10 (2019) 3647–3656.
[97] B. Kumru, M. Antonietti, B.V.K.J. Schmidt, Enhanced dispersibility of graphitic carbon nitride particles in aqueous and organic media via a one-pot grafting approach, ACS Publ. 33 (2017) 9897–9906.
[98] K.S. Novoselov, A.K. Geim, S.V. Morozov, D. Jiang, Y. Zhang, S.V. Dubonos, I. V. Grigorieva, A.A. Firsov, Electric field effect in atomically thin carbon films, Science 306 (2004) 666–669.
[99] H. Jamal, B.-S. Kang, H. Lee, J.-S. Yu, C.-S. Lee, Comparative studies of electrochemical performance and characterization of TiO_2/graphene nanocomposites as anode materials for Li-secondary batteries, J. Ind. Eng. Chem. 64 (2018) 151–166.
[100] A.A. Lahcen, S. Rauf, T. Beduk, C. Durmus, A. Aljedaibi, S. Timur, H.N. Alshareef, A. Amine, O.S. Wolfbeis, K.N. Salama, Electrochemical sensors and biosensors using laser-derived graphene: a comprehensive review, Biosens. Bioelectron. 168 (2020) 112565.
[101] R. Zhou, C. Wang, Y. Huang, K. Huang, Y. Wang, W. Xu, L. Xie, Y. Ying, Label-free terahertz microfluidic biosensor for sensitive DNA detection using graphene-metasurface hybrid structures, Biosens. Bioelectron. 188 (2021) 113336.
[102] U. Kamran, K.Y. Rhee, S.-Y. Lee, S.-J. Park, Innovative progress in graphene derivative-based composite hybrid membranes for the removal of contaminants in wastewater: a review, Chemosphere 306 (2022) 135590.
[103] R. Goldoni, M. Farronato, S.T. Connelly, G.M. Tartaglia, W.-H. Yeo, Recent advances in graphene-based nanobiosensors for salivary biomarker detection, Biosens. Bioelectron. 171 (2021) 112723.
[104] P.L. Yap, S. Kabiri, Y.L. Auyoong, D.N.H. Tran, D. Losic, Tuning the multifunctional surface chemistry of reduced graphene oxide via combined elemental doping and chemical modifications, ACS Omega 4 (2019) 19787–19798.
[105] K. Ling, H. Jiang, Y. Li, X. Tao, C. Qiu, F.-R. Li, A self-assembling RNA aptamer-based graphene oxide sensor for the turn-on detection of theophylline in serum, Biosens. Bioelectron. 86 (2016) 8–13.
[106] Q. Liu, G.-R. Xu, Graphene oxide (GO) as functional material in tailoring polyamide thin film composite (PA-TFC) reverse osmosis (RO) membranes, Desalination 394 (2016) 162–175.
[107] B. Kurt Urhan, Ü. Demir, T. Öznülüer Özer, H. Öztürk Doğan, Electrochemical fabrication of Ni nanoparticles-decorated electrochemically reduced graphene oxide composite electrode for non-enzymatic glucose detection, Thin Solid Films 693 (2020) 137695.
[108] K.K. Reza, Md.A. Ali, S. Srivastava, V.V. Agrawal, A.M. Biradar, Tyrosinase conjugated reduced graphene oxide based biointerface for bisphenol A sensor, Biosens. Bioelectron. 74 (2015) 644–651.
[109] U. Kamran, Y.-J. Heo, B.-G. Min, I. In, S.-J. Park, Effect of nickel ion doping in MnO_2/reduced graphene oxide nanocomposites for lithium adsorption and recovery from aqueous media, RSC Adv. 10 (2020) 9245–9257.
[110] F. Liu, J.Y. Choi, T.S. Seo, Graphene oxide arrays for detecting specific DNA hybridization by fluorescence resonance energy transfer, Biosens. Bioelectron. 25 (2010) 2361–2365.
[111] Q. Gong, H. Han, H. Yang, M. Zhang, X. Sun, Y. Liang, Z. Liu, W. Zhang, J. Qiao, Sensitive electrochemical DNA sensor for the detection of HIV based on a polyaniline/graphene nanocomposite, J. Materiomics. 5 (2019) 313–319.
[112] C.I.L. Justino, A.C. Duarte, T.A.P. Rocha-Santos, Critical overview on the application of sensors and biosensors for clinical analysis, TrAC, Trends Anal. Chem. 85 (2016) 36–60.
[113] S.M. Mousavi, F.W. Low, S.A. Hashemi, C.W. Lai, Y. Ghasemi, S. Soroshnia, A. Savardashtaki, A. Babapoor, N. Pynadathu Rumjit, S.M. Goh, N. Amin, S. K. Tiong, Development of graphene based nanocomposites towards medical and biological applications, Artif. Cells, Nanomed. Biotechnol. 48 (2020) 1189–1205.
[114] Q. Gong, Y. Wang, H. Yang, A sensitive impedimetric DNA biosensor for the determination of the HIV gene based on graphene-Nafion composite film, Biosens. Bioelectron. 89 (2017) 565–569.
[115] W. Yu, L. Sisi, Y. Haiyan, L. Jie, Progress in the functional modification of graphene/graphene oxide: a review, RSC Adv. 10 (2020) 15328–15345.
[116] S. Wang, M.Z. Hossain, K. Shinozuka, N. Shimizu, S. Kitada, T. Suzuki, R. Ichige, A. Kuwana, H. Kobayashi, Graphene field-effect transistor biosensor for detection of biotin with ultrahigh sensitivity and specificity, Biosens. Bioelectron. 165 (2020) 112363.
[117] N. Muthuchamy, K.-P. Lee, A.-I. Gopalan, Enhanced photoelectrochemical biosensing performances for graphene (2D) – titanium dioxide nanowire (1D) heterojunction polymer conductive nanosponges, Biosens. Bioelectron. 89 (2017) 390–399.
[118] R. Jijie, K. Kahlouche, A. Barras, N. Yamakawa, J. Bouckaert, T. Gharbi, S. Szunerits, R. Boukherroub, Reduced graphene oxide/polyethylenimine based immunosensor for the selective and sensitive electrochemical detection of uropathogenic Escherichia coli, Sensor. Actuator. B Chem. 260 (2018) 255–263.
[119] Y. Song, Y. Luo, C. Zhu, H. Li, D. Du, Y. Lin, Recent advances in electrochemical biosensors based on graphene two-dimensional nanomaterials, Biosens. Bioelectron. 76 (2016) 195–212.
[120] S. Xu, Y. Liu, W. Zhao, Q. Wu, Y. Chen, X. Huang, Z. Sun, Y. Zhu, X. Liu, Hierarchical 0D-2D bio-composite film based on enzyme-loaded polymeric nanoparticles decorating graphene nanosheets as a high-performance bio-sensing platform, Biosens. Bioelectron. 156 (2020) 112134.
[121] X. Jiang, A.V. Kuklin, A. Baev, Y. Ge, H. Ågren, H. Zhang, P.N. Prasad, Two-dimensional MXenes: from morphological to optical, electric, and magnetic properties and applications, Phys. Rep. 848 (2020) 1–58.
[122] B. Bhattacharjee, M. Ahmaruzzaman, R. Djellabi, E. Elimian, S. Rtimi, Advances in 2D MXenes-based materials for water purification and disinfection: synthesis approaches and photocatalytic mechanistic pathways, J. Environ. Manag. 324 (2022) 116387.
[123] D.H. Ho, Y.Y. Choi, S.B. Jo, J.-M. Myoung, J.H. Cho, Sensing with MXenes: progress and prospects, Adv. Mater. 33 (2021) 2005846.
[124] H. Park, S. Kim, S. Kim, M. Kim, Y. Kang, S. Amirthalingam, S. Lee, N.S. Hwang, K. Yang, H.D. Kim, Bioactive inorganic compound MXene and its application in tissue engineering and regenerative medicine, J. Ind. Eng. Chem. 117 (2023) 38–53.
[125] X. Ren, M. Huo, M. Wang, H. Lin, X. Zhang, J. Yin, Y. Chen, H. Chen, Highly catalytic niobium carbide (MXene) promotes hematopoietic recovery after radiation by free radical scavenging, ACS Nano 13 (2019) 6438–6454.
[126] W. Feng, R. Wang, Y. Zhou, L. Ding, X. Gao, B. Zhou, P. Hu, Y. Chen, Ultrathin molybdenum carbide MXene with fast biodegradability for highly efficient theory-oriented photonic tumor hyperthermia, Adv. Funct. Mater. 29 (2019) 1901942.
[127] C. Xing, S. Chen, X. Liang, Q. Liu, M. Qu, Q. Zou, J. Li, H. Tan, L. Liu, D. Fan, H. Zhang, Two-dimensional MXene (Ti_3C_2)-integrated cellulose hydrogels: toward smart three-dimensional network nanoplatforms exhibiting light-induced swelling and bimodal photothermal/chemotherapy anticancer activity, ACS Appl. Mater. Interfaces 10 (2018) 27631–27643.
[128] X. Han, J. Huang, H. Lin, Z. Wang, P. Li, Y. Chen, 2D ultrathin MXene-based drug-delivery nanoplatform for synergistic photothermal ablation and chemotherapy of cancer, Adv. Healthcare Mater. 7 (2018) 1701394.
[129] A. Szuplewska, D. Kulpińska, A. Dybko, A.M. Jastrzębska, T. Wojciechowski, A. Rozmysłowska, M. Chudy, I. Grabowska-Jadach, W. Ziemkowska, Z. Brzózka, A. Olszyna, 2D Ti_2C (MXene) as a novel highly efficient and selective agent for photothermal therapy, Mater. Sci. Eng. C 98 (2019) 874–886.
[130] Z. Li, H. Zhang, J. Han, Y. Chen, H. Lin, T. Yang, Surface nanopore engineering of 2D MXenes for targeted and synergistic multitherapies of hepatocellular carcinoma, Adv. Mater. 30 (2018) 1706981.
[131] L. Zong, H. Wu, H. Lin, Y. Chen, A polyoxometalate-functionalized two-dimensional titanium carbide composite MXene for effective cancer theranostics, Nano Res. 11 (2018) 4149–4168.
[132] P. Balakrishnan, V.G. Geethamma, M. Sreekala, S. Thomas, Polymeric Biomaterials: State-Of-The-Art and New Challenges, 2018, pp. 1–20.
[133] R.B. Rakhi, P. Nayak, C. Xia, H.N. Alshareef, Novel amperometric glucose biosensor based on MXene nanocomposite, Sci. Rep. 6 (2016) 36422.
[134] M. Sharifuzzaman, M.A. Zahed, M.S. Reza, M. Asaduzzaman, S. Jeong, H. Song, D. K. Kim, S. Zhang, J.Y. Park, MXene/fluoropolymer-derived laser-carbonaceous all-fibrous nanohybrid patch for soft wearable bioelectronics, Adv. Funct. Mater. 33 (2023) 2208894.
[135] F. Wang, C. Yang, M. Duan, Y. Tang, J. Zhu, TiO_2 nanoparticle modified organ-like Ti_3C_2 MXene nanocomposite encapsulating hemoglobin for a mediator-free biosensor with excellent performances, Biosens. Bioelectron. 74 (2015) 1022–1028.
[136] S. Zhou, C. Gu, Z. Li, L. Yang, L. He, M. Wang, X. Huang, N. Zhou, Z. Zhang, $Ti_3C_2T_x$ MXene and polyoxometalate nanohybrid embedded with polypyrrole: ultra-sensitive platform for the detection of osteopontin, Appl. Surf. Sci. 498 (2019) 143889.
[137] Y. Hu, H. Zhuo, Q. Luo, Y. Wu, R. Wen, Z. Chen, L. Liu, L. Zhong, X. Peng, R. Sun, Biomass polymer-assisted fabrication of aerogels from MXenes with ultrahigh compression elasticity and pressure sensitivity, J. Mater. Chem. A 7 (2019) 10273–10281.
[138] X. Lin, Z. Li, J. Qiu, Q. Wang, J. Wang, H. Zhang, T. Chen, Fascinating MXene nanomaterials: emerging opportunities in the biomedical field, Biomater. Sci. 9 (2021) 5437–5471.
[139] S. A, K. D, D. A, C. M, J. Am, O. A, B. Z, Future applications of MXenes in biotechnology, nanomedicine, and sensors, Trends Biotechnol. 38 (2020).
[140] H. Huang, R. Jiang, Y. Feng, H. Ouyang, N. Zhou, X. Zhang, Y. Wei, Recent development and prospects of surface modification and biomedical applications of MXenes, Nanoscale 12 (2020) 1325–1338.

[141] C. Xing, J. Zhang, J. Jing, J. Li, F. Shi, Preparations, properties and applications of low-dimensional black phosphorus, Chem. Eng. J. 370 (2019) 120–135.
[142] S. Anju, J. Ashtami, P.V. Mohanan, Black phosphorus, a prospective graphene substitute for biomedical applications, Mater. Sci. Eng. C 97 (2019) 978–993.
[143] D.K. Sang, H. Wang, Z. Guo, N. Xie, H. Zhang, Recent developments in stability and passivation techniques of phosphorene toward next-generation device applications, Adv. Funct. Mater. 29 (2019) 1903419.
[144] J.S. Shaikh, N.S. Shaikh, S. Sabale, N. Parveen, S.P. Patil, Y.K. Mishra, P. Kanjanaboos, S. Praserthdam, C.D. Lokhande, A phosphorus integrated strategy for supercapacitor: 2D black phosphorus–doped and phosphorus-doped materials, Mater. Today Chem. 21 (2021) 100480.
[145] Q. Li, J.-T. Wu, Y. Liu, X.-M. Qi, H.-G. Jin, C. Yang, J. Liu, G.-L. Li, Q.-G. He, Recent advances in black phosphorus-based electrochemical sensors: a review, Anal. Chim. Acta 1170 (2021) 338480.
[146] A.K. Tareen, K. Khan, S. Rehman, M. Iqbal, J. Yu, Nasir mahmood, Z. Zhou, J. Yin, Chuan li, H. Zhang, Recent development in emerging phosphorene based novel materials: progress, challenges, prospects and their fascinating sensing applications, Prog. Solid State Chem. 65 (2022) 100336.
[147] J.R. Choi, K.W. Yong, J.Y. Choi, A. Nilghaz, Y. Lin, J. Xu, X. Lu, Black phosphorus and its biomedical applications, Theranostics 8 (2018) 1005–1026.
[148] N. Sultana, A. Degg, S. Upadhyaya, T. Nilges, N.S. Sarma, Synthesis, modification, and application of black phosphorus, few-layer black phosphorus (FLBP), and phosphorene: a detailed review, Mater. Adv. 3 (2022) 5557–5574.
[149] G. He, T. Dong, Z. Yang, P. Ohlckers, Tuning 2D black phosphorus: defect tailoring and surface functionalization, Chem. Mater. 31 (2019) 9917–9938.
[150] Y. Teng Yew, Z. Sofer, C.C. Mayorga-Martinez, M. Pumera, Black phosphorus nanoparticles as a novel fluorescent sensing platform for nucleic acid detection, Mater. Chem. Front. 1 (2017) 1130–1136.
[151] X. Ge, Z. Xia, S. Guo, Recent advances on black phosphorus for biomedicine and biosensing, Adv. Funct. Mater. 29 (2019) 1900318.
[152] H. Liu, K. Hu, D. Yan, R. Chen, Y. Zou, H. Liu, S. Wang, Recent advances on black phosphorus for energy storage, catalysis, and sensor applications, Adv. Mater. 30 (2018) 1800295.
[153] L. Tan, M. Li, Z. Luo, K. Cai, Y. Hu, Black phosphorus biomaterials for photo-controlled bone tissue engineering, Composites, Part B 246 (2022) 110245.
[154] J. Li, C. Chen, S. Liu, J. Lu, W.P. Goh, H. Fang, Z. Qiu, B. Tian, Z. Chen, C. Yao, W. Liu, H. Yan, Y. Yu, D. Wang, Y. Wang, M. Lin, C. Su, J. Lu, Ultrafast electrochemical expansion of black phosphorus toward high-yield synthesis of few-layer phosphorene, Chem. Mater. 30 (2018) 2742–2749.
[155] C. Li, Y. Wu, B. Deng, Y. Xie, Q. Guo, S. Yuan, X. Chen, M. Bhuiyan, Z. Wu, K. Watanabe, T. Taniguchi, H. Wang, J.J. Cha, M. Snure, Y. Fei, F. Xia, Synthesis of crystalline black phosphorus thin film on sapphire, Adv. Mater. 30 (2018) 1703748.
[156] W. Lei, G. Liu, J. Zhang, M. Liu, Black phosphorus nanostructures: recent advances in hybridization, doping and functionalization, Chem. Soc. Rev. 46 (2017) 3492–3509.
[157] D. Scelta, A. Baldassarre, M. Serrano-Ruiz, K. Dziubek, A.B. Cairns, M. Peruzzini, R. Bini, M. Ceppatelli, Interlayer bond formation in black phosphorus at high pressure, Angew. Chem. 129 (2017) 14323–14328.
[158] Y. Cao, X. Tian, J. Gu, B. Liu, B. Zhang, S. Song, F. Fan, Y. Chen, Covalent functionalization of black phosphorus with conjugated polymer for information storage, Angew. Chem. Int. Ed. 57 (2018) 4543–4548.
[159] Y. Zhao, Y.-H. Zhang, Z. Zhuge, Y.-H. Tang, J.-W. Tao, Y. Chen, Synthesis of a poly-l-lysine/black phosphorus hybrid for biosensors, Anal. Chem. 90 (2018) 3149–3155.
[160] S. Chandra Barman, M. Sharifuzzaman, M.A. Zahed, C. Park, S.H. Yoon, S. Zhang, H. Kim, H. Yoon, J.Y. Park, A highly selective and stable cationic polyelectrolyte encapsulated black phosphorene based impedimetric immunosensor for Interleukin-6 biomarker detection, Biosens. Bioelectron. 186 (2021) 113287.
[161] L. Zhou, C. Liu, Z. Sun, H. Mao, L. Zhang, X. Yu, J. Zhao, X. Chen, Black phosphorus based fiber optic biosensor for ultrasensitive cancer diagnosis, Biosens. Bioelectron. 137 (2019) 140–147.
[162] T.D. Thanh, N.D. Chuong, H.V. Hien, T. Kshetri, L.H. Tuan, N.H. Kim, J.H. Lee, Recent advances in two-dimensional transition metal dichalcogenides-graphene heterostructured materials for electrochemical applications, Prog. Mater. Sci. 96 (2018) 51–85.
[163] S. Kaushik, U.K. Tiwari, A. Deep, R.K. Sinha, Two-dimensional transition metal dichalcogenides assisted biofunctionalized optical fiber SPR biosensor for efficient and rapid detection of bovine serum albumin, Sci. Rep. 9 (2019) 6987.
[164] Z. Li, S.L. Wong, Functionalization of 2D transition metal dichalcogenides for biomedical applications, Mater. Sci. Eng. C 70 (2017) 1095–1106.
[165] H. Hu, A. Zavabeti, H. Quan, W. Zhu, H. Wei, D. Chen, J.Z. Ou, Recent advances in two-dimensional transition metal dichalcogenides for biological sensing, Biosens. Bioelectron. 142 (2019) 111573.
[166] P. Goswami, G. Gupta, Recent progress of flexible NO_2 and NH_3 gas sensors based on transition metal dichalcogenides for room temperature sensing, Mater. Today Chem. 23 (2022) 100726.
[167] J. Azadmanjiri, J. Wang, C.C. Berndt, A. Yu, 2D layered organic–inorganic heterostructures for clean energy applications, J. Mater. Chem. A 6 (2018) 3824–3849.
[168] M.T. Rahman, A.A. Maruf, S. Faisal, R. Pathak, K.M. Reza, A. Gurung, M. Hummel, Z. Gu, M.A.R. Laskar, S.I. Rahman, B.S. Lamsal, Q. Qiao, Metallic 1T phase tungsten disulfide microflowers for trace level detection of Hg^{2+} ions, Adv. Sustain. Syst. 4 (2020) 2000068.
[169] K. Kalantar-zadeh, J.Z. Ou, T. Daeneke, M.S. Strano, M. Pumera, S.L. Gras, Two-dimensional transition metal dichalcogenides in biosystems, Adv. Funct. Mater. 25 (2015) 5086–5099.
[170] H.-I. Kim, D. Yim, S.-J. Jeon, T.W. Kang, I.-J. Hwang, S. Lee, J.-K. Yang, J.-M. Ju, Y. So, J.-H. Kim, Modulation of oligonucleotide-binding dynamics on WS_2 nanosheet interfaces for detection of Alzheimer's disease biomarkers, Biosens. Bioelectron. 165 (2020) 112401.
[171] J. Yang, H. Lee, I. Hwang, H. Kim, D. Yim, J. Kim, Fluorescent 2D WS_2 nanosheets bearing chemical affinity elements for the recognition of glycated hemoglobin, Adv. Healthcare Mater. 7 (2018) 1701496.
[172] F. Li, X. Cui, Y. Zheng, Q. Wang, Y. Zhou, H. Yin, Photoelectrochemical biosensor for DNA formylation based on WS_2 nanosheets@polydopamine and MoS_2 nanosheets, Biosens. Bioelectron. X 10 (2022) 100104.
[173] T. Hu, X. Mei, Y. Wang, X. Weng, R. Liang, M. Wei, Two-dimensional nanomaterials: fascinating materials in biomedical field, Sci. Bull. 64 (2019) 1707–1727.
[174] M. Moharramnejad, A. Ehsani, M. Shahi, S. Gharanli, H. Saremi, R.E. Malekshah, Z.S. Basmenj, S. Salmani, M. Mohammadi, MOF as nanoscale drug delivery devices: synthesis and recent progress in biomedical applications, J. Drug Deliv. Sci. Technol. 81 (2023) 104285.
[175] S. Zhang, X. Pei, H. Gao, S. Chen, J. Wang, Metal-organic framework-based nanomaterials for biomedical applications, Chin. Chem. Lett. 31 (2020) 1060–1070.
[176] I. Soni, P. Kumar, G. Kudur Jayaprakash, Recent advancements in the synthesis and electrocatalytic activity of two-dimensional metal–organic framework with bimetallic nodes for energy-related applications, Coord. Chem. Rev. 472 (2022) 214782.
[177] M.G. Campbell, S.F. Liu, T.M. Swager, M. Dincă, Chemiresistive sensor arrays from conductive 2D metal–organic frameworks, J. Am. Chem. Soc. 137 (2015) 13780–13783.
[178] S.A. Younis, D.-K. Lim, K.-H. Kim, A. Deep, Metalloporphyrinic metal-organic frameworks: controlled synthesis for catalytic applications in environmental and biological media, Adv. Colloid Interface Sci. 277 (2020) 102108.
[179] B. Pramanik, R. Sahoo, M.C. Das, pH-stable MOFs: design principles and applications, Coord. Chem. Rev. 493 (2023) 215301.
[180] Y. Xue, S. Zheng, H. Xue, H. Pang, Metal–organic framework composites and their electrochemical applications, J. Mater. Chem. A 7 (2019) 7301–7327.
[181] H. Serati-Nouri, A. Jafari, L. Roshangar, M. Dadashpour, Y. Pilehvar-Soltanahmadi, N. Zarghami, Biomedical applications of zeolite-based materials: a review, Mater. Sci. Eng. C 116 (2020) 111225.
[182] X. Liao, H. Fu, T. Yan, J. Lei, Electroactive metal–organic framework composites: design and biosensing application, Biosens. Bioelectron. 146 (2019) 111743.
[183] J. Liu, T. Liu, P. Du, L. Zhang, J. Lei, Metal–organic framework (MOF) hybrid as a tandem catalyst for enhanced therapy against hypoxic tumor cells, Angew. Chem. Int. Ed. 58 (2019) 7808–7812.
[184] B. Liu, M. Jiang, D. Zhu, J. Zhang, G. Wei, Metal-organic frameworks functionalized with nucleic acids and amino acids for structure- and function-specific applications: a tutorial review, Chem. Eng. J. 428 (2022) 131118.
[185] W. Zhang, D. Duan, S. Liu, Y. Zhang, L. Leng, X. Li, N. Chen, Y. Zhang, Metal-organic framework-based molecularly imprinted polymer as a high sensitive and selective hybrid for the determination of dopamine in injections and human serum samples, Biosens. Bioelectron. 118 (2018) 129–136.
[186] B.V.K.J. Schmidt, Metal-organic frameworks in polymer science: polymerization catalysis, polymerization environment, and hybrid materials, macromol, Rapid Commun. 41 (2020) 1900333.
[187] K. Zhou, D. Shen, X. Li, Y. Chen, L. Hou, Y. Zhang, J. Sha, Molybdenum oxide-based metal-organic framework/polypyrrole nanocomposites for enhancing electrochemical detection of dopamine, Talanta 209 (2020) 120507.
[188] L. Jiao, J.Y.R. Seow, W.S. Skinner, Z.U. Wang, H.-L. Jiang, Metal–organic frameworks: structures and functional applications, Mater. Today 27 (2019) 43–68.
[189] M. Kalaj, K.C. Bentz, S.Jr. Ayala, J.M. Palomba, K.S. Barcus, Y. Katayama, S. M. Cohen, MOF-polymer hybrid materials: from simple composites to tailored architectures, Chem. Rev. 120 (2020) 8267–8302.
[190] L. Du, W. Chen, P. Zhu, Y. Tian, Y. Chen, C. Wu, Applications of functional metal-organic frameworks in biosensors, Biotechnol. J. 16 (2021) 1900424.
[191] S. Chen, D. Liu, N. Song, C. Wang, X. Lu, Promoting non-enzymatic electrochemical sensing performance toward glucose by the integration of conducting polypyrrole with metal-organic framework, Compos. Commun. 30 (2022) 101074.
[192] J. Liu, B. Yin, X. Liu, C. Yang, S. Zang, S. Wu, Enhancing electrochemical properties of a two-dimensional zeolitic imidazole framework by incorporating a conductive polymer for dopamine detection, Analyst 148 (2023) 4525–4532.
[193] J. Gao, C. Wang, H. Tan, Dual-emissive polystyrene@zeolitic imidazolate framework-8 composite for ratiometric detection of singlet oxygen, J. Mater. Chem. B 5 (2017) 9175–9182.
[194] D.I. Osman, S.M. El-Sheikh, S.M. Sheta, O.I. Ali, A.M. Salem, W.G. Shousha, S. F. El-Khamisy, S.M. Shawky, Nucleic acids biosensors based on metal-organic framework (MOF): paving the way to clinical laboratory diagnosis, Biosens. Bioelectron. 141 (2019) 111451.
[195] N.A. Khan, Z. Hasan, S.H. Jhung, Beyond pristine metal-organic frameworks: preparation and application of nanostructured, nanosized, and analogous MOFs, Coord. Chem. Rev. 376 (2018) 20–45.
[196] J. Chang, X. Wang, J. Wang, H. Li, F. Li, Nucleic acid-functionalized metal–organic framework-based homogeneous electrochemical biosensor for

simultaneous detection of multiple tumor biomarkers, Anal. Chem. 91 (2019) 3604–3610.
[197] S. Yang, V.V. Karve, A. Justin, I. Kochetygov, J. Espín, M. Asgari, O. Trukhina, D. T. Sun, L. Peng, W.L. Queen, Enhancing MOF performance through the introduction of polymer guests, Coord. Chem. Rev. 427 (2021) 213525.
[198] S.A. Kumar, B. Balasubramaniam, S. Bhunia, M.K. Jaiswal, K. Verma, Prateek, A. Khademhosseini, R.K. Gupta, A.K. Gaharwar, Two-dimensional metal organic frameworks for biomedical applications, Wiley Interdiscip. Rev. Nanomed. Nanobiotechnol. 13 (2021) e1674.
[199] A.K. Sundramoorthy, T.H. Vignesh Kumar, S. Gunasekaran, Chapter 12 - Graphene-Based Nanosensors and Smart Food Packaging Systems for Food Safety and Quality Monitoring, Elsevier, 2018, pp. 267–306.
[200] F. Shi, B. Wang, L. Yan, B. Wang, Y. Niu, L. Wang, W. Sun, In-situ growth of nitrogen-doped carbonized polymer dots on black phosphorus for electrochemical DNA biosensor of Escherichia coli O157: H7, Bioelectrochemistry 148 (2022) 108226.
[201] C. Singh, Md.A. Ali, V. Kumar, R. Ahmad, G. Sumana, Functionalized MoS_2 nanosheets assembled microfluidic immunosensor for highly sensitive detection of food pathogen, Sensor. Actuator. B Chem. 259 (2018) 1090–1098.
[202] Q. Zhou, D. Tang, Recent advances in photoelectrochemical biosensors for analysis of mycotoxins in food, TrAC, Trends Anal. Chem. 124 (2020) 115814.
[203] W. Wu, Y. Li, Q. Xu, N. Long, P. Song, J. Wang, L. Zhou, B. Fu, W. Kong, Polydopamine-coated HKUST MOFs-based strip lateral flow immunoassay for on-site ultrasensitive detection of aflatoxin B1 in foods, Food Control 152 (2023) 109864.
[204] A.M. Al-Dhahebi, R. Jose, M. Mustapha, M.S.M. Saheed, Ultrasensitive aptasensor using electrospun MXene/polyvinylidene fluoride nanofiber composite for Ochratoxin A detection, Food Chem. 390 (2022) 133105.
[205] H. Nasiri, H. Baghban, R. Teimuri-Mofrad, A. Mokhtarzadeh, Graphitic carbon nitride/magnetic chitosan composite for rapid electrochemical detection of lactose, Int. Dairy J. 136 (2023) 105489.
[206] X. Zhuang, C. Tian, F. Luan, X. Wu, L. Chen, One-step electrochemical fabrication of a nickel oxide nanoparticle/polyaniline nanowire/graphene oxide hybrid on a glassy carbon electrode for use as a non-enzymatic glucose biosensor, RSC Adv. 6 (2016) 92541–92546.
[207] D. Mathivanan, K.S. Shalini Devi, G. Sathiyan, A. Tyagi, V.A.O.P. da Silva, B. C. Janegitz, J. Prakash, R.K. Gupta, Novel polypyrrole-graphene oxide-gold nanocomposite for high performance hydrogen peroxide sensing application, Sens. Actuators Phys. 328 (2021) 112769.
[208] C. Liu, X. Chen, B. Zong, S. Mao, Recent advances in sensitive and rapid mercury determination with graphene-based sensors, J. Mater. Chem. A 7 (2019) 6616–6630.
[209] U. Kamran, S.-Y. Lee, K.Y. Rhee, S.-J. Park, Rice husk valorization into sustainable Ni@TiO_2/biochar nanocomposite for highly selective Pb (II) ions removal from an aqueous media, Chemosphere 323 (2023) 138210.
[210] S. Zhang, D. Zhang, X. Zhang, D. Shang, Z. Xue, D. Shan, X. Lu, Ultratrace naked-eye colorimetric detection of Hg^{2+} in wastewater and serum utilizing mercury-stimulated peroxidase mimetic activity of reduced graphene oxide-PEI-Pd nanohybrids, Anal. Chem. 89 (2017) 3538–3544.
[211] N. Ruecha, N. Rodthongkum, D.M. Cate, J. Volckens, O. Chailapakul, C.S. Henry, Sensitive electrochemical sensor using a graphene–polyaniline nanocomposite for simultaneous detection of Zn(II), Cd(II), and Pb(II), Anal. Chim. Acta 874 (2015) 40–48.
[212] M. Eswaran, P.-C. Tsai, M.-T. Wu, V.K. Ponnusamy, Novel nano-engineered environmental sensor based on polymelamine/graphitic-carbon nitride nanohybrid material for sensitive and simultaneous monitoring of toxic heavy metals, J. Hazard Mater. 418 (2021) 126267.
[213] A. Saljooqi, T. Shamspur, A. Mostafavi, A sensitive electrochemical sensor based on graphene oxide nanosheets decorated by Fe_3O_4@Au nanostructure stabilized on polypyrrole for efficient triclosan sensing, Electroanalysis 32 (2020) 1297–1303.
[214] S.-J. Choi, S.-J. Kim, I.-D. Kim, Ultrafast optical reduction of graphene oxide sheets on colorless polyimide film for wearable chemical sensors, NPG Asia Mater. 8 (2016) e315, e315.
[215] D. Tyagi, H. Wang, W. Huang, L. Hu, Y. Tang, Z. Guo, Z. Ouyang, H. Zhang, Recent advances in two-dimensional-material-based sensing technology toward health and environmental monitoring applications, Nanoscale 12 (2020) 3535–3559.
[216] Y. Li, Y. Li, X. Yu, Y. Sun, Electrochemical determination of carbofuran in tomatoes by a concanavalin A (con A) polydopamine (PDA)-Reduced graphene oxide (RGO)-Gold nanoparticle (GNP) glassy carbon electrode (GCE) with immobilized acetylcholinesterase (AChE), Anal. Lett. 52 (2019) 2283–2299.
[217] J.K. Aronson, R.E. Ferner, Biomarkers—a general review, Curr. Protoc. Pharmacol. 76 (2017) 9.23.1–9.23.17.
[218] S. Joshi, K.A. Raj, M.R. Rao, R. Ghosh, An electronic biosensor based on semiconducting tetrazine polymer immobilizing matrix coated on rGO for carcinoembryonic antigen, Sci. Rep. 12 (2022) 3006.
[219] H. Zhang, Z. Wang, Q. Zhang, F. Wang, Y. Liu, Ti_3C_2 MXenes nanosheets catalyzed highly efficient electrogenerated chemiluminescence biosensor for the detection of exosomes, Biosens. Bioelectron. 124–125 (2019) 184–190.
[220] F. Liu, B. An, J. Zhang, S. Niu, J. Wan, Electrochemical determination of hydrogen peroxide using a novel prussian blue–polythiophene–graphene oxide membrane-modified glassy carbon electrode, Instrum. Sci. Technol. 46 (2018) 207–221.
[221] V. Kumar, J.R. Brent, M. Shorie, H. Kaur, G. Chadha, A.G. Thomas, E.A. Lewis, A. P. Rooney, L. Nguyen, X.L. Zhong, M.G. Burke, S.J. Haigh, A. Walton, P. D. McNaughter, A.A. Tedstone, N. Savjani, C.A. Muryn, P. O'Brien, A.K. Ganguli, D.J. Lewis, P. Sabherwal, Nanostructured aptamer-functionalized black phosphorus sensing platform for label-free detection of myoglobin, a cardiovascular disease biomarker, ACS Appl. Mater. Interfaces 8 (2016) 22860–22868.
[222] T. Li, Y. Li, T. Zhang, Materials, structures, and functions for flexible and stretchable biomimetic sensors, Acc. Chem. Res. 52 (2019) 288–296.
[223] H. Yang, T. Xue, F. Li, W. Liu, Y. Song, Graphene: diversified flexible 2D material for wearable vital signs monitoring, Adv. Mater. Technol. 4 (2019) 1800574.
[224] L. Chen, F. Chen, G. Liu, H. Lin, Y. Bao, D. Han, W. Wang, Y. Ma, B. Zhang, L. Niu, Superhydrophobic functionalized $Ti_3C_2T_x$ MXene-based skin-attachable and wearable electrochemical pH sensor for real-time sweat detection, Anal. Chem. 94 (2022) 7319–7328.
[225] H. Guo, C. Lan, Z. Zhou, P. Sun, D. Wei, C. Li, Transparent, flexible, and stretchable WS_2 based humidity sensors for electronic skin, Nanoscale 9 (2017) 6246–6253.
[226] Y.-W. Cai, X.-N. Zhang, G.-G. Wang, G.-Z. Li, D.-Q. Zhao, N. Sun, F. Li, H.-Y. Zhang, J.-C. Han, Y. Yang, A flexible ultra-sensitive triboelectric tactile sensor of wrinkled PDMS/MXene composite films for E-skin, Nano Energy 81 (2021) 105663.
[227] Z. Chen, Y. Hu, H. Zhuo, L. Liu, S. Jing, L. Zhong, X. Peng, R. Sun, Compressible, elastic, and pressure-sensitive carbon aerogels derived from 2D titanium carbide nanosheets and bacterial cellulose for wearable sensors, Chem. Mater. 31 (2019) 3301–3312.
[228] W. Tao, X. Zhu, X. Yu, X. Zeng, Q. Xiao, X. Zhang, X. Ji, X. Wang, J. Shi, H. Zhang, L. Mei, Black phosphorus nanosheets as a robust delivery platform for cancer theranostics, Adv. Mater. 29 (2017) 1603276.
[229] W.Y. Chen, X. Jiang, S.-N. Lai, D. Peroulis, L. Stanciu, Nanohybrids of a MXene and transition metal dichalcogenide for selective detection of volatile organic compounds, Nat. Commun. 11 (2020) 1302.
[230] M. Amiri, H. Salehniya, A. Habibi-Yangjeh, Graphitic carbon nitride/chitosan composite for adsorption and electrochemical determination of mercury in real samples, Ind. Eng. Chem. Res. 55 (2016) 8114–8122.
[231] S. Palanisamy, V. Velusamy, S.-W. Chen, T.C.K. Yang, S. Balu, C.E. Banks, Enhanced reversible redox activity of hemin on cellulose microfiber integrated reduced graphene oxide for H_2O_2 biosensor applications, Carbohydr. Polym. 204 (2019) 152–160.
[232] P. Teengam, W. Siangproh, A. Tuantranont, C.S. Henry, T. Vilaivan, O. Chailapakul, Electrochemical paper-based peptide nucleic acid biosensor for detecting human papillomavirus, Anal. Chim. Acta 952 (2017) 32–40.
[233] S. Wu, J. Hao, S. Yang, Y. Sun, Y. Wang, W. Zhang, H. Mao, X.-M. Song, Layer-by-layer self-assembly film of PEI-reduced graphene oxide composites and cholesterol oxidase for ultrasensitive cholesterol biosensing, Sensor. Actuator. B Chem. 298 (2019) 126856.
[234] A. Cui, P. Meng, J. Hu, H. Yang, Z. Yang, H. Li, Y. Sun, Fabrication of high-performance cell-imprinted polymers based on AuNPs/MXene composites via metal-free visible light-induced ATRP, Analyst 148 (2023) 1058–1067.
[235] X. Liu, Y. Qiu, D. Jiang, F. Li, Y. Gan, Y. Zhu, Y. Pan, H. Wan, P. Wang, Covalently grafting first-generation PAMAM dendrimers onto MXenes with self-adsorbed AuNPs for use as a functional nanoplatform for highly sensitive electrochemical biosensing of cTnT, Microsyst. Nanoeng. 8 (2022) 1–15.
[236] H. Jiang, Q. Xia, D. Liu, K. Ling, Calcium-cation-doped polydopamine-modified 2D black phosphorus nanosheets as a robust platform for sensitive and specific biomolecule sensing, Anal. Chim. Acta 1121 (2020) 1–10.
[237] Y. Zhao, Z. Zhuge, Y.-H. Tang, J.-W. Tao, Synthesis of a CuNP/chitosan/black phosphorus nanocomposite for non-enzymatic hydrogen peroxide sensing, Analyst 145 (2020) 7260–7266.
[238] Y. Li, Z. Shi, C. Zhang, X. Wu, L. Liu, C. Guo, C.M. Li, Highly stable branched cationic polymer-functionalized black phosphorus electrochemical sensor for fast and direct ultratrace detection of copper ion, J. Colloid Interface Sci. 603 (2021) 131–140.
[239] R. Yang, J. Zhao, M. Chen, T. Yang, S. Luo, K. Jiao, Electrocatalytic determination of chloramphenicol based on molybdenum disulfide nanosheets and self-doped polyaniline, Talanta 131 (2015) 619–623.
[240] T. Yang, L. Meng, H. Chen, S. Luo, W. Li, K. Jiao, Synthesis of thin-layered molybdenum disulfide-based polyaniline nanointerfaces for enhanced direct electrochemical DNA detection, Adv. Mater. Interfac. 3 (2016) 1500700.
[241] A. Soni, C.M. Pandey, M.K. Pandey, G. Sumana, Highly efficient Polyaniline-MoS_2 hybrid nanostructures based biosensor for cancer biomarker detection, Anal. Chim. Acta 1055 (2019) 26–35.
[242] J. Yang, L. Gao, C. Peng, W. Zhang, Construction of self-signal DNA electrochemical biosensor employing WS_2 nanosheets combined with PIn6COOH, RSC Adv. 9 (2019) 9613–9619.
[243] Z. Zhang, J. Xu, Y. Wen, T. Wang, A highly-sensitive VB_2 electrochemical sensor based on one-step co-electrodeposited molecularly imprinted WS_2-PEDOT film supported on graphene oxide-SWCNTs nanocomposite, Mater. Sci. Eng. C 92 (2018) 77–87.
[244] S.P. Selvam, A.N. Kadam, K.R. Maiyelvaganan, M. Prakash, S. Cho, Novel SeS_2-loaded Co MOF with Au@PANI comprised electroanalytical molecularly imprinted polymer-based disposable sensor for patulin mycotoxin, Biosens. Bioelectron. 187 (2021) 113302.
[245] W. Yang, G. Zhang, W. Weng, B. Qiu, L. Guo, Z. Lin, G. Chen, Signal on fluorescence biosensor for MMP-2 based on FRET between semiconducting polymer dots and a metal organic framework, RSC Adv. 4 (2014) 58852–58857.
[246] A. Gupta, S.K. Bhardwaj, A.L. Sharma, K.-H. Kim, A. Deep, Development of an advanced electrochemical biosensing platform for E. coli using hybrid metal-organic framework/polyaniline composite, Environ. Res. 171 (2019) 395–402.

[247] S. Wang, J. Liu, Y. Huang, N. Yang, Selective sensing of Mn^{2+} based on ZnCdS/ZnS QD/carboxymethyl chitosan/g-C_3N_4 nanosheet nanocomposite film by the conformational regulation of polymer chain, Appl. Surf. Sci. 530 (2020) 147255.
[248] X. Lu, S. Li, W. Guo, F. Zhang, F. Qu, A covalent organic polymer–TiO_2/Ti_3C_2 heterostructure as nonenzymatic biosensor for voltammetric detection of dopamine and uric acid, Microchim. Acta 188 (2021) 95.
[249] K. Salimiyan Rizi, B. Hatamluyi, M. Darroudi, Z. Meshkat, E. Aryan, S. Soleimanpour, M. Rezayi, PCR-free electrochemical genosensor for *Mycobacterium tuberculosis* complex detection based on two-dimensional Ti_3C_2 Mxene-polypyrrole signal amplification, Microchem. J. 179 (2022) 107467.
[250] M. Fatkullin, V. Menzelintsev, A. Lipovka, E. Dogadina, E. Plotnikov, K. Brazovskiy, S. Li, L. Ma, C. Cheng, E. Porokhova, I. Khlusov, L. Qiu, R. D. Rodriguez, E. Sheremet, Smart graphene textiles for biopotential monitoring: laser-tailored electrochemical property enhancement, ACS Sens. 9 (2024) 1809–1819.

Tahreem Zahra received her Bachelor of Science degree from the University of Narowal, Pakistan, in 2023. Her main research interests include the design and fabrication of nanomaterials for applications in water remediation and biosensors.

Umme Javeria received her Bachelor of Science degree from the University of Narowal, Pakistan, in 2023. Her research efforts primarily focus on materials science, biotechnology, and energy conversion/storage devices.

Hasan Jamal completed his Masters from Keimyung University. He worked as a researcher in Division of Energy Technology, Daegu Gyeongbuk Institute of Science & Technology, South Korea. His research area included energy storage, Li-metal batteries, all soild state electrolytes, and polymer membrane.

Mirza Mahmood Baig is working as a Postdoctoral researcher in Chemistry department, university of ulsan, South Korea. His research area is design of novel 2D materials and their composites for environmental remediation, energy storage and energy harvesting.

Farid Akhtar working as a Professor in Luleå University of Technology since 2014. He received doctorate in Materials Science and Engineering from University of Science and Technology Beijing, China. He worked as postdoctoral research at Department of Materials and Environmental Chemistry at Stockholm University (2007). His research focuses on synthesis and processing of porous materials for gas separation and gas storage and designing and tailoring of microstructure and properties of metallic, intermetallic and ceramic materials for high temperature applications.

Urooj Kamran is currently working as an excellent postdoctoral researcher at Luleå University of Technology, Sweden. In 2023, she also worked as a research professor at the Institute of Advanced Machinery Design Technology at Korea University, South Korea. She also worked as a postdoctoral researcher in the Department of Mechanical Engineering at Kyung Hee University, South Korea. She obtained her PhD degree in 2022 from the Department of Chemistry at Inha University (South Korea). Her research expertise includes innovative material fabrications, including biocomposites, nanocomposites, nanomaterials, and microporous carbonaceous materials for wastewater treatment and carbon dioxide capture.